Topics In Cosmology and Theoretical High Energy Physics:
Dark Astronomical Compact Objects (DACOs), Heavy Mirror Mesons.

Dat Quoc Duong
Da Nang, Viet Nam

B.Sc Physics, Hue, Vietnam 2013

A Dissertation presented to
the Graduate Faculty of the University of Virginia
in Candidacy for the Degree of
Doctor of Phylosophy

Department of Physics
University of Virginia
April, 2019

ACKNOWLEDGEMENTS

To begin my thesis, I would like to express my deepest gratitude to my mentor, Dr. Pham Quang Hung for his guidance to me through the field of High Energy Physics. His profound knowledge and his creative way of thinking really inspires me in different ways to keep exploring new challenges both in and out of Physics. This thesis could not be completed without his encouragement, discussion and support.

I would like to thank all of the faculty and staffs of the Department of Physics. I would like to thank Dr. Marshall, Dr. Bychkov for supporting me when I was a teaching assistant. They did not just show me how Physics should be properly conveyed through experiments, but also gave me opportunity to look at Physics from a different perspective and to stimulate the excitement and joy of stuyding Physics in my students. I would like thank Dr. Hirosky for his interesting course in Computational Physics, which helped me a lot in completing this thesis as well as being able use computer programming for my studying on different fields. I am also truly grateful for all members of the the committee for their understanding and support.

I want to thank my lovely wife Truc Le for her unconditioned love and support, my little son Daniel whose smiles and babbling encourage me like nothing else. Finally, I would like to thank my family for always supporting me in everything I do.

Contents

List of Figures

List of Tables

Chapter 1

Summary of the Standard Model

1.1 Particles and interactions

The Standard Model (SM) in particle physics is a relativistic quantum field theory which describes three out of four fundamental interactions in nature. The SM includes quantum chromodynamics, a theory of unbroken $SU(3)$ symmetry that describes the strong interaction, and the electroweak model, a theory of a broken $SU(2)_L \times U(1)_Y$ symmetry that describes the electromagnetic and weak interactions [1].

In the SM, particles are divided into fermions and bosons, which are identified by their spin quantum numbers. Fermions are particles that follow Fermi - Dirac statistics, which include fundamental particles whose spin is 1/2 and any composite particle that has odd number of these fundamental particles. Bosons are particles that follow Bose - Eistein statistics, which always have integer spin quantum numbers. Fermions are building blocks of matter while bosons are mainly mediators for fundamental forces described earlier.

Fermions in the SM include quarks and leptons, which come in 3 generations.

- **Quarks** are particles whose combination creates hadrons and have never been observed as free particles. Bound states of a quark and an antiquark are called mesons while bound states of three quarks are called baryons. Quarks come in up and down isospin doublets. Based on quarks' charge, they are classified into "up" type and "down" type. Quark charges are calculated by using the generalized Gell-Mann-Nishijima formula [2]:

$$Q = T_3 + \frac{Y}{2}, \tag{1.1}$$

where T_3 is the isospin quantum number (+1/2 for u, c, t quarks and -1/2 for d, s, b quarks) and $Y/2$ is the hypercharge (1/6 for quark doublets). From this, we can verify the charges of all SM quarks:

$$\begin{aligned} Q(u, c, t) &= T_3 + \frac{Y}{2} = \frac{1}{2} + \frac{1}{6} = \frac{2}{3}, \\ Q(d, s, b) &= T_3 + \frac{Y}{2} = -\frac{1}{2} + \frac{1}{6} = -\frac{1}{3}. \end{aligned} \tag{1.2}$$

There are 6 flavors of quarks that fall into three "generations" or "families" as summarized in Figure (1.1). Each quark flavor comes with three different color charges, which enable them to interact via the strong interaction. Every quark has a corresponding antiquark with the same mass, the same mean lifetime and the same spin but with an opposite charge. Due to the color confinement of hadrons in QCD, quarks cannot exist as free particles. We can only find quarks as part of compound particles like mesons (a combination of one quark and one antiquark) and baryons (combinations of three quarks).

- **Leptons** are also fermions of spin 1/2 which exist in 6 different flavors that are grouped into three generations as described in Figure (1.1). Unlike quarks whose charges are not integers, each generation of lepton has one neutral and one negatively charged particle. For example, the first generation includes one electron neutrino ν_e which is electrically neutral and one electron with charge -e. Leptons' charge also follows the Gell-Man-Nishijima formula. With all neutrinos having $T_3 = +1/2$, electron, muon and tau having $T_3 = -1/2$ and all leptons having $Y/2 = -1/2$, we can verify leptons' charges:

$$\begin{aligned} Q(\nu) &= T_3 + \frac{Y}{2} = \frac{1}{2} - \frac{1}{2} = 0, \\ Q(e) &= T_3 + \frac{Y}{2} = -\frac{1}{2} - \frac{1}{2} = -1. \end{aligned} \tag{1.3}$$

Each lepton described above has a corresponding anti-partner. For example, antiparticle of an electron is the positron, whose mass is equal to that of the

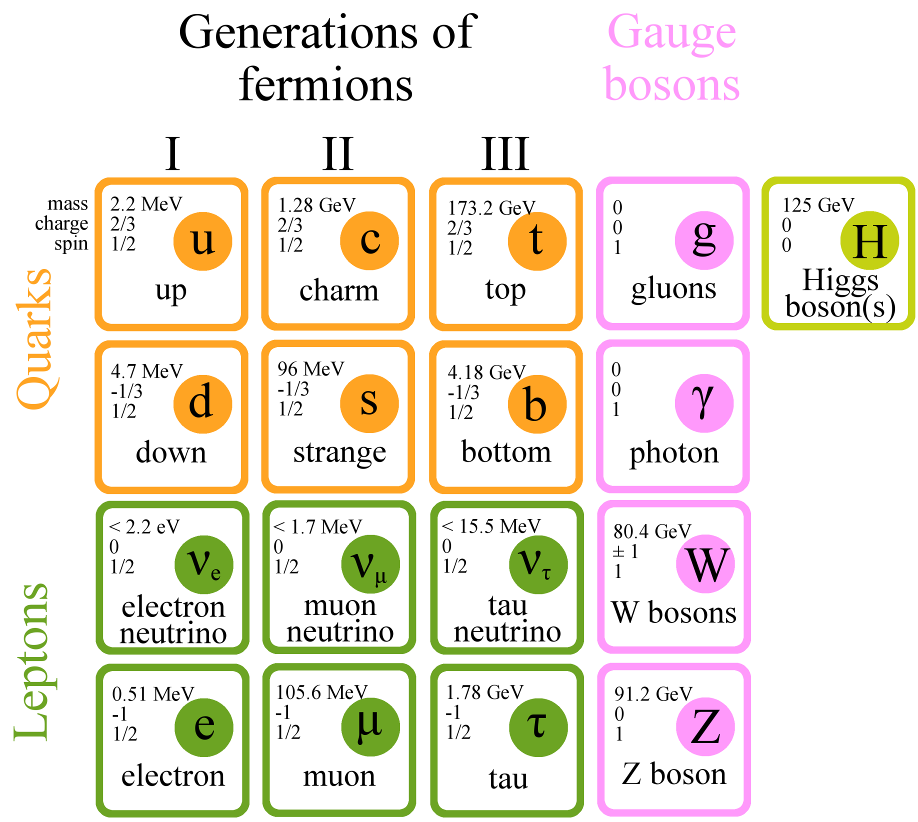

Figure 1.1: Standard Model of Elementary particles [3]

electron and has a charge of +e. One important point of the SM for leptons is that it predicts masses of neutrinos to be zero while in fact they are not. This is considered to be one the biggest issues of the SM. In contrast to quarks, leptons can be observed to be free particles. The charged leptons interact with other charged particles via electromagnetic and weak interactions while light lepton $(\nu_e, \nu_\mu, \nu_\tau)$ can only interact with other leptons via weak forces. These interactions will be discussed in more detail in subsequent sections.

While fermions are the building blocks that make up the world of matter, bosons are responsible for mediating the interaction between fermions, which include strong interaction, electroweak interaction and gravitational interaction. Bosons follow Bose - Einstein statistics and carry integer spin quantum numbers $(0, \pm 1, \pm 2, ...)$. Elementary particles interact with each other by exchanging the corresponding gauge bosons, which are gluons, photons, $W^{\pm}$ and Z bosons.

- **Gluons** are mediators for the strong interaction between quarks. There are 8 gluons in the SM as this is the number of generators for the $SU(3)$ color gauge group: $3^2 - 1 = 8$. Just like quarks, gluons have color charges and cannot be observed as free particles due to the color confinement that limits the effective range for strong interactions to about the size of an atomic nucleus.

- The photon is the mediator for electromagnetic interactions which are described by Quantum Electrodynamics (QED). Electrically charged particles interact with each other by exchanging photons in electric interactions.

- $\mathbf{W}^{\pm}$ and $\mathbf{Z}$ bosons are mediators for weak interactions, which are behind many processes like beta decay of a neutron into a proton and a W^- boson followed by the decay of W^- into electron and antielectron neutrino: $n \to p + e^- + \bar{\nu}_e$. In the SM, the weak and electromagnetic interactions are unified into the electroweak interaction under the $SU(2) \times U(1)$ gauge group, which will be explained in more detail in the next section.

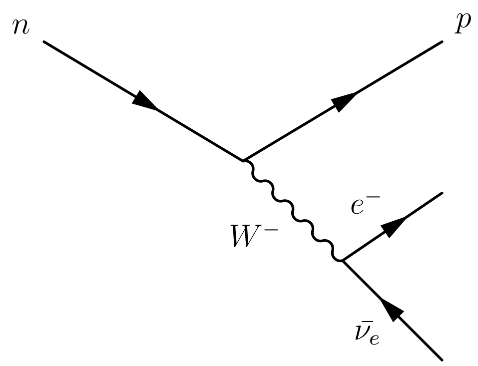

Figure 1.2: Beta decay of neutron

- The last boson of the SM is the Higgs boson which is a complex doublet. Following the process called “Higgs mechanism”, gauge bosons like $W^{\pm}$ and Z acquire masses after absorbing 3 out of 4 components of the Higgs doublet. The Higgs boson is also responsible for generating masses of quarks and leptons by coupling with them via a Higgs field. This important part will be explained in detail in the next sections.

1.2 The SM gauge theory

1.2.1 Lagrangian Field Theory

In Quantum Field Theory(QFT) [4], the Lagrangian density $\mathcal{L}$, which is the function of the fields of particles and their derivatives, gives us information about the kinetics of particles and how they interact with each other. The action, which is the time integral of the Lagrangian, is written as:

$$S = \int L dt = \int \mathcal{L}(\phi, \partial_\mu \phi) d^4 x. \tag{1.4}$$

When the action is minimized, field equations can be obtained:

$$\begin{aligned} 0 = \delta S &= \int d^4x \left\{ \frac{\partial L}{\partial \phi} \delta\phi + \frac{\partial L}{\partial(\partial\phi)} \delta(\partial_\mu \phi) \right\} \\ &= \int d^4x \left\{ \frac{\partial \mathcal{L}}{\partial \phi} \delta\phi - \partial_\mu \left(\frac{\partial \mathcal{L}}{\partial(\partial_\mu x)} \right) \delta\phi + \partial_\mu \left(\frac{\partial \mathcal{L}}{\partial(\partial_\mu x)} \delta\phi \right) \right\}, \end{aligned} \tag{1.5}$$

where $\delta\phi$ is the infinitesimal deformation of the field. As the integral of the final term in the equation above can be turned into a surface integration of the spacetime region of integral, which evaluates to zero, the field equation is then expressed as in the following form, which is also known as Euler-Lagrange equation:

$$\frac{\partial \mathcal{L}}{\partial \phi} - \partial_\mu \left(\frac{\partial \mathcal{L}}{\partial(\partial_\mu \phi)} \right) = 0. \tag{1.6}$$

If there is more than one field described in the Lagrangian, each field must have a corresponding Euler-Lagrange equation. As a simple example, let us consider the Lagrangian of a single real scalar field $\phi(x)$:

$$\mathcal{L} = \frac{1}{2}(\partial_\mu \phi)^2 - \frac{1}{2} m \phi^2. \tag{1.7}$$

By taking derivatives of $\mathcal{L}$ with respect to ϕ and $\partial_\mu \phi$, one can derive the equation of motion for $\phi(x)$, which is given by:

$$(\partial^\mu \partial_\mu + m^2)\phi(x) = 0, \tag{1.8}$$

which is well known as the Klein-Gordon equation.

1.2.2 Noether's Theorem

Noether's theorem is the theorem that states the relationship between symmetries and conservation laws, which can be applied in both classical and quantum field theories. This theorem is particularly important as it provides the analysis of charge conservation in the SM. For an infinitesimal deformation of the field given in the following form:

$$\phi(x) \to \phi'(x) = \phi(x) + \alpha\Delta\phi(x) \tag{1.9}$$

where α is infinitesimally small and $\Delta\phi$ is the deformation of the field. Such transformation is said to be symmetric if it leaves the equation of motion unchanged, which means that the action has to be invariant under such transformation. Generally, this will also be true if we allow the action to change by a surface term because that term can always be turned into a surface integral and evaluated to zero. Therefore, under the field transformation, the Lagrangian must transform as:

$$\mathcal{L}(x) \to \mathcal{L}'(x) + \alpha\partial_\mu \mathcal{J}^\mu(x) \tag{1.10}$$

by some $\mathcal{J}^\mu(x)$ function. The variation of the Lagrangian corresponding to the field variation is given by:

$$\begin{aligned} \alpha\Delta\mathcal{L}(x) &= \frac{\partial\mathcal{L}}{\partial\phi}(\alpha\Delta\phi) + \left(\frac{\partial\mathcal{L}}{\partial(\partial_\mu\phi)}\right)\partial_\mu(\alpha\Delta\phi) \\ &= \alpha\partial_\mu\left(\frac{\partial\mathcal{L}}{\partial(\partial_\mu\phi)}\Delta\phi\right) + \alpha\left[\frac{\mathcal{L}}{\partial\phi} - \partial_\mu\left(\frac{\mathcal{L}}{\partial(\partial_\mu\phi)}\right)\right]\Delta\phi. \end{aligned} \tag{1.11}$$

The second term in equation (1.11) is equal to 0 by the result of Euler - Lagrange equation. By comparing the remaining term in equation (1.110 with equation (1.10), we get:

$$\alpha\partial_\mu\mathcal{J}^\mu(x) = \alpha\partial_\mu\left(\frac{\partial\mathcal{L}}{\partial(\partial_\mu\phi)}\Delta\phi\right), \tag{1.12}$$

or equivalently, we can put this in the following form:

$$\partial_\mu j^\mu = 0 \text{ where } j^\mu = \frac{\partial\mathcal{L}}{\partial(\partial_\mu\phi)}\Delta\phi - \mathcal{J}^\mu(x). \tag{1.13}$$

The result we come up here means that for each continuous symmetry $\mathcal{L}$, we have a corresponding conserved current j^μ. The conserved charge in this case is given by:

$$Q = \int_{\text{all space}} j^0 d^3x. \tag{1.14}$$

where the integral is constant over time.

1.2.3 Chiral Symmetry

In deriving Euler - Lagrange equation, we have given an example of solving the equation of motion of real scalar field. A similar approach can give us the equation of motion of Dirac fields which represent fermionic particles. Such equation is called Dirac equation:

$$(i\gamma^\mu \partial_\mu - m)\psi(x) = 0, \tag{1.15}$$

with $\psi(x)$ denoting the field and m denoting fermion's mass. The term γ^μ in the equation above are gamma matrices, which are expressed in the Weyl basis as [4]:

$$\gamma^0 = \begin{pmatrix} 0 & I \\ I & 0 \end{pmatrix}, \gamma^i = \begin{pmatrix} 0 & \tau^i \\ -\tau^i & 0 \end{pmatrix}, \gamma^5 = \begin{pmatrix} -I & 0 \\ 0 & I \end{pmatrix}, \tag{1.16}$$

where I is the identity matrix and $\tau^i (i = 1, 2, 3)$ are the Pauli matrices.

The solution of the Dirac equation can be split into two 2-dimensional representations:

$$\psi = \begin{pmatrix} \psi_L \\ \psi_R \end{pmatrix}, \tag{1.17}$$

where ψ_L, ψ_R are related to ψ by the projection operators:

$$P_\pm = \frac{1}{2}(I \pm \gamma^5). \tag{1.18}$$

Under this transformation, each Weyl spinor transforms independently as:

$$\psi_L = P_- \psi, \ \psi_R = P_+ \psi \tag{1.19}$$

$$\bar{\psi_L} = \bar{\psi} P_-, \ \bar{\psi_R} = \bar{\psi} P+ \tag{1.20}$$

where $\bar{\psi} = \psi^+ \gamma^0$ is the Dirac adjoint of ψ. From the explicit form of γ^5, we can see that ψ_L and ψ_R are two eigenstates of γ^5 with eigenvalues of -1 and $+1$, respectively:

$$\gamma^5 \psi_L = -\psi_L \text{ and } \gamma^5 \psi_R = \psi_R. \tag{1.21}$$

By expressing the fermion fields as the sum of the left and right-handed components, we can see that the mass term that is proportional to $\bar{\psi}\psi$ will not be allowed as it would break the symmetry under the chiral transformation above. From this, we can rewrite the Dirac Lagrangian of a massless fermion as the sum of left and right-handed components as:

$$\mathcal{L}_{\text{Dirac}} = i\bar{\psi}\gamma^\mu \partial_\mu \psi = i\bar{\psi_L}\gamma^\mu \partial_\mu \psi_L + i\bar{\psi_R}\gamma^\mu \partial_\mu \psi_R. \tag{1.22}$$

In case of two flavors, one can have the freedom to make a $SU(2) \otimes U(1)$ transformations for each of the L and R components independently:

$$\psi_L \to U_L \psi_L,\ \ \psi_R \to U_R \psi_R. \tag{1.23}$$

The symmetry describing such transformations is called chiral symmetry. In terms of ψ_L and ψ_R, the Dirac equation, which is derived from Dirac Lagrangian above can be written as:

$$(i\gamma^\mu \partial_\mu - m)\psi = \begin{pmatrix} -m & i(\partial_0 + \boldsymbol{\sigma}.\boldsymbol{\nabla}) \\ i(\partial_0 - \boldsymbol{\sigma}.\boldsymbol{\nabla}) & -m \end{pmatrix} \begin{pmatrix} \psi_L \\ \psi_R \end{pmatrix} = 0 \tag{1.24}$$

In the limit where $m \to 0$, the equation above is split into system of two independent equations:

$$\begin{aligned} i(\partial_0 - \boldsymbol{\sigma}.\boldsymbol{\nabla})\psi_L = 0 \\ i(\partial_0 + \boldsymbol{\sigma}.\boldsymbol{\nabla})\psi_R = 0. \end{aligned} \tag{1.25}$$

The solution of Dirac equations above can be written as a linear combination of plane waves with positive frequency waves given by:

$$\psi(x) = u(p)e^{-ip.x},\ \ p^2 = m^2,\ \ p^0 > 0. \tag{1.26}$$

With this substitution, equation (1.25) becomes:

$$\begin{aligned} (E + \boldsymbol{\sigma}.\boldsymbol{p})\psi_L = 0 \\ (E - \boldsymbol{\sigma}.\boldsymbol{p})\psi_R = 0, \end{aligned} \tag{1.27}$$

where $E \to |p|$ in the limit that $m \to 0$. Therefore, we can rewrite the equation (1.27) as:

$$h\psi_L = -\frac{1}{2}\psi_L,\ \ h\psi_R = +\frac{1}{2}\psi_R, \tag{1.28}$$

where $h = \frac{1}{2}\boldsymbol{\sigma}.\boldsymbol{p}/|\boldsymbol{p}|$ is the helicity operator with eigenvalues $+\frac{1}{2}, -\frac{1}{2}$ for right and left-handed fermions, respectively. The helicity operator projects the direction of the angular momentum on the direction of linear momentum. For massive particles, direction of linear momentum depends on its selection of reference frame as one can select a reference frame that reverses the linear momentum direction while angular momentum remains the same. Hence helicity of massive fermions depends on the choice of reference frame. For a massless particle, the direction of the linear momentum does not depend on the choice of reference frame. Therefore, helicities of massless fermionos are independent of reference frame. In general, fermions are not massless. However, in the high energy limit where kinetic energy is much larger than the fermion's mass, chiral symmetry is usually utilized.

1.3 Quantum Electrodynamics

In the previous part, we have discussed the invariance of the field equation under the global phase transformation, which means that the transformation does not depend of the space-time coordinates. If we generalize the transformation in such a way that it is a function of space-time:

$$\psi(x) \to e^{i\alpha(x)}\psi(x), \tag{1.29}$$

where α is some functions of space-time, we will a transformation that is known as a local gauge transformation. However, this transformation does not guarantee that the Lagrangian of the field will be invariant. For example, the Dirac Lagrangian of a fermion field is given by:

$$\mathcal{L} = i\bar{\psi}\gamma^\mu\partial_\mu\psi - m\bar{\psi}\psi. \tag{1.30}$$

Under local transformation (1.29), the last term of $\mathcal{L}$ is invariant as:

$$\bar{\psi}\psi \to \bar{\psi}e^{-i\alpha(x)}e^{i\alpha(x)}\psi = \bar{\psi}\psi. \tag{1.31}$$

However, the first term in the Lagrangian is not invariant as it contains the derivative of the fermion field:

$$\partial_\mu\psi \to e^{i\alpha(x)}\partial_\mu\psi + ie^{i\alpha(x)}\psi\partial_\mu\alpha(x), \tag{1.32}$$

and the term containing $\partial_\mu\alpha(x)$ breaks the invariance of the Lagrangian. Up to this point, there is nothing crucial about this. However, if we insist on having the Lagrangian invariant under local transformations as it does in global transformation, we have to modify the derivative ∂_μ so that the term $\partial_\mu\alpha(x)$ will not appear after such transformation. In other word, the expected derivative must transform the same way ψ transforms:

$$\begin{aligned} \psi &\to e^{i\alpha(x)}\psi, \\ \mathcal{D}_\mu\psi &\to e^{i\alpha(x)}\mathcal{D}_\mu\psi \end{aligned} \tag{1.33}$$

The expected derivative is called "covariant" derivative as it has the same form of transformation as that of the field. To be able to achieve that goal, a vector field A_μ was introduced which transforms locally in such a way that the term containing derivative of the phase is canceled out. This is done by replacing ∂_μ by $\mathcal{D}_\mu$:

$$\mathcal{D}_\mu = \partial_\mu - ieA_\mu \tag{1.34}$$

where the vector field A_μ transforms as:

$$A_\mu \to A_\mu + \frac{1}{e}\partial_\mu \alpha(x). \tag{1.35}$$

We can confirm that the covariant derivative actually has the property that we expect: under the local phase transformation, we have:

$$\begin{aligned} \mathcal{D}_\mu \psi = (\partial_\mu - ieA_\mu)\psi \to \left[\partial_\mu - ie\left(A_\mu + \frac{1}{e}\partial_\mu \alpha(x)\right)\right](e^{i\alpha(x)}\psi) \\ = e^{i\alpha(x)}\left(\partial_\mu - ieA_\mu\right)\psi = e^{i\alpha(x)}\mathcal{D}_\mu \psi. \end{aligned} \tag{1.36}$$

After the replacement, the Lagrangian is invariant under the local transformation (1.29). However, the form of the Lagrangian is also altered:

$$\begin{aligned} \mathcal{L} &= i\bar{\psi}\gamma^\mu \mathcal{D}_\mu \psi - m\bar{\psi}\psi \\ &= i\bar{\psi}\gamma^\mu \partial_\mu \psi - m\bar{\psi}\psi + e\bar{\psi}\gamma^\mu \psi A_\mu. \end{aligned} \tag{1.37}$$

Thus, by requiring that the Dirac Lagrangian must be invariant under local phase transformation, we are required to introduce a gauge vector field A_μ that couples to the Dirac particle of charge e. To complete the Lagrangian, we must add to the Lagrangian the kinetic term for the newly added vector field A_μ. Again, to have an invariant Lagrangian, the kinetic term must also be invariant under (1.29). It can be checked that a field strength tensor $F_{\mu\nu} = \partial_\mu A_\nu - \partial_\nu A_\mu$ is gauge invariant. From this, we get the Lagrangian of QED:

$$\mathcal{L}_{QED} = \bar{\psi}(i\gamma^\mu \partial_\mu - m)\psi + e\bar{\psi}\gamma^\mu \psi A_\mu - \frac{1}{4}F_{\mu\nu}F^{\mu\nu}. \tag{1.38}$$

We did not include the mass term for the vector field because a mass term of $1/2m^2 A_\mu A^\mu$ would break the invariance of the Lagrangian, which explains why photon must be massless. The factor of $1/4$ for the kinetic term of the photon is to recover the Maxwell's equations. The Euler - Lagrange equation for the photon field A_μ is given by

$$\partial_\mu F^{\mu\nu} = j^\nu_{em}, \tag{1.39}$$

where the electric current j^ν_{em} is given by $j^\nu_{em} = e\bar{\psi}\gamma^\nu\psi$. We can check to see that the current corresponding to the photon field is conserved:

$$\partial_\mu j^\mu_{em} = e\partial_\mu\bar{\psi}\gamma^\mu\psi + e\bar{\psi}\gamma^\mu\partial_\mu\psi = (iem\bar{\psi})\psi + \bar{\psi}(-iem\psi) = 0. \tag{1.40}$$

In summary, we have looked into the scenario where Dirac Lagrangian variance is broken by a local phase transformation. To retain this invariance, the photon field A_μ was introduced that resulted in the interacting field theory of QED.

1.4 Yang-Mills Theory

In the previous section, the interacting field theory of QED was constructed based on the idea of preserving the local phase transformation invariance of the Lagrangian of fermion field. The original Yang and Mill's paper [5] proposed the invariance of the Lagrangian for proton - neutron doublet under transformation in isotopic spin space. In generalization of that argument, Yang - Mill theory can be applied to prove that fermion field Lagrangian must be invariant under any continuous symmetry group. Let us consider a fermion field described by an N multiplet: $\psi = (\psi_1, \psi_2, ..., \psi_N)$. Under the $SU(N)$ local phase transformation, the field will transform as:

$$\psi'_j(x) = exp\left[-i\frac{T_a\theta_a(x)}{2}\right]\psi_j(x) = U(\theta(x))\psi_j(x), \tag{1.41}$$

where T_a are the generators of the group which follow the commutator relation:

$$[T_a, T_b] = if_{abc}T_c, \tag{1.42}$$

where f_{abc} are called structure constants of the group. Again, by requiring that the Lagrangian must be invariant under this locally continuous phase transformation, we are forced to replace the field derivative by a covariant derivative which comes with additional vector fields. The symmetry group that describes electrodynamics is called Abelian symmetry and the generalized theory is called non-Abelian symmetry.

Starting from the free Lagrangian of the multiplet fermion field:

$$\mathcal{L} = \bar{\psi}_j(x)(i\gamma^\mu\partial_\mu - m_j)\psi_j(x), \tag{1.43}$$

where the field derivative will transform as:

$$\partial_\mu\psi \to \partial_\mu(U(\theta)\psi) = U(\theta(x))\partial_\mu\psi + \psi\partial_\mu(U(x)), \tag{1.44}$$

which certainly destroys the invariance of this fermion field Lagrangian. If we require that the Lagrangian must be invariant under transformation (1.41), we have to replace the old field derivative with covariant derivative so that the term containing $\partial_\mu(U(x))$ is canceled out of the derivative. Let us introduce the covariant derivative as

$$\partial_\mu\psi \to \mathcal{D}_\mu(\psi(x)) = \left(\partial_\mu - ig\frac{T_a A_\mu^a}{2}\right)\psi \tag{1.45}$$

that contains gauge vector field A_μ^a and g being the coupling constant of the theory, which is similar to electric charge in quantum electrodynamics. As we expect the covariant $\mathcal{D}_\mu$ to transform as $\mathcal{D}_\psi \to U(\theta(x))\mathcal{D}_\mu\psi$, we must have the vector field A_μ transformed as:

$$T^a A_\mu^{\prime a} = U(\theta(x))T^a A_\mu^a U^{-1}(\theta(x)) - \frac{i}{g}[\partial_\mu U(\theta(x))]U^{-1}(\theta(x)), \tag{1.46}$$

where $U(\theta(x) \approx 1 + -\frac{i}{2}T^a\theta^a(x)$ for infinitesimal $\theta^a(x)$. This means, the field A_μ^a must transform as:

$$A_\mu^a \to A_\mu^a - \frac{1}{g}\partial_\mu\theta^a + f_{abc}\theta^b A_\mu^c. \tag{1.47}$$

The transform of the vector field ensures that the covariant derivative of ψ has the same form with ψ and ensures that the Lagrangian of the fermion field is invariant under local phase transformations. The field tensor is defined by:

$$[\mathcal{D}_\mu, \mathcal{D}_\nu] = -i\frac{g}{2}F_{\mu\nu}^a T^a, \tag{1.48}$$

or equivalently:

$$F_{\mu\nu}^a = \partial_\mu A_\nu^a - \partial_\nu A_\mu^a + gf^{abc}A_\mu^b A_\nu^c, \tag{1.49}$$

whose infinitesimal transformation is:

$$F_{\mu\nu}^a \to F_{\mu\nu}^a - f^{abc}\theta^b F_{\mu\nu}^c. \tag{1.50}$$

The complete Lagrangian for Yang-Mills theory is then:

$$\mathcal{L}_{YM} = i\bar{\psi}_j(\gamma^\mu \mathcal{D}_\mu - m)\psi_j - \frac{1}{4}F^a_{\mu\nu}F^{a\mu\nu}. \tag{1.51}$$

It can be seen that the mass term for the vector field would break the symmetry under local phase transformations and therefore is forbidden. This explains the fact that vector gauge bosons in this theory are always massless. The number of massless gauge bosons in the group is also equal to the number of generators of the gauge symmetry.

In this section, we have discussed the general cases of Yang - Mill's theory, whose original paper described the proton - neutron doublet transformed under isotopic spin. In the next section, we will look at the example of Yang-Mill's theory being applied to describe QCD.

1.5 Quantum Chromodynamics

In the previous section, we have discussed the Yang-Mills theory, which can be applied to describe behaviors of fermionic particles using non-Abelian Lie groups. In this section, we will discuss the application of Yang-Mills theory to Quantum Chromodynamics (QCD), the theory that describes strong interaction between quarks and gluons, which are elementary particles that carry color charges. One important property of QCD is that the strong coupling constant is not a constant but rather decreases when the energy scale increases. This phenomenon is known as asymptotic freedom and was discovered in 1973 and the theory of QCD we are about to discuss has the ability to explain the physics behind it.

As presented in the beginning of the chapter, there are 6 flavors of quarks: u, d, s, c, b, t. Experimental evidence [6] shows that each quark comes in three color charges. One of such measurement is the R ratio of cross sections of the process $e^+e^- \to$ hadrons to that of the process $e^+e^- \to \mu^+\mu^-$:

$$R = \frac{e^+e^- \to \text{ hadrons}}{e^+e^- \to \mu^+\mu^-} = 3\sum_q e_q^2, \tag{1.52}$$

where e_q is the fractional charge of quarks and the factor of 3 comes from the assumption that each quark has three different color charges.

The color charges are named red (r), green (g), blue (b) with the corresponding color states:

$$r = \begin{pmatrix} 1 \\ 0 \\ 0 \end{pmatrix}, b = \begin{pmatrix} 0 \\ 1 \\ 0 \end{pmatrix}, g = \begin{pmatrix} 0 \\ 0 \\ 1 \end{pmatrix}, \tag{1.53}$$

The QCD theory is then the Yang - Mill's theory of $SU(3)$ where each quark flavor transforms as the fundamental triplet representations $\mathbf{3}$ and $\bar{\mathbf{3}}$. Stable hadrons observed in nature are all colorless, or more precisely, they are all in color singlet states. For hadrons to be invariant under $SU(3)$ color symmetry, they must belong to one of the following types of combinations:

$$\bar{q}^i q_i, \quad \epsilon^{ijk} q_i q_j q_k, \quad \epsilon_{ijk} \bar{q}^i \bar{q}^j \bar{q}^k, \tag{1.54}$$

which represent mesons, baryons. The color singlet state is given by:

$$\frac{\bar{r}r + \bar{g}g + \bar{b}b}{\sqrt{3}}. \tag{1.55}$$

In addition, we also have 8 mixed color states that are used for describing color states of gluons:

$$\begin{aligned} &(r\bar{b} + b\bar{r})/\sqrt{2}, \quad -i(r\bar{b} - b\bar{r})/\sqrt{2}, \quad (r\bar{g} + g\bar{r})/\sqrt{2}, \quad -i(r\bar{g} - g\bar{r})/\sqrt{2}, \\ &(b\bar{g} + g\bar{b})/\sqrt{2}, \quad -i(b\bar{g} - g\bar{b})/\sqrt{2}, \quad (r\bar{r} - b\bar{b})/\sqrt{2}, \quad (r\bar{r} + b\bar{b} - 2g\bar{g})/\sqrt{6}, \end{aligned} \tag{1.56}$$

which are linearly independent to each other. Following the theory structure we have shown in the Yang - Mill theory, we can contruct the Lagrangian of QCD as:

$$L_{QCD} = \bar{Q}_j (i\gamma^\mu \mathcal{D}_\mu - m_{q_j}) Q_j - \frac{1}{4} G^{a\mu\nu} G_{a\mu\nu}, \tag{1.57}$$

where the covariant derivative and field streng tensor are defined as usual:

$$\begin{aligned} \mathcal{D}^\mu &= \partial^\mu + i\frac{g}{2}\lambda_a A^\mu_a, \\ G^a_{\mu\nu} &= \partial_\mu A_\nu - \partial_\nu A_\mu + g f^{abc} A^b_\mu A^c_\nu. \end{aligned} \tag{1.58}$$

The 8 generators of the $SU(3)$ symmetry group are 3×3 Hermitian matrices that satisfy the relation:

$$[\lambda_a, \lambda_b] = i f_{abc} \lambda_c, \tag{1.59}$$

and are represented by [1]:

$$\lambda_1 = \begin{pmatrix} 0 & 1 & 0 \\ 1 & 0 & 0 \\ 0 & 0 & 0 \end{pmatrix}, \lambda_2 = \begin{pmatrix} 0 & -i & 0 \\ i & 0 & 0 \\ 0 & 0 & 0 \end{pmatrix}, \lambda_3 = \begin{pmatrix} 1 & 0 & 0 \\ 0 & -1 & 0 \\ 0 & 0 & 0 \end{pmatrix}, \lambda_4 = \begin{pmatrix} 0 & 0 & 1 \\ 0 & 0 & 0 \\ 1 & 0 & 0 \end{pmatrix}$$
$$\lambda_5 = \begin{pmatrix} 0 & 0 & -i \\ 0 & 0 & 0 \\ i & 0 & 0 \end{pmatrix}, \lambda_6 = \begin{pmatrix} 0 & 0 & 0 \\ 0 & 0 & 1 \\ 0 & 1 & 0 \end{pmatrix}, \lambda_7 = \begin{pmatrix} 0 & 0 & 0 \\ 0 & 0 & -i \\ 0 & i & 0 \end{pmatrix}, \lambda_8 = \frac{1}{\sqrt{3}} \begin{pmatrix} 1 & 0 & 0 \\ 0 & 1 & 0 \\ 0 & 0 & -2 \end{pmatrix}. \tag{1.60}$$

As for any physics theories which is only appropriate for a specific energy scale and are described by a certain set of parameters, the theory of QCD is dependent on the energy scale. The QCD theory is renormalizable in the sense that the set of parameters for a certain energy scale can be used to infer the set belonging to other scales. For QCD, the rule of inference for the coupling constant g is described by the renormalization group equation [4]:

$$\frac{d}{d\log(Q/M)}\bar{g} = \beta(\bar{g}), \tag{1.61}$$

where the initial condition is $\alpha_s(M) = \alpha_s = g^2(M)/4\pi$ at some certain scale M. The equation $\beta(\bar{g})$ gives us the information about how the coupling constant $\bar{g}$ varies with energy scale M and the momentum transfer scale Q. For QCD of $n_c = 3$ colors and n_f flavors, β function is evaluated by:

$$\beta(g) = -\frac{b_0}{(4\pi)^2} \text{ where } b_0 = 11 - \frac{2n_f}{n_c}. \tag{1.62}$$

From this, the dependence of the coupling constant $\alpha_s = g_s^2/4\pi$ can be evaluated as:

$$\alpha_s(Q^2) = \frac{12\pi}{(11n_c - 2f)\ln\left(|Q^2|/M^2\right)}, \tag{1.63}$$

Experimental results show that the range for M is from 100 to 500 MeV. From this dependence, we can see that at large seperation between quarks where the momentum transfer is small, the coupling constant becomes larger and prevents further seperation between them. This is the reason for quark confinement, which states that quarks cannot exist in color singlet states. In other words, when the distance of a quark to its host hadron is larger than the length of the theory, the strong force will pull and confine the quark back to its hadron.

1.6 Higgs Mechanism

In previous section, we have discussed the requirement of an invariance of Lagrangian under local phase transformation of $U(1)$ and $SU(3)$ symmetries, which explains the mass of photon and gluons being zero. However, this cannot be applied to the weak interaction because the masses of the weak interaction gauge bosons W and Z are non-zero. By manually adding masses for W and Z boson, the weak interaction will become unrenormalizable. In this section, we will discuss a method for introducing mass for gauge boson without breaking local phase invariance.

1.6.1 Spontaneous Symmetry Breaking

Mass of a particle as given in example (1.7) is said to be added manually by hand. The other way to generate mass for particle is via spontaneous symmetry breaking. Given the Lagrangian of a scalar field below:

$$\mathcal{L} = T + V = \frac{1}{2}(\partial_\mu \phi)^2 - \left(\frac{1}{2}\mu^2\phi^2 + \frac{\lambda}{4}\phi^4\right), \tag{1.64}$$

where $\lambda > 0$, which is symmetric under the reflection transformation $\phi \to -\phi$. The case of $\mu^2 > 0$ was examined to represent a scalar of mass μ with a 4-particle vertex with coupling λ. For the case where $\mu^2 < 0$, the particle's potential has local minima at:

$$\frac{\partial_V}{\partial \phi} = 0 \leftrightarrow \mu^2 + \lambda\phi^2 = 0 \leftrightarrow \phi = \pm v, \tag{1.65}$$

where $v = \sqrt{-\mu^2/\lambda}$. With no loss of generality, we can shift the variable to the bottom of the potential well at v with the following transformation:

$$\phi(x) = v + \eta(x). \tag{1.66}$$

The Lagrangian is now read:

$$\mathcal{L}' = \frac{1}{2}(\partial_\mu \eta)^2 - \lambda v^2\eta^2 - \lambda\eta^3 - \frac{1}{4}\lambda\eta^4 + \text{const.}. \tag{1.67}$$

It can be understood that $\mathcal{L}$ and $\mathcal{L}'$ are equivalent mathematically. However, $\mathcal{L}'$ is now containing a massive scalar of mass $m_\eta = \sqrt{2\lambda v^2} = \sqrt{-2\mu^2}$. What is the difference between $\mathcal{L}$ and $\mathcal{L}'$ that makes $\mathcal{L}'$ able to generate mass for its scalar field? The answer is that $\phi = 0$ is not a local minima in $\mathcal{L}$, which makes it unstable under perturbation of the field. When shifting the coordinate to the ground at local minima, we can stably do perturbation calculations.

Next, let us examine another example of spontaneous breaking of global gauge symmetry of Lagrangian that describes a complex scalar field $\phi = (\phi_1 + i\phi_2)/\sqrt{2}$:

$$\mathcal{L} = \partial_\mu \phi * \partial^\mu \phi - \mu(\phi * \phi) - \lambda(\phi * \phi)^2. \tag{1.68}$$

The Lagrangian is invariant under global phase transformation $\phi \to e^{i\alpha}\phi$, which is a $U(1)$ gauge symmetry. We can rewrite the Lagrangian as:

$$\mathcal{L} = \frac{1}{2}(\partial_\mu \phi_1)^2 + \frac{1}{2}(\partial_\mu \phi_2)^2 - \frac{\mu^2}{2}(\phi_1^2 + \phi_2^2) - \frac{\lambda}{4}(\phi_1^2 + \phi_2^2)^2, \tag{1.69}$$

Minima of the potential are now given by:

$$\phi_1^2 + \phi_2^2 = v^2, \text{ where } v^2 = -\frac{\mu^2}{\lambda}. \tag{1.70}$$

By selecting the ground to be at $(\phi_1, \phi_2) = (v, 0)$ and expand the Lagrangian around that point by having $\phi(x) = [v + \eta(x) + i\xi(x)]/\sqrt{2}$, we will come up with the Lagrangian:

$$\mathcal{L}' = \frac{1}{2}(\eta)^2 + \frac{1}{2}(\xi)^2 + \mu^2\eta^2 + C, \tag{1.71}$$

where C contains constants and term that are in cubic and quadratic of ξ and η. From this form, we can see that now our field η has acquired a mass given by $m_\eta = \sqrt{-2\mu^2}$. However, there is now a scalar field with no corresponding mass term ξ, which is called Goldstone - Nambu boson. From this, the next step is to find out a way to solve the problem of the existence of this massless boson.

1.6.2 Higgs Mechanism

As an extension to the previous part, let us discuss the spontaneous symmetry breaking of the local phase transformation of $U(1)$ symmetry. As we have mentioned earlier, the transformation is represented by:

$$\phi(x) \to e^{i\alpha(x)}\phi(x). \tag{1.72}$$

The gauge invariant Lagrangian is then:

$$\mathcal{L} = (\mathcal{D}_\mu \phi) * (\mathcal{D}^\mu \phi) - \mu^2\phi^2 - \lambda(\phi^2)^2 - \frac{1}{4}F_{\mu\nu}F^{\mu\nu}, \tag{1.73}$$

where $\mathcal{D}_\mu = \partial_\mu - ieA_\mu$ and A_μ transforms as $A_\mu \to A_\mu + \frac{1}{e}\partial_\mu A$. In the previous section, we have examined the case where $\mu^2 > 0$, which is just QED theory for charged scalar particle of mass μ. To generate mass spontaneously as we have done in the two examples earlier, let us assume that $\mu^2 < 0$. Again, the original symmetry will be broken by shifting the field to its true ground state with $\phi(x) = \frac{1}{\sqrt{2}}(v + \eta(x) + i\xi(x))$. The resulting Lagrangian is then:

$$\mathcal{L}' = \frac{1}{2}(\partial_\mu \xi)^2 + \frac{1}{2}(\partial_\mu \eta)^2 - v^2\lambda\mu^2 + \frac{1}{2}e^2v^2A_\mu A^\mu - evA_\mu\partial^\mu\xi ... \tag{1.74}$$

This form of Lagrangian indicates that we now have $m_\xi = 0, m_A = ev, m_\eta = \sqrt{2\lambda v^2}$. As observed earlier, we now have an unwanted massless Goldstone - Nambu boson ξ and massive gauge bosons η, A. However, there are some problems with this field translation. First, there is now a term $A_\mu \partial^\mu \xi$, which describes the transformation of a particle into another, which is not physical. Second, by giving mass to vector field A_μ, its degrees of freedom changes from 2 to 3, which cannot happen if all we did was just translating the coordinates of the fields. Therefore, we have to select an gauge transform that eliminates the appearance of unphysical particles. The appropriate choice is:

$$\begin{aligned} \phi \to& \frac{1}{\sqrt{2}}(v + h(x))e^{i\theta(x)/v} \\ A_\mu \to& A_\mu + \frac{1}{ev}\partial_\mu\theta, \end{aligned} \tag{1.75}$$

where h is real. With this choice of gauge transformation, the Lagrangian is written as:

$$\begin{aligned} \mathcal{L} =& \frac{1}{2}(\partial_\mu h)^2 - \lambda v^2 h^2 + \frac{1}{2}e^2v^2A_\mu^2 - \lambda v h^3 - \frac{1}{4}\lambda h^4 \\ &+ \frac{1}{2}e^2A_\mu^2 h^2 + ve^2A_\mu^2 h - \frac{1}{4}F_{\mu\nu}F^{\mu\nu}. \end{aligned} \tag{1.76}$$

What we have here in the new Lagrangian are the absence of the massless Goldstone - Nambu boson, and the existence of the massive gauge boson A_μ and massive scalar field h, which is called Higgs particle. The massless Goldstone-Nambu boson was transformed into the longitudinal polarization of the massive gauge boson A_μ to give it its mass. This whole process is called "Higgs mechanism".

Another example of Higgs mechanism is in the spontaneous symmetry breaking of local $SU(2)$ gauge symmetry. The Lagrangian of this theory is given by:

$$\mathcal{L} = (\partial_\mu \phi)^\dagger(\partial^\mu \phi) - \mu^2\phi^\dagger\phi - \lambda(\phi^\dagger\phi)^2, \tag{1.77}$$

where ϕ is a complex scalar field of $SU(2)$:

$$\phi = \frac{1}{\sqrt{2}} \begin{pmatrix} \phi_1 + i\phi_2 \\ \phi_3 + i\phi 4 \end{pmatrix}. \tag{1.78}$$

Under the local phase transformation:

$$\phi(x) \to \phi'(x) = e^{i\alpha(x).\tau(x)/2}\phi(x), \tag{1.79}$$

the Lagrangian is kept invariant by replacing the normal derivative with the covariant derivative $\mathcal{D}_\mu = \partial_\mu + ig\frac{\tau_a}{2}W_\mu^a$, with the three vector fields $W_\mu^a (a = 1, 2, 3)$ vary as:

$$W_\mu \to W_\mu - \frac{1}{g}\partial_\mu\alpha - \alpha \times W_\mu. \tag{1.80}$$

With such field transformation, the gauge invariant is then:

$$\mathcal{L} = (\mathcal{D}_\mu\phi)^\dagger(\mathcal{D}^\mu\phi) - \mu^2\phi^\dagger\phi - \lambda(\phi^\dagger\phi)^2 - \frac{1}{4}W^{\mu\nu}W_{\mu\nu}, \tag{1.81}$$

where $W_{\mu\nu} = \partial_\mu W_\nu - \partial_\nu W_\mu - gW_\mu \times W_\nu$. The cross-product of vector fields appear due to the non-Abelian property of the group as mentioned in the previous section. For $\mu^2 > 0$, the theory describes the four scalar fields interacting with three massless vector fields. The scenario we are interested in is when $\mu^2 < 0$, where the potential proportional to $\phi^\dagger\phi$ has minima locating on:

$$\phi^\dagger\phi = \frac{1}{2}(\phi_1^2 + \phi_2^2 + \phi_3^2 + \phi_4^2) = -\frac{\mu^2}{2\lambda}. \tag{1.82}$$

As usual, we will pick a particular minima and expands the field in vicinity to that position. The choice of minima is this case will be $\phi_1 = \phi_2 = \phi_4 = 0, \phi_3 = -\mu^2/2\lambda$. Our field is then expanded as:

$$\phi(x) = \frac{1}{\sqrt{2}} \begin{pmatrix} 0 \\ v + h(x) \end{pmatrix}. \tag{1.83}$$

From this, we can find the mass generated for the three massless gauge bosons. The mass terms for the gauge boson will then be embedded inside of the covariant derivative:

$$\begin{aligned} \left| ig\frac{1}{2}\tau.W_\mu\phi \right|^2 &= \frac{g^2}{8} \left| \begin{pmatrix} W_\mu^3 & W_\mu^1 - iW_\mu^2 \\ W_\mu^1 + iW_\mu^2 & W_\mu^3 \end{pmatrix} \begin{pmatrix} 0 \\ v \end{pmatrix} \right| \\ &= \frac{g^2v^2}{8}\left[(W_\mu^1)^2 + (W_\mu^2)^2 + (W_\mu^3)^2\right]. \end{aligned} \tag{1.84}$$

This tells us that the spontaneous symmetry breaking of $SU(2)$ under local phase transformation has generated a mass of $M = gv/2$ for the vector bosons. What we have after this spontaneous symmetry breaking are the three massive bosons W_μ and a scalar Higgs field h. The masses of the vector bosons come from the fact that massless Goldstone-Nambu bosons were "eaten" by the vector fields. This is one other example of Higgs mechanism.

It can be seen that Higgs mechanism has helped generating masses for vector bosons while preserving renormalizability of the theory, which cannot be achieved if we manually add masses for vector bosons by hand. For that reason, it is widely believed that gauge principles are responsible for generating structures of all interactions in the universe. In the next section, we will discuss how gauge principles are used to combine electromagnetic and weak interactions with three weak bosons being massive and photon being massless.

1.7 Electroweak Theory

The electroweak theory is the theory that unifies two out of four interactions in nature: the weak interaction and electromagnetic interaction. The initial idea of unifying the two interactions was proposed by Glashow, which had a flaw that the theory is not renormalizable since W boson masses had to be inserted manually by hand. The problem was then solved by Weinberg and Salam independently by proposing that the masses of the vector bosons will be generated by a process called Higgs mechanism.

As we have described in the previous section, Higgs mechansim has the ability to generate masses for gauge bosons while preserving renormalizability of the theory. Experimental data have confirmed that the weak and electromagnetic interactions are invariant under weak isospin $SU(2)_L$ and weak hypercharge $U(1)_Y$ transformation. In this section, we will discuss how the invariant Lagrangian of $SU(2)_L \times U(1)_Y$ was created.

By requiring the invariance of Lagrangian under local $U(1)$ gauge transformation, we come up with the interacting Lagrangian for fermions:

$$\mathcal{L} = \bar{\psi}(i\gamma^\mu \partial_\mu - m)\psi - eQ\bar{\psi}\gamma^\mu \psi A_\mu - \frac{1}{4}F_{\mu\nu}F^{\mu\nu}, \tag{1.85}$$

where Q is the charge of the fermion and the interaction term can be expressed as the coupling of electromagnetic current to the vector boson:

$$-eQ\bar{\psi}\gamma^\mu \psi A_\mu = -ej_\mu^{em} A^\mu. \tag{1.86}$$

To be able to describe the weak processes, we have to replace the electromagnetic interaction with the weak interaction between the fermions with coupling g and weak gauge bosons W_μ and vector boson B_μ with fermions carrying weak hypercharge with coupling $g'/2$. The interaction terms are then described by:

$$g\mathbf{J}_\mu.\mathbf{W}^\mu + \frac{g'}{2}j_\mu^Y B^\mu = \bar{\chi}_L\gamma_\mu \mathbf{T}.\mathbf{W}^\mu \chi_L + \frac{g'}{2}(\bar{\chi_L}\gamma_\mu Y \chi_L + \bar{\chi_R}\gamma_\mu Y \chi_R)B^\mu, \tag{1.87}$$

where $\mathbf{T}$ and Y are generators of $SU(2)_L$ and $U(1)_Y$ groups. In the expressions above, χ_L is the isospin doublet of the left-handed fermions and χ_R is the right-handed isosinglets. Some examples of these fields are those of the first generation where

$$\chi_L = \begin{pmatrix} \nu_e \\ e^- \end{pmatrix}_L, \quad \chi_R = e_R^- \tag{1.88}$$

for leptons and:

$$\chi_L = \begin{pmatrix} u \\ d \end{pmatrix}_L, \quad \chi_R = u_R, d_R \tag{1.89}$$

for quarks. The generators of $U(1)_{em}$, $SU(2)_L$ and $U(1)_Y$ are related by:

$$Q = T^3 + \frac{Y}{2}, \tag{1.90}$$

which means:

$$j_\mu^{em} = J_\mu^3 + \frac{1}{2}j_\mu^Y. \tag{1.91}$$

By having two physical fields A_μ and Z_μ being orthogonal combinations of B_μ and W_3 with mixing angle θ_W, one can have

$$\begin{aligned} gJ_\mu^3 W^3 + \frac{g'}{2}j_\mu^Y B_\mu = & \left(g\sin\theta_W J_\mu^3 + g'\cos\theta_W \frac{j_\mu^Y}{2}\right)A^\mu \\ & + \left(g\cos\theta_W J_\mu^3 - g'\sin\theta_W \frac{j_\mu^Y}{2}\right)Z^\mu. \end{aligned} \tag{1.92}$$

which must contain $ej_\mu^{em}A_\mu$. From there, we can easily find the relation between g, g' and e as:

$$e = g\sin\theta_W = g'\cos\theta_W. \tag{1.93}$$

At this point, we have came up with the electroweak Lagrangian that is invariant under $SU(2)_L \times U(1)_Y$ local phase transformation:

$$\begin{aligned}\mathcal{L} = \bar{\chi}_L\gamma^\mu &\left[i\partial_\mu - g\frac{1}{2}\tau.\mathbf{W}_\mu - g'\left(-\frac{1}{2}\right)B_\mu\right]\chi_L \\ &+ \bar{e}_R\gamma^\mu\left[i\partial_\mu - g'(-1)B_\mu\right]e_R - \frac{1}{4}W_{\mu\nu}W^{\mu\nu} - \frac{1}{4}B_{\mu\nu}B^{\mu\nu}.\end{aligned} \tag{1.94}$$

where $Y_L = -1$ and $Y_R = 2$. However, adding any mass term for the gauge bosons or the fermions will break the invariance. In order to generate masses for the gauge bosons as well as those of fermions, we have to invoke the Higgs mechanism as discussed in the previous section of the chapter. The result from this is that we will have massive $W^\pm$ and Z bosons while having the photon massless.

To do this, we need to introduce the scalar field ϕ_i and add its new $SU(2)\times U(1)$ gauge invariant Lagrangian to the old Lagrangian:

$$\mathcal{L}_\phi = \left|\left(i\partial_\mu - g\mathbf{T}.\mathbf{W}_\mu - g'\frac{Y}{2}B_\mu\right)\phi\right|^2 - V(\phi). \tag{1.95}$$

where ϕ belongs to the multiplets of $SU(2)\times U(1)$ to keep $\mathcal{L}_\phi$ invariant. The most economical choice was selected by Weinberg with $Y = 1$:

$$\phi = \begin{pmatrix}\phi^+ \\ \phi^0\end{pmatrix} = \frac{1}{\sqrt{2}}\begin{pmatrix}\phi_1 + i\phi_2 \\ \phi_3 + i\phi_4\end{pmatrix}. \tag{1.96}$$

The potential is as usual:

$$V(\phi) = \mu^2\phi^\dagger\phi + \lambda(\phi^\dagger\phi)^2 \tag{1.97}$$

with $\mu^2 < 0$ and $\lambda > 0$. The choice of vacuum expectation value is again:

$$\phi_0 = \frac{1}{\sqrt{2}}\begin{pmatrix}0 \\ v\end{pmatrix}. \tag{1.98}$$

This choice with $T = 1/2, T^3 = -1/2$ and $Y = 1$ will break both $SU(2)$ and $U(1)_Y$ symmetry. However, the $U(1)_{em}$ will remain unbroken as:

$$Q = T^3 + \frac{Y}{2} \rightarrow Q\phi_0 = 0\phi_0. \tag{1.99}$$

For this reason, the mass of photon will be zero while other bosons will acquire masses. The mass of other bosons can obtained by replacing ϕ with ϕ_0 to the Lagrangian $\mathcal{L}_\phi$. The term containing mass terms is:

$$\begin{aligned}
&\left|\left(-ig\frac{\tau}{2}.\mathbf{W}_\mu - i\frac{g'}{2}B_\mu\right)\phi\right|^2 \\
&= \frac{1}{8}\left|\begin{pmatrix} gW^3_\mu + g'B_\mu & g(W^1_\mu - iW^2_\mu) \\ g(W^1_\mu + iW^2_\mu) & gW^3_\mu + g'B_\mu \end{pmatrix}\begin{pmatrix} 0 \\ v \end{pmatrix}\right|^2 \\
&= \frac{1}{8}v^2g^2\left[(W^1_\mu)^2 + (W^2_\mu)^2\right] + \frac{1}{8}v^2(g'B_\mu - gW^3_\mu)(g'B^\mu - gW^{3\mu}) \\
&= \left(\frac{1}{2}gv\right)^2 W^+_\mu W^{\mu -} + \frac{1}{8}v^2(W^3_\mu, B_\mu)\begin{pmatrix} g^2 & -gg' \\ -gg' & g'^2 \end{pmatrix}\begin{pmatrix} W^{3\mu} \\ B^\mu \end{pmatrix},
\end{aligned} \tag{1.100}$$

from which, we can obtain mass for W bosons:

$$M_W = \frac{1}{2}gv. \tag{1.101}$$

The second term in the equation (1.100) can be expressed as:

$$\frac{1}{2}v^2\left[g^2(W^3_\mu)^2 - 2gg'W^3_\mu B^\mu + g'^2B^2_\mu\right] = \frac{1}{8}v^2\left(gW^3_\mu - g'B_\mu\right)^2 + 0\left(g'W^3_\mu + gB_\mu\right)^2. \tag{1.102}$$

By identifying this result with the mass term for Z_μ and A_μ bosons:

$$\frac{1}{2}M^2_Z Z^2_\mu + \frac{1}{2}M^2_A A^2_\mu, \tag{1.103}$$

one can get state of Z_μ and A_μ as mixed states of Z^μ_3 and B^μ as:

$$\begin{aligned}
A_\mu &= \frac{g'W^3_\mu + gB_\mu}{\sqrt{g^2 + g'^2}} \quad \text{with } M_A = 0, \\
Z_\mu &= \frac{gW^3_\mu - g'B_\mu}{\sqrt{g^2 + g'^2}} \quad \text{with } M_Z = \frac{v}{2}\sqrt{g^2 + g'^2}.
\end{aligned} \tag{1.104}$$

From equation (1.93), we can get $\tan\theta_W = g'/g$, which can be used to rewrite (1.104) as:

$$\begin{aligned}
A_\mu &= \cos\theta_W B_\mu + \sin\theta_W W^3_\mu, \\
Z_\mu &= -\sin\theta_W B_\mu + \cos\theta_W W^3_\mu.
\end{aligned} \tag{1.105}$$

From equation (1.101) and (1.104), we can find that $M_W/M_Z = \cos\theta_W$. It is worth mentioning that the same Higgs doublet used to generate masses for the bosons can also be used generate masses for the fermions [4]. However, their actual masses cannot be predicted as in cases of W and Z bosons.

Chapter 2

Introduction to Cosmology

2.1 Observations

Up to present where many great discoveries in cosmology have been made, we are still lacking a good data source for scientists to work on. The cosmological observables we have so far include the expansion of the Universe, the Hubble constant H_0; the deceleration of the Universe q_0, the age of the universe t_0; the density of the universe ρ_0; the cosmic microwave background radiation; the abundance of light elements which include D, ^{3}He, ^{4}He, ^{7}Li; the baryon number in the Universe; and the galaxies and larger structures' distribution in the Universe where the subscripts 0 indicates the present values. In this section, we will discuss the physical meanings of these observables.

- The expansion rate:

  The expansion of the Universe has been observed by the fact that many nearby galaxies are red shifting with typical red shift value z in the range of 0.94 to 4.7. For an astronomical object of luminosity L, its luminosity distance is given by $d_L = (L/4\pi F)^{1/2}$. The red shift for such object is then given by:

  $$z = H_0 d_L - \frac{1}{2}(1 - q_0)^2 + ... \tag{2.1}$$

  The linear relationship between the red shift and the liminosity distance has been observed in [37]. However, the value of the Hubble constant can only be extracted from these observations with a large uncertainty. Its current value is given by [50]:

$$H_0 = 100h \text{ km s}^{-1}\text{Mpc}^{-1} = 74.03 \pm 1.42 \text{ km s}^{-1}\text{Mpc}^{-1}, \tag{2.2}$$

where the variable h shows the fact that the precise measurement of the Hubble constant is an ongoing effort. TheThe Hubble time or Hubble distance is defined as the inverse of Hubble constant:

$$H_0^{-1} = 9.78h^{-1} \times 10^9 yr = 9.25h^{-1} \times 10^{27} cm. \tag{2.3}$$

- The age of the Universe:

  The age of the Universe is a very important test for any cosmological model. It can be calculated in many different ways, which yield a consistent range from 10 to 20 Gyr. By estimating the age of the Universe by Hubble time, one can get a range of 9.8 to 24.5 Gyr. The other way to determine age of the Universe is to compare Hertzsprung-Russell diagram from ages of the oldest globular clusters. Most estimates by this method give the age of the Universe in the range of 10 to 20 Gyr. One other method is to use radioactive elements like ^{232}Th, ^{235}U, ^{238}U, ^{87}Rb, ^{187}Re to date the Universe and other astronomical objects in it. For example, the use of ^{235}U and ^{238}U estimates the age of the Universe to be about 6.6 Gyr. A newer method conducted by Winget, et al is to use the cooling of the white dwarf stars to determine the age of the Galaxy. Based on the observations of oldest white dwarfs and their white dwarf model, the age of the Universe is estimated to be 13.80 ± 0.02 Gyr [8].

- Cosmic microwave background radiation (CMBR):

  The fact that the CMBR fluctuation across the Universe is extrememly small ($\Delta T/T \sim 10^{-4}$) indicates that the Universe started from a hot Big Bang. The wavelength of the CMBR ranging from 70 cm to 0.1 cm corresponds to the black body radiation of temperature 2.75 ± 0.01 K and the present number of photon density of 422cm^{-3}. The density fluctuation required to initiate structure formation can be used to predict temperature fluctuation in the CMBR. Therefore, the anisotropies of the CMBR can provide a test for theories of how how large-scale structures are formed.

- Light-element abundances:

  Shortly after Big Bang, nucleonsysthesis starts to take place, which results in large amounts of many light elements like D (with $log_{10}(D/H) = -4.5940 \pm 0.0056$ [51]), ^{3}He (with $n_{^3He}/n_H \sim (1.1 \pm 0.2) \times 10^{-5}$), ^{4}He (with mass fraction $Y \sim 0.24709 \pm 0.00017$[52]) and ^{7}Li (with $n_{Li}/n_H \sim 10^{-10}$).

  By comparing the predicted light-element abundance with these observations, we can have a test for the standard cosmology. The primordial nucleosynthesis also provides precise estimates of baryon density in the Universe as well as important constraints on the existence of light hypothetical particles.

- Dark matter in the Universe:

  The existence of Dark Matter (DM) is widely accepted to explain the discrepancy between the observations of rotational velocity and what is expected from dynamical mechanics. Let us assume that the galaxy number density in the Universe is n and each galaxy has an average mass M, the mass density of the Universe will then be:

  $$\langle \rho \rangle = nM. \tag{2.4}$$

  To measure the mass of a galaxy dynamically, one has to find the velocity of objects orbiting that galaxy at different distances r. Following Kepler's 3^{rd} law:

  $$GM(r) = v^2 r, \tag{2.5}$$

  where $M(r)$ is the mass enclosed in the distance r from the center of the galaxy. By using this method, we can find the ratio of luminous mass or visible mass density ρ to that of the critical density ρ_C, which will be explained in later section, is about:

  $$\Omega_{LUM} = \frac{\rho_{LUM}}{\rho_C} \leq 0.01, \tag{2.6}$$

  By applying the same technique for objects that are much further away from the center of a galaxy where light corresponding to luminous matter ceases, $M(r)$ is not a constant as expected but rather increases with r. The rotational velocity is not proportional to $r^{-1/2}$ but stays constant with distance r, which requires that the mass $M(r) \sim r$. The mass that is accountable for this

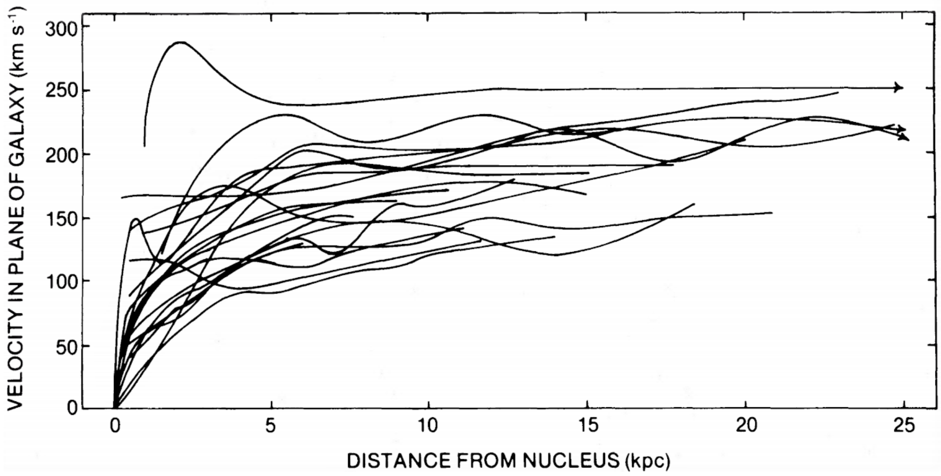

Figure 2.1: Rotational curves of 21 Sc galaxies [9].

unexpected velocity behavior has no detectable radiation and is considered "dark". The rotational curves of 21 Sc galaxies can bee seen in Fig. (2.1).

The mass accounted for the this rotational velocity distribution can be up to 10 times the mass of luminous matter:

$$\Omega_{DM} \geq 0.1 \simeq 10\Omega_{LUM}, \tag{2.7}$$

indicating that DM is actually dominating the Universe. The average mass of galaxy in a cluster can also be found using virial theory. Suppose that the cluster has mass M, the velocity of the galaxy is then:

$$GM = \frac{2\left\langle v^2 \right\rangle}{\left\langle r^{-1} \right\rangle}, \tag{2.8}$$

giving the estimate of $\Omega \sim 0.1$ to 0.3, which is consistent with the previous method and again confirming that luminous matter cannot account for the majority of the mass of the galaxy. We can safely say that the total amount of dark matter and luminous matter can be:

$$\Omega_{matter} = 0.2 \pm 0.1. \tag{2.9}$$

These observations give us the great insight into how the Universe operates. As more and more data are collected through many experiments, we will have more chances to look further to the history of the Universe, to understand what makes up the Universe and to confirm the predictions that many scientists are contributing to the understanding of Cosmology.

2.2 The Robertson - Walker Metric

2.2.1 Open, closed, and flat spatial models

For a region in space that is as large as our present Hubble length, our Universe can be considered to be homogeneous and isotropic even though there is no such guarantee in a bigger region. That smooth region is considered to be homogeneous and isotropic for a time duration comparable to the Hubble time, which was estimated to be at least 10 Gyr in the previous section. The metric for such a region in space is described by the Robertson - Walker (RW) metric [10], which is given by:

$$ds^2 = dt^2 + R^2(t)\left[\frac{dr^2}{1-kr^2} + r^2 d\theta^2 + r^2 + \sin^2\theta d\phi^2\right], \tag{2.10}$$

where the set of t, r, θ, ϕ is space-time coordinates and $R(t)$ is the cosmic scale factor. The constant k can be $+1, -1, 0$ corresponding to the positve, negative or zero spatial curvature, respectively. The time component in the metric is the proper time, which means it is measured by an observer that is at rest in that frame.

The spatial part of the metric is:

$$\vec{dl}^2 = h_{ij}dx^i dx^j, h_{ij} = -g_{ij}, \tag{2.11}$$

where $i, j = 1, 2, 3$. Some important quantities of the metric are defined as:

$$\begin{aligned} \text{Riemann tensor} \quad {}^3R_{ijkl} &= \frac{k}{R^2(t)}(h_{ik}h_{jl} - h_{il}h_{kj}), \\ \text{Ricci tensor} \quad {}^3R_{ij} &= \frac{2k}{R^2(t)}h_{ij}, \\ \text{Ricci scalar} \quad {}^3\mathcal{R} &= \frac{6k}{R^2(t)}. \end{aligned} \tag{2.12}$$

The construction of the RW metric can be explained by the method of embedding a two-sphere (two-dimensional curved space) in a three-dimensional Cartesian space. For example, consider a two-sphere in a three dimensional Cartesian space x_1, x_2, x_3 with its radius given by:

$$R^2 = x_1^2 + x_2^2 + x_3^2 \rightarrow x_3^2 = R^2 - x_1^2 - x_2^2, \tag{2.13}$$

where x_3 is the fictitious spatial component as it would not be available in two dimensional space. An element of length is calculated by:

$$\vec{dl}^2 = dx_1^2 + dx_2^2 + dx_3^2 = dx_1^2 + dx_2^2 + \frac{(x_1dx_1 + x_2dx_2)}{R^2 - x_1^2 - x_2^2}. \tag{2.14}$$

Now, we can replace the coordinate x_1 and x_2 by r' and θ:

$$x_1 = r'\cos\theta, \quad x_2 = r'\sin\theta, \tag{2.15}$$

which leads to:

$$\vec{dl}^2 = \frac{R^2 dr'^2}{R^2 - r'^2} + r'^2 d\theta^2 = R^2\left[\frac{dr^2}{1-r^2} + r^2 d\theta^2\right], \tag{2.16}$$

where $r = r'/R$. This is the spatial part of the RW metric with $k = 1$ with R being the radius of the sphere.

We can also use the polar coordinates to describe the two-sphere with:

$$x_1 = R\sin\theta\cos\phi, \quad x_2 = R\sin\theta\sin\phi, \quad x_3 = R\cos\theta, \tag{2.17}$$

giving the length element as:

$$\vec{dl}^2 = R^2(d\theta^2 + \sin^2\theta d\phi^2), \tag{2.18}$$

from which, sphere's volume can be calculated to give $V = 4\pi R^2$. It must be noted that as the Universe is assumed to be homogeneous and isotropic, the scale factor R can only be a function of time. As the Universe expands, the coordinates r and θ are unchanged. However, the distance between two comoving points in the space will be scaled by factor of $R(t)$.

To get the equivalent explanation for negative curvature or with zero curvature, one has to replace $R \to iR$ or $R \to \infty$, respectively. However, for the zero curvature case, the scale factor is no longer related to the physical distance between two comoving points. It only describes the fact that the spatial distance between any two points scales with the expansion or contraction of the Universe.

To generalize this approach to three spatial dimensions, one has to embed a three-sphere into a four dimensional space with the fourth dimension being fictitious. The radius and a length element are calculated by:

$$\begin{aligned} R^2 &= x_1^2 + x_2^2 + x_3^2 + x_4^2 \\ \vec{dl}^2 &= dx_1^2 + dx_2^2 + dx_3^2 + dx_4^2. \end{aligned} \tag{2.19}$$

By eliminating the forth dimension, we get:

$$\vec{dl}^2 = dx_1^2 + dx_2^2 + dx_3^2 + \frac{(x_1 dx_1 + x_2 dx_2 + x_3 dx_3)^2}{R^2 - x_1^2 - x_2^2 - x_3^2}. \tag{2.20}$$

By expressing $x_1 = r' \sin\theta \cos\phi, x_2 = r' \sin\theta \sin\phi, x_3 = r' \cos\theta, r = r'/R$, we come up with the spatial component of the RW metric with $k = 1$. By expressing the three-sphere using 3 angular coordinates: $x_1 = R \sin\chi \sin\theta \cos\phi$, $x_2 = R \sin\chi \sin\theta \sin\chi$, $x_3 = R \sin\chi \cos\theta$, $x_4 = R \cos\chi$ as:

$$\vec{dl}^2 = R^2 \left[d\chi^2 + \sin^2\chi (d\theta^2 + \sin^2\theta d\phi^2) \right], \tag{2.21}$$

which leads to the volumes of the-three sphere as $V = 2\pi^2 R^3$. The approach for negative and zero curvature models are similar to what was explained in two dimensions.

We can also replace the time component of the metric dt^2 by "conformal time", which is $d\eta = dt/R(t)$:

$$\vec{dl}^2 = R^2(t) \left[d\eta^2 - \frac{dr^2}{1 - kr^2} - r^2 d\theta^2 - r^2 \sin^2\theta d\phi^2 \right], \tag{2.22}$$

which is conformal to the Minkowski space for flat model of $k = 0$. In addition, it can also be proved that all the metric models are locally conformal to the Minkowski space, which makes it a reasonable choice for local coordinates.

2.2.2 Particle Kinematics

Having defined the Robertson - Walker metrics, we can now discuss how it can be applied to describe the kinetics of both massless and massive particles in the RW metric. For a massless particle, for example a photon, assuming that a light source emits photon at time $t = 0$ at $r = r_H$, it will hit the observer at position $r_0 = 0$ at time t. We do not need to pay attention to other coordinates θ and ϕ as the RW metric was assumed to be a homogeneous and isotropic space. The light will follow the geodesics with $ds^2 = 0$. From the RW metric, we can obtain:

$$\int_0^t \frac{dt'}{R(t')} = \int_0^{r_H} \frac{dr}{\sqrt{1 - kr^2}}. \tag{2.23}$$

The proper distance of r_H at the time we catch the photon t is:

$$d_H(t) = R(t) \int_0^{r_H} \sqrt{g_{rr}} dr = R(t) \int_0^{r_H} \frac{dr}{\sqrt{1 - kr^2}} = R(t) \int_0^t \frac{dt'}{R(t')}, \tag{2.24}$$

meaning that the proper distance d_H could be infinity depending how $R(t)$ behaves around $t = 0$. From the form of metric as written in equation (2.22), we can have:

$$d_H(t) = R(t)[\eta(t) - \eta(t = 0)]. \tag{2.25}$$

For a massive particle, the condition $ds^2 = 0$ is no longer correct. The geodesics equation is now following:

$$\frac{du^\mu}{d\lambda} + \Gamma^\mu_{\nu\alpha} u^\nu \frac{dx^\alpha}{d\lambda} = 0, \tag{2.26}$$

where $u^\mu = dx^\mu/ds$ and $\Gamma^\mu_{\nu\alpha}$ is defined as:

$$\Gamma^\mu_{\alpha\nu} = \frac{1}{2} g^{\mu\beta}(g_{\beta\alpha,\nu} + g_{\beta\mu,\alpha} - g_{\alpha\nu,\beta}), \quad g_{\alpha\beta,\mu} = \frac{\partial g_{\alpha\beta}}{\partial x^\mu}. \tag{2.27}$$

Choose the affine parameter λ to be the proper length, the $\mu = 0$ component of the geodesics equation is:

$$\begin{aligned} \frac{du^0}{ds} + \Gamma^0_{\nu\alpha} u^\nu u^\alpha = 0 \rightarrow \frac{du^0}{ds} + \Gamma^0_{ij} u^i u^j = 0 \\ \rightarrow \frac{du^0}{ds} + \frac{\dot{R}}{R} |\vec{u}|^2 = 0 \end{aligned} \tag{2.28}$$

As $u_0^2 - |\vec{u}|^2 = 1 \rightarrow u_0 du_0 = |\vec{u}| d|\vec{u}|$ and $u^0 = dt/ds$, the equation above leads to:

$$\frac{|\dot{\vec{u}}|}{|\vec{u}|} = -\frac{\dot{R}}{R} \rightarrow |\vec{u}| \sim R^{-1}. \tag{2.29}$$

This tells us that the momentum $p_\mu = m u_\mu$ of a freely moving particle in space scale as R^{-1}. Note that the term ds in the equation (2.28) disappears eventually, meaning that the argument above is true for both massive and massless particles.

2.2.3 Kinematics of Robertson - Walker Metric

In the previous section, we have shown that the momentum of a massive or massless particle is proportional to the R^{-1} as the Universe expands. This means that a photon of wavelength l_1 at time t_1 will has its wavelength changed to l_0 at time t_0 with l_0 given by:

$$\frac{\lambda_1}{\lambda_0} = \frac{R(t_1)}{R(t_0)}. \tag{2.30}$$

This relation means that the red shift of the photon is caused by the expansion of the Universe. The red shift z is defined in terms of the ratio of the detected wavelength to the wavelength when it was emitted:

$$1 + z = \frac{\lambda_0}{\lambda_1} = \frac{R(t_0)}{R(t_1)}. \tag{2.31}$$

From the RW metric, we can come up with the Hubble's law, which describes the relationship between the distance from us to a galaxy and its red shift. Consider a galaxy of luminosity $\mathcal{L}$ and measured flux $\mathcal{F}$. The luminosity distance of that galaxy is defined as:

$$d_L = \frac{\mathcal{L}}{4\pi\mathcal{F}}, \tag{2.32}$$

However, to calculate d_L, we have to consider the fact that the Universe expands. Suppose that the light is emitted at r_1 at time t_1 and is detected at locatioin $r_0 = 0$ at time t_0. At t_1, the distance between the two locations is $R(t_1)(r_1 - r_0) = R(t_1)r_1$. However, at the detected time, we have to replace $R(t_1)$ by $R(t_0)$ and add the red shift, which means that the physical distance is now:

$$d_L = R(t_0)r_1(1+z). \tag{2.33}$$

By using the Taylor's expansion on $R(t)/R(t_0)$, we have:

$$\frac{R(t)}{R(t_0)} = 1 + H_0(t-t_0) - \frac{1}{2}q_0H_0^2(t-t_0)^2 + \mathcal{O}\left((t-t_0)^3\right), \tag{2.34}$$

where

$$H_0 = R(\dot{t_0})/R(t_0), \quad q_0 = -\frac{\ddot{R}}{RH_0^2}. \tag{2.35}$$

H_0 is called Hubble rate of expansion and q_0 is called rate of deceleration. The subscript "0" indicates these values are at present. As $1 + z = R(t_0)/R(t)$, we get:

$$\begin{aligned} z &= H_0(t_0 - t) + \left(1 + \frac{1}{2}\right) H_0^2(t_0-t)^2 + ... \\ \rightarrow (t - t_0) &= H_0^{-1}\left[z - \left(1 + \frac{q_0}{2}\right) z^2 + ...\right] \end{aligned} \tag{2.36}$$

To obtain the expression for r_1 in term of z, we have to use the fact that the geodesic that photons follow is:

$$ds^2 = 0 \rightarrow \int_{t_1}^{t_0} \frac{dt}{R(t)} = \int_0^{r_1} \frac{dr}{\sqrt{1-kr^2}} \approx r_1 \text{ for small } r_1. \tag{2.37}$$

By using the Taylor's expansion above:

$$\begin{aligned} r_1 &= \int_{t_1}^{t_0} \frac{dt}{R(t)} = \int_{t_1}^{t_0} \frac{dt}{R(t_0)} \left(1 - H_0(t-t_0) + \frac{1}{2}q_0H_0^2(t-t_0)^2\right) \\ r_1 &= \frac{1}{R(t_0)}\left[(t_0 - t_1) + \frac{1}{2}H_0(t_0-t_1)^2 + ..\right] \\ r_1 &= \frac{1}{R(t_0)H_0}\left[z - \frac{1}{2}(1+q_0)z^2 + ...\right]. \end{aligned} \tag{2.38}$$

From this, we can recover the Hubble's law:

$$\begin{aligned} d_L &= R(t_0)r_1(1+z) = \frac{1}{H_0}\left[z + \frac{1}{2}(1-q_0)z^2 + ...\right] \\ \rightarrow H_0 d_L &= z + \frac{1}{2}(1-q_0)z^2 + ... \end{aligned} \tag{2.39}$$

In principle, one could use the Hubble diagram (d_L vs z) to find q_0. However, this approach requires the existence of a star or galaxy of known luminosity that can be detectable at cosmological distance and with little variance. In addition to this model dependent relationship, there are some other relationships that are model independent. The simplest one is the measured surface brightness, which is calculated by the energy flux per solid angle. These model independent relationships help testing whether an astronomical or observational problem affects model-dependent relationships.

2.3 The Expanding Universe

In the previous section, we have discussed how kinematics of the Universe depends on the scale factor $R(t)$. To really have a picture of how the scale factor R is governed, we have to use the help of Einstein equations [11]:

$$R_{\mu\nu} - \frac{1}{2}\mathcal{R}g_{\mu\nu} = 8\pi G T_{\mu\nu} + \Lambda g_{\mu\nu}, \tag{2.40}$$

where $G_{\mu\nu}$ is the Einstein tensor, $T_{\mu\nu}$ is the stress-energy tensor for all matter, radiation and Λ is the cosmological constant. The simplest form of the stress-energy tensor is that of the perfect fluid that is described by the energy density $\rho(t)$ and the pressure $p(t)$. Perfect fluid is the fluid in such a frame that pressure is the same in all direction and is perpendicular to the surface on which it acts. On perfect fluid, there is no heat conduction and no viscosity. The form of the stress energy tensor $T^{\mu\nu}$ for perfect fluid is:

$$T_\mu^\nu = \begin{pmatrix} \rho & 0 & 0 & 0 \\ 0 & -p & 0 & 0 \\ 0 & 0 & -p & 0 \\ 0 & 0 & 0 & -p \end{pmatrix} \tag{2.41}$$

The conservation of energy-momentum is expressed as:

$$\frac{\partial t^{\mu\nu}}{\partial x^\nu} \equiv T^{\mu\nu}_{;\nu} = 0, \tag{2.42}$$

which can be used to derive the 1st law of thermodynamics in the curved space:

$$d(\rho R^2) = -pd^3(R^3), \tag{2.43}$$

or equivalently:

$$d\left[R^3(\rho+p)\right] = R^3 dp. \tag{2.44}$$

The physical meaning of the conservation of energy-momentum described by the equation above can be explained that the change in energy in a comoving volume element $d(\rho R^3)$ is equal to the negative of the pressure times the change in volumes $-pd^3R$. With the equation of state given by $p = w\rho$, the energy density will depend on the scale factor as:

$$\rho \sim R^{-3(1+w)}. \tag{2.45}$$

For a radiation-dominated universe whose equation of state is $p = \rho/3$, the density energy evolves with scale factor as $\rho \sim R^{-4}$. For matter-dominated universe, we have $p = 0$, leading to $\rho \sim R^{-3}$. It should be emphasized that describing the stress - energy tensor with the equation of state $p = w\rho$ is actually a quite good approximation for the stress - energy tensor in RW metric, which is also a good approximation to the space-time in our Hubble volume.

From the Einstein equation, one can find the evolution of the scale factor R. Starting from the RW metric, we have:

$$\begin{aligned} R_{00} &= -3\frac{\ddot{R}}{R}, \\ R_{ij} &= -\left[\frac{\ddot{R}}{R} + 2\frac{\dot{R}^2}{R^2} + \frac{2k}{R^2}\right] g_{ij}, \\ \mathcal{R} &= -6\left[\frac{\ddot{R}}{R} + \frac{\dot{R}^2}{R^2} + \frac{k}{R^2}\right]. \end{aligned} \tag{2.46}$$

where $R_{\mu\nu}$ is the Ricci tensor and $\mathcal{R}$ is the Ricci scalar as we have shown in the previous section. From this, the 0 - 0 component of the Einstein equation, which is also known as the Friedmann equation, is given by:

$$\frac{\dot{R}^2}{R^2} + \frac{k}{R^2} = \frac{8\pi G}{3}\rho, \tag{2.47}$$

and the i - i components are expressed as:

$$2\frac{\ddot{R}}{R} + \frac{\dot{R}^2}{R^2} + \frac{k}{R^2} = -8\pi G p. \tag{2.48}$$

By subtracting the two equations above side by side, we get:

$$\frac{\ddot{R}}{R} = -\frac{4\pi G}{3}(\rho + 3p). \tag{2.49}$$

As the Universe is expanding, we have $\dot{R} > 0$. If the term $\rho + 3p$ has always been positive, it would be an indication that there was a time when $R = 0$, which is usually referred to as the Big Bang.

The Hubble rate, which indicates the rate of expansion of the Universe, is calculated as $H = \dot{R}/R$ and can be inferred from the Friedmann equation:

$$\frac{k}{H^2 R^2} = \frac{\rho}{2H^2/8\pi G} - 1 \equiv \Omega - 1 = \frac{\rho}{\rho_C} - 1, \tag{2.50}$$

where ρ_C is the critical density: $\rho_C = 3H^2/8\pi G$. From this, we can see that there is a relation between the sign of k and the value of Ω: if $k = 1$ (for closed universe), $\Omega > 1$; if $k = 0$ (for flat universe), $\Omega = 1$; if $k = -1$ (for open universe), $\Omega < 1$.

It must be emphasized that the critical density ρ_C is not a constant but varies as the Universe expands. At early times of the Universe, the curvature term k/H^2R^2 is close to 0, meaning that $\rho \sim 1 \to H^2 \sim \rho$. From equation (2.45), the expansion rate varies as $H^2 \sim R^{-3}$ for a matter-dominated Universe and $H^2 \sim R^{-4}$ for a radiation-dominated Universe.

At the present time, the quantity $|\Omega - 1| \approx 1$ and the Universe is matter dominated:

$$|\Omega - 1| = |\Omega_0 - 1| \frac{H_0^2 R_0^2}{H^2 R} = \frac{R}{R_0} = \frac{1}{1+z} \tag{2.51}$$

Tracing back to the time before matter-radiation equilibrium, the Universe was radiation-dominated:

$$|\Omega - 1| = |\Omega_{EQ} - 1| \frac{H_0^2 R_0^2}{H^2 R} = |\Omega_{EQ} - 1| \frac{R^2}{R_{EQ}^2} = \frac{R_{EQ}}{R_0} \frac{R^2}{R_{EQ}^2} \approx 10^4 (1+z)^{-2}, \tag{2.52}$$

which tells us that the radiation dominated early Universe has an energy density that is very close to the critical density.

To get an idea of how the scale factor varies with time, one has to integrate the Friedmann equations:

$$\begin{aligned} \left(\frac{\dot{R}}{R_0}\right)^2 + \frac{k}{R_0^2} &= \frac{8\pi G}{3} \rho_0 \frac{R_0}{R} \qquad (MD), \\ \left(\frac{\dot{R}}{R_0}\right)^2 + \frac{k}{R_0^2} &= \frac{8\pi G}{3} \rho_0 \frac{R_0^2}{R^2} \qquad (RD). \end{aligned} \tag{2.53}$$

By utilizing equation (2.50), one can integrate the equations above to find the variation of the scale factor R as a function of time as:

$$R \sim t^{2/3(1+w)}, \tag{2.54}$$

with $w = 1/3$ for a radiation-dominated Universe and $w = 0$ for a matter-dominated Universe.

2.4 Equilibrium Thermodynamics

In cosmology, thermal equilibrium of a species refers to the state for which interaction rate among that species is larger than the expansion rate of the Universe. If that condition is maintained, the number density, energy density and pressure are given by:

$$\begin{aligned} n &= \frac{g}{(2\pi)^3}\int f(\vec{p})d^3p, \\ \rho &= \frac{g}{(2\pi)^3}\int E(\vec{p})f(\vec{p})d^3p, \\ p &= \frac{g}{(2\pi)^3}\int \frac{|\vec{p}|^2}{3E}f(\vec{p})d^3p. \end{aligned} \tag{2.55}$$

where the bosons and fermions follow Bose - Einsteins and Fermi - Dirac distribution respectively:

$$f(\vec{p}) = \frac{1}{e^{\frac{E-\mu}{T}} \pm 1}, \tag{2.56}$$

where "+" is for Fermi - Dirac distribution and "−" is for Bose - Eistein distribution. μ is the chemical potential of particle. From this, we can come up with some special cases as follows: [10]:

- For the relativistic limit ($T \gg m$), $T \gg \mu$:

$$\begin{aligned} \rho &= \frac{\pi^2}{30}gT^4 \text{ (BOSE) } ; \frac{7}{8}\frac{\pi^2}{30}gT^4 \text{ (FERMI)}, \\ n &= \frac{\zeta(3)}{\pi^2}gT^3 \text{ (BOSE) } ; \frac{3}{4}\frac{\zeta(3)}{\pi^2}gT^3 \text{ (FERMI) }, \\ p &= \frac{\rho}{3}. \end{aligned} \tag{2.57}$$

- For degenerate fermions ($\mu \gg T \gg m$):

$$\begin{aligned} \rho &= \frac{1}{8\pi^2}g\mu^4, \\ n &= \frac{1}{6\pi^2}g\mu^3, \\ p &= \frac{1}{24\mu^2}g\mu^3. \end{aligned} \tag{2.58}$$

- For relativistic bosons or fermions with $\mu < 0$:

$$\begin{aligned} n &= \exp(\mu/T)\frac{g}{\pi^2}T^3, \\ \rho &= \exp(\mu/T)\frac{3g}{\pi^2}T^4, \\ p &= \exp(\mu/T)\frac{g}{\pi^2}T^4. \end{aligned} \tag{2.59}$$

- For the nonrelativistic limit ($m \gg T$):

$$\begin{aligned} n &= g\left(\frac{mT}{2\pi}\right)^{3/2}\exp\left[-(m-\mu)/T\right], \\ \rho &= mn, \\ p &= \frac{\rho}{3}. \end{aligned} \tag{2.60}$$

One important quantity in Cosmology is the difference between the number density of fermions over corresponding antifermions:

$$\begin{aligned} \Delta n = n_+ - n_- &= n(\mu) - n(-\mu) = \\ &= \frac{gT^3}{6\pi^2}\left[\pi^2\left(\frac{\mu}{T}\right) + \left(\frac{\mu}{T}\right)^3\right] \quad (T \gg m) \\ &= 2g\left(\frac{mT}{2\pi}\right)^{3/2}\sinh\left(\mu/T\right)\exp(-m/T) \quad (T \ll m). \end{aligned} \tag{2.61}$$

As we can see, the energy and momentum of all the species are dominated by all that are in relativistic limit. Therefore, we can safely approximate the energy and momentum density by those of the relativistic particles:

$$\begin{aligned} \rho_R &= \frac{\pi^2}{30}g_\star T^4 \\ p_R &= \frac{\rho_R}{3}. \end{aligned} \tag{2.62}$$

The effective degrees of freedom $g_\star$ in the expression above is calculated in such a way that only particles that are relativistic at temperature T are taken into account:

$$g_\star = \sum_{\text{bosons}} g_i\left(\frac{T_i}{T}\right)^4 + \frac{7}{8}\sum_{\text{fermions}} g_i\left(\frac{T_i}{T}\right)^4. \tag{2.63}$$

For $T \ll$ MeV, $g_\star = 3.36$ as only photons and neutrinos are relativistic. For 1 MeV $< T <$ 100 MeV, $g_\star = 10.75$ as we now have electrons and positrons added to the list of relativistic particles. For $T >$ 100 GeV, $g_\star = 106.75$ as all particles in the SM are relativistic.

Some important and useful relations for radiation-dominated epochs are:

$$\begin{aligned} R(t) &\sim t^{1/2} \\ H &= 1.66 g_\star^{1/2} \frac{T^2}{m_{Pl}} \\ t &= 0.301 g_\star^{-1/2} \frac{m_{Pl}}{T^2}. \end{aligned} \tag{2.64}$$

As we have mentioned in the beginning of the section, the local thermal equilibrium will be maintained as long as the interaction rate is larger than the expansion rate of the Universe. If the condition is satisfied, the second law of thermal dynamics can be applied to the comoving volume:

$$TdS = d(\rho V) + pdV = d[(\rho + p)V] - Vdp. \tag{2.65}$$

Combining this with the first law of thermal dynamics:

$$d[(\rho + p)V] = Vdp, \tag{2.66}$$

it can be shown that the entropy per comoving volumn is conserved:

$$ds = 0 \text{ where entropy } s = \frac{\rho + p}{T}. \tag{2.67}$$

As relativistic particles contribute the most to the entropy density, to a good approximation, we have:

$$\begin{aligned} s &= \frac{2\pi^2}{45} g_{\star S} T^3 \\ g_{\star S} &= \sum_{\text{bosons}} g_i \left(\frac{T_i}{T}\right)^3 + \frac{7}{8} \sum_{\text{fermions}} g_i \left(\frac{T_i}{T}\right)^3. \end{aligned} \tag{2.68}$$

Because the entropy density is constant, it means that the total entropy is also constant:

$$S \sim sR^3 \sim g_{\star S} T^3 R^3 = \text{const}, \tag{2.69}$$

which means that the temperature will scale as $T \sim g_{\star S}^{-1/3} R^{-1}$. What we are interested in here is what happens to a species after the time that its interaction rate cannot keep up with the expansion rate. If that is the case, the species will decouple from the heat reservoir and vary differently from those which are still in thermal equilibrium. Consider a massless species that decouples at time t_D and temperature

T_D and the scale factor R_D. At time t_D, the distribution follows Bose - Einstein or Fermi - Dirac distributions:

$$f(\vec{p}, t_D) = \frac{1}{\exp(E/T_D) \pm 1}. \tag{2.70}$$

After decoupling, the energy scales as R^{-1}, the momentum scale as R^{-1}, meaning that the distribution $f(\vec{p}) = d^3n/d^3p$ is constant:

$$f(\vec{p}, t) = f(\frac{R\vec{p}}{R_D}, t_D) \Leftrightarrow \frac{1}{\exp(E/T) \pm 1} = \frac{1}{\exp(ER/R_D T_D) \pm 1}. \tag{2.71}$$

This means that after decoupling, the temperature of the massless particle drops as:

$$T_{\text{massless}} = T_D \frac{R_D}{R} \sim R^{-1}. \tag{2.72}$$

In case the particle is massive and nonrelativistic, its momentum scales as $T = T_D R_D/R$ after decoupling, meaning that its energy will scale as R^{-2}. Again, we must have that the distribution is unchanged at t and t_D:

$$f(\vec{p}, t) = f(\frac{R\vec{p}}{R_D}, t_D) \Leftrightarrow \frac{1}{\exp(E/T) \pm 1} = \frac{1}{\exp(ER^2/R_D^2 T_D) \pm 1}, \tag{2.73}$$

or equivalently:

$$T_{\text{massive}} = T_D \left(\frac{R_D}{R}\right)^2 \sim R^{-2}. \tag{2.74}$$

In summary, both massive and massless particles maintain their equilibrium phase space distribution after decoupling. After decoupling, massless particles have their temperature scaled with R^{-1} while that of massive particles is scaled as R^{-2}.

2.5 History of the Universe

In the previous section, we have shown how a species that is in local thermal equilibrium evolves with the expansion of the Universe and how it does after decoupling from the thermal equilibrium. The key mechanism that controls whether or not a species in thermal equilibrium is the balance between the interaction rate involving that species and the expansion rate of the Universe. Approximately, if the interaction rate of a species is less than the expansion rate of the Universe, the number of particles of that species per comoving volume will decrease and that species will decouple from the local thermal equilibrium. We have also determined the thermal behaviors of massive and massless species after decoupling. Generally speaking, a massless species will have its temperature scaled as R^{-1} while a massive species will scale as R^{-2} after decoupling.

To illustrate this argument, let us consider the interactions mediated by massless vector bosons and by massive vector bosons.

- Massless vector boson (γ):
  The interaction cross section is $\sigma \sim \alpha^2/T^2$, which gives the interaction rate as $\Gamma \sim n\sigma|v| \sim \alpha^2/T$. From equation (2.64), the expansion rate varies with the temperature as $H \sim T^2/m_{Pl}$ in the radiation epoch. The ratio $\Gamma/H \sim \alpha^2 m_{Pl}/T$. This means that when the temperature drops below $\alpha^2 m_{Pl} \sim 10^{16}$ GeV, particles whose interaction is mediated by photons will be in local thermal equilibrium.

- Massive vector bosons ($W^{\pm}, Z$):
  If $T \gg m_X$ where m_X is the mass of the gauge bosons, the cross section will be the same as in the first case of massless gauge boson. If $T < m_X$, the cross section is $\sigma \sim G_X^2 T^2$ where $G_X = \alpha/m_X^2$. From this we can have: $\Gamma \sim n\sigma|v|\sigma G_X^2 T^5 \rightarrow \Gamma/H \sim G_X^2 m_{Pl} T^3$. The critical temperature above which the species is in local thermal equilibrium is $m_X > T > G_X^{-2/3} m_{Pl}^{-1/3} \sim (m_X/100 \text{ GeV})^{4/3}$ MeV.

From this brief calculation, we can basically get an overall picture of the history of the Universe. When the temperature is above 10^{16} GeV, the Universe might contain only highly relativistic particles, which are quarks, leptons, gauge bosons, Higgs. As our calculation has shown, these particles are not in local thermal equilibrium as their interaction rate cannot keep up with the expansion rate of the Universe. At around 10^{16} to 10^{14} GeV, the Grand Unification Theory (GUT) phase transition will occur. Around 300 GeV, the electroweak spontaneous symmetry breaking will occur. As a result, the electroweak gauge bosons start to acquire masses and the particles that interact via those gauge bosons will decouple from the thermal equilibrium where the order of decoupling depends on the mass of the gauge bosons as we have shown above. As the temperature drops to 100 $\sim$ 300 MeV, the transition related to the chiral symmetry breaking and color-confinement will occur. The primordial nucleosynthesis occurrs around $T = 10 \sim 0.1$ MeV where the Universe changes from radiation-dominated to matter-dominated. This time marks the beginning of structure formation. Finally, at the time around 10^{13} (s), atoms are created as ions and electrons are combined together, matter and radiation decouple from thermal equilibrium.

Some details of important marks in the history of the Universe:

- **Neutrino Decoupling**: In the early Universe, neutrinos are kept in the thermal equilibrium by processes like $\bar{\nu}\nu \leftrightarrow e^+e^-, \nu e \leftrightarrow \nu e$, etc. With the number density of massless neutrinos $n \sim T^3$ and the cross section $\sigma \approx G_F^2 T^2$ where G_F is the Fermi constant, we have the interaction rate calculated by:

$$\Gamma = n\sigma|v| \approx G_F^2 T^5. \tag{2.75}$$

The ratio of interaction over expansion rate is then:

$$\frac{\Gamma}{H} \approx \frac{G_F^2 T^5}{T^2/m_{Pl}} \approx \left(\frac{T}{1MeV}\right)^3. \tag{2.76}$$

From this, at the temperature above 1 MeV, interaction rate is higher than the expansion rate, which means that neutrinos are in good thermal equilibrium with the plasma. When the temperature drops below 1 MeV, neutrino decouples from the plasma and its temperature T_ν will scale with the form factor as $T_\nu \sim R^{-1}$ as we have shown in the previous section. If the temperature continues to drop below m_e, the effective degrees of freedom will change from $g_* = 11/2$ (which includes that of the photon $g_\gamma = 2$ and the $e^\pm$ pair $g_{e^\pm} = 4$) to $g_* = e$ (which includes only that of the photon). As $g_*(RT)^3 = const$ before and after $e^\pm$ decoupling while $RT_\nu = const$ after neutrino decoupling, we have the present temperature of the relic neutrinos:

$$T_\nu = T_\gamma \left(\frac{2}{11/2}\right)^{1/3} = 1.96(K), \tag{2.77}$$

given that the temperature of the CMBR is about 2.73 (K).

- **Radiation - Matter equilibrium**: After decoupling, matter energy density varies as $\rho_M \sim R^{-3}$ while radiation energy density varies as $\rho_R \sim R^{-4}$, which means that if we trace back to the time of radiation - matter equilibrium, we must have:

$$\frac{\rho_R}{\rho_M} \sim \frac{R_0}{R} = 1 + z, \tag{2.78}$$

from which, the ratio of radiation energy density ρ_{R-EQ} to matter energy density ρ_{M-EQ} at equilibirium is:

$$1 = \frac{\rho_{R-EQ}}{\rho_{M-EQ}} = \frac{\rho_{R-0}}{\rho_{M-0}} \frac{R_0}{R_{EQ}}, \tag{2.79}$$

given that at present time $\rho_{M_0} = 1.88 \times 10^{-29} \Omega_0 h^2 \text{g cm}^{-3}$ and $\rho_{R_0} = 8.09 \times 10^{-34} \text{g cm}^{-3}$ [11].From this, we have:

$$\frac{R_0}{R_E} = 1 + z_{EQ} = \frac{\rho_{M_0}}{\rho_{R_0}} = \frac{8 \times 10^{-34}}{1.88 \times 10^{-29} \Omega_0 h^2} = 2.3 \times 10^5 \Omega_0 h^2, \tag{2.80}$$

which leads to:

$$\begin{aligned} T_{EQ} &= T_0(1 + z_{EQ}) = 5.5 \Omega_0 h^2 (eV) \\ t_{EQ} &= \frac{2}{3} H_0^2 \Omega_0^{-1/2} (1 + z_{EQ})^{-3/2}. \end{aligned} \tag{2.81}$$

In summary, in this chapter, we have discussed some background understandings of cosmology. Starting from key cosmological observation, we have discussed the derivation of the Robertson - Walker metric and used to investigate kinetics of object in an expanding Universe. We have also discussed the Boltzmann equation and how it helps explaining the origin of matter in the expanding Universe by taking into account the fact that particles interact with each other and the effect of the expanding Universe. This background is the foundation for our research on dark matter in this thesis.

Chapter 3

Dark Astronomical Compact Objects (DACOs)

3.1 Introduction

The nature of dark matter is one of the most pressing questions in particle physics and cosmology. It goes without saying that the search for dark matter is one of the most attractive endeavors in astroparticle physics. So far, it eludes all search attempts despite the fact that various cosmological observations hinted at its existence.

The most popular cosmological scenario for dark matter and dark energy is the so-called ΛCDM model [12], where the candidate for dark energy is characterized by the unknown cosmological constant Λ, although there exists a few problems with this scenario that need to be resolved. First, there seems to be some tension between numerical simulations of collisionless cold dark matter for central density profiles for dwarf galaxies and galaxy cluster halos (cusp-like) and observations which indicate a flat core. Second, numerical simulation predicts the number of Milky Way satellites to be much more than these observed ones, the so-called missing satellite problem [13]. Third, the so-called too-big-to-fail problem suggests that the largest subhalos of the Milky Way are too massive to host the brightest observed dwarf spheroidal galaxy satellites as suggested by numerical simulations of ΛCMD. In the next sections, we are going to discuss these problems in more detail. There are several proposals for solving these aforementioned problems, one of which goes under the name “self-interacting dark matter”.

An explicit model of self-interacting dark matter was constructed in Refs. [14, 15, 16]. Dark matter and luminous matter are unified at a high energy scale called Λ_{DUT} into a DUT gauge group $SU(6)$, which subsequently breaks into $SU(4) \times SU(2)_W \times U(1)_{DM}$. In this scenario, the Standard Model (SM) gauge group $SU(3)_C(QCD)$ and $U(1)_Y$ are merely spectator gauge groups. The weak gauge group $SU(2)$ is denoted by $SU(2)_W$ for the reason that the model contains “mirror fermions” with opposite chiralities to the SM fermions and allows for the existence of non-sterile right-handed Majorana neutrinos with masses which are proportional to the electroweak scale $\Lambda_{EW} \sim 246$ GeV [17]. Furthermore, the existence of mirror fermions ensures that the DUT gauge group $SU(6)$ is anomaly-free. Below Λ_{DUT}, the symmetry group is $SU(4) \times U(1)_{DM} \times SM$ where $SM \equiv SU(3)_C \times SU(2)_W \times U(1)_Y$. In the brief review given in the next section, it will be shown that DM particles are singlets under the SM gauge group and transform as $\chi = (4, Q_M)$ under $SU(4)_{DM} \times U(1)_{DM}$, where Q_M is the quantum number of $SU(4)_{DM}$.

At the DUT scale, the gauge couplings of $SU(4), SU(2)_W$ and $U(1)_{DM}$ are *equal* and, by running $\alpha_4 = g_4^2/4\pi$ from Λ_{DUT} down to $\alpha_4 \sim \mathcal{O}(1)$, it was found that Λ_4 can range from a few hundred GeVs to a few hundred TeVs [18]. When the confinement of $SU(4)$ occurs, the singlet state appears in the form of dark “baryons” formed out of four χs called CHIMP [15] whose spin is zero and hence are considered as massive bosons. Typically, these dark baryons have masses of $\mathcal{O}(4\Lambda_4)$. As discussed in [15], there exists very light dark pions which are $\bar{\chi}\chi$ states and which couple to the dark “baryons”.

Let us assume that, below Λ_4, one has a gas of massive bosonic dark baryons. Under some certain conditions that will be discussed in the next sections, these dark “baryons” can be gravitationally clumped together into compact objects. We shall call these objects by the name DACO, which stands for Dark Astronomical Compact Object. In order to form stable compact objects while these dark “baryons” gravitationally attract each other, an energy dissipation mechanism is needed. It will be shown below that such a mechanism indeed exists: the “Bremsstrahlung” of dark pions from the dark “baryons” while they fall into the gravitational potential well.

1) How heavy can a DACO be? In other words, what would be the minimum and maximum masses of a stable DACO? In paricular, considering the fact that dark "baryons" are bosons which we will assume to have spin 0, is there a mechanism which prevents DACOs from being too massive and collapse into black holes?

2) How can they be detected? We suggest here three methods which might be applicable to search for DACOs. Two of these methods are based on the assumption that stars can capture DACOs, which have "solar-planetory system" masses and, as a result, the search for exoplanets appears to be the best way to look for DACOs. The most promising methods are: 1) the radial velocity method based on the Doppler effect of spectral lines which get shifted due to the motion of the star-planet system around its center of mass; 2) the pulsar timing method; 3) This last method is a long shot but it is worth mentioning. It is not impossible that DACOs can cluster into mini dark galaxies which the physical size of say a neutron star and with a total mass of a few tenths of the mass of the Sun. The merging of such two galaxies could in principle generate gravitational waves. Since DACOs are supposed to be "transparent", the absence of the signal using the transit methods, in conjunction of radial velocity method with a positive signal would point to a presence of DACOs orbiting such a star.

In discussing #1 and #2 above, we will be leaving out many issues which are beyond the scope of this thesis such as the distribution of DACOs in the galaxies and clusters of galaxies and the detail of the search for DACOs.

It must be emphasized that DACOs can be created from any heavy dark bosons with the only requirement being the existence of a cooling mechanism for the highly energetic dark bosons to lose their energy. Therefore, this approach can be applied to other models when this condition is applicable. The structure of the chapter is as follows: first, we discuss the condition under which DACOs can be formed out of dark bosonic baryons. In particular, we derive the minimum and maximum mass of such object. Second, we give a brief review of the Luminogenesis model, which was proposed in Refs. [15, 16] and expanded in Ref. [18] as an example model that proposes new dark bosonic baryon. Last but not least, we propose various methods to search for DACOs using exoplanet searches as well as those being used in detection of gravitational waves.

3.2 Current problems of Cold Dark Matter

In the previous chapter, we have introduced the reasons behind the argument that there must be dark matter in the Universe that makes up 23% of the Universe. We, however, have not mentioned the nature of dark matter. The constraints we have on dark matter particles are that they must be electrically neutral, they cannot consist of SM baryons; their interactions with each other may have effects on structure formation of the Universe as they can transfer energy and momentum in their interactions. The theories of Cold Dark Matter are among the most popular theories of Dark Matter. Candidates for Cold DM fall into three categories: axions, MACHOs (Massive Compact Halo Objects) and WIMPs (Weakly Interacting Massive Particles) among which, WIMPs have a great attraction for researches.

WIMPs interact with each other at the scale of the weak interaction and have masses on the order of 100 GeV. The WIMP origin is thought to begin in the early Universe where they are in thermal equilibrium with other particles. As the Universe expands, the equilibrium is no longer maintained and the number density of WIMPs decreases exponentially to the point where the annihilation of the WIMP particles and anti-particles no longer occurs. From this point to the present, the number density of the WIMPs remains constant. For a WIMP self-interaction of the strength of that of the weak interaction and mass at the order of 100 GeV, the WIMPs self interaction cross section can be estimated to be $\sigma_{ann} \approx \alpha_W^2/m^2$. By using the Boltzmann equation, one can get the present number density of WIMPs, which matches the number density calculated from cosmological constrains [39]. This coincidence is known as "WIMP miracle".

Despite being the standard paradigm for structure formation in the Universe, the Cold Dark Matter cosmology contains many issues. One of the problems known as the "core versus cusp" problem is as follows: N-body simulations of Cold Dark Matter seem to predict that the density of the galaxies increases as a power law function toward the center of the galaxies. The typical density distribution of the galaxies taken from N-body simulations is given as:

$$\rho_{DM}(x) = \frac{\rho_0}{x^\alpha (x+1)^{3-\alpha}}, \tag{3.1}$$

where $\alpha = 1.0$ for Navarro-Frenk-White model [40], and 1.5 for Fukushige - Makino

- Moore model [41]. However, recent observations on the nearby low mass galaxies or low surface-brightness galaxies show that the density distribution of these halos are relatively constant at the centers of these galaxies. In Fig. 3.1, the dark matter density profiles of 7 galaxies taken from "The HI Nearby Galaxy Survey" shows in detail the discrepancies between the simulations of Cold Dark Matter and the observations [42]. It can be seen that while the NFW density profile predicts a core of that peaks at the center of the galaxy. The observation fits show densities that are up to one order of magnitude smaller than predictions.

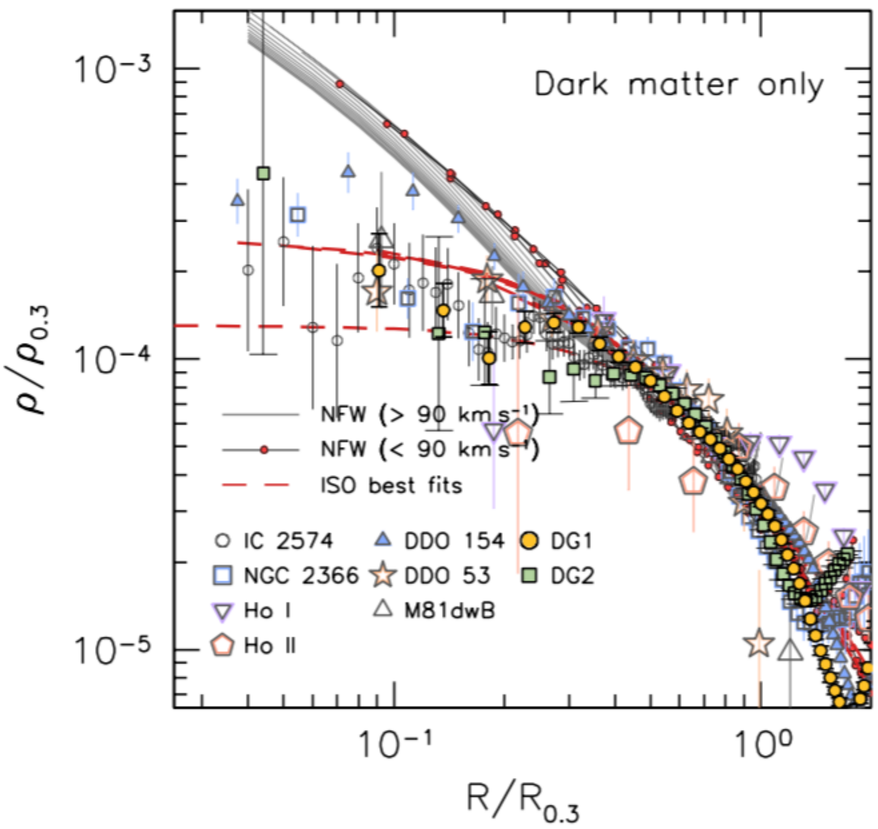

Figure 3.1: Density profile of simulated galaxies versus the observations from 7 nearby galaxies [42].

The second challenge of the Cold Dark Matter scenario is what is known as the "missing satellites" problem. In the analysis of Anatoly et al,. [48] it was shown that by using N-body simulation with ΛCDM model, the expected number of satellites of a halo with the same size as that of our galaxy is much less than what we have from cosmological observations. In Fig. 3.2, the circular velocity distibution of the number of satellites are shown in the region of $200h^{-1}$kpc from the center of the

Milky Way and Andromeda galaxies [43]. From the plot, we can see that for the circular velocity $V_{circ} > 50$ km/s, N-body simulations and cosmological observations are in good statistical agreements with each other. However, for $V_{circ} < 50$ km/s, the simulation shows predictions that are up to one order of magnitude bigger than the observations.

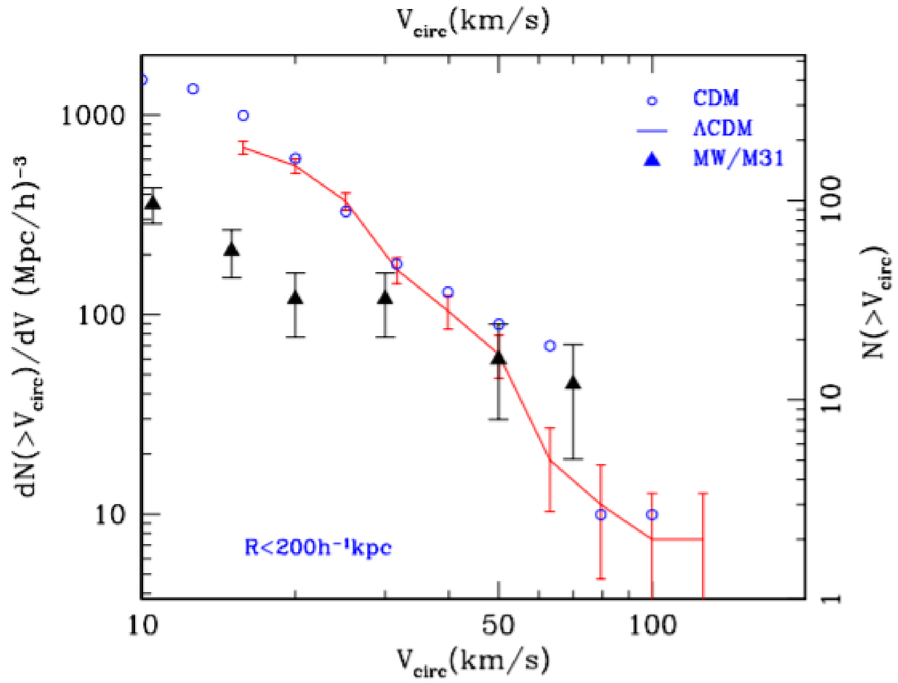

Figure 3.2: Missing satellite problem: The simulated circular velocity distribution of number of satellites are different from cosmological observation in regions where $V_{circ} < 50$ km/s [43].

In addition, CDM has some more additional challenges that are not satisfactorilly addressed. From this, it is natural to steer our imagination to the direction where dark matter is not weakly interacting particles but rather strongly self-interacting particles. In the next sections, we will discuss in detail the behaviors of compact cosmological objects that are made from strongly self-interacting particles.

3.3 Evolution of Bosonic Astronomical Compact Objects

Bosonic astronomical compact objects are made of bosons that are bound together only by their gravitational attraction. In the early Universe, matter was highly energetic and the gravitational potential might not have been large enough to cluster bosonic particles or any other particles together to form astronomical structures. Therefore, a mechanism for these high energy bosons to lower their energy is a requirement for bosonic astronomical compact objects to be created.

For any model that has a dark composite bosonic particle and a cooling mechanism, conditions for the formation of a bosonic astronomical compact object are satisfied. It must be reiterated that the dark boson being considered is composite particle whose constituents are dark fermions. The next question one may ask is how stable that object is gravitationally, what would happen if the stability condition were broken? To answer these questions [19], we can start with the stability conditions for a Bose star [49] by using the argument of James Jeans. Consider a static universe with a uniform and static energy density ρ and pressure p. Suppose that the energy density ρ_1 fluctuates around the average energy density, the relation between the energy density fluctuation ρ_1, the pressure p and the sound velocity through this medium v_s is governed by: [11]

$$\frac{\partial^2 \rho_1}{\partial t^2} = v_s^2 \nabla^2 \rho_1 + 4\pi G \rho \rho_1, \tag{3.2}$$

where $v_s^2 = \delta p / \delta \rho$. The solution of this equation has the form of:

$$\rho_1 \propto exp(i\vec{k}\vec{x} - i\omega t), \tag{3.3}$$

where ω and the wave number $\vec{k}$ are related by:

$$\omega^2 = \vec{k}^2 v_s^2 - 4\pi G\rho = v_s^2 \left[\vec{k}^2 - (4\pi G\rho / v_s^2) \right]. \tag{3.4}$$

The Jeans wave number is defined by:

$$k_{Jeans} = (4\pi G\rho / v_s^2)^{1/2}. \tag{3.5}$$

The solution for the energy density fluctuation is a function of the wave number k.

- For $k > k_{Jeans} \to \omega^2 > 0 \to \omega$ is a real number, the energy density fluctuation ρ_1 varies sinusoidally with time.

- For $k < k_{Jeans} \to \omega^2 < 0 \to \omega$ is an imaginary number, the energy density fluctuation ρ_1 will then increase exponentially with time.

For an astronomical structure to be created, it must be true that some point in its history, the energy density fluctuation increases well above the average energy density. Therefore, the wave number k must be less than the Jeans wave number for a new astronomical structure to be created.

In an expanding universe, the wave number varies with the scale factor as $1/R$. For a comoving sphere of radius given by $R = 2\pi/|\vec{k}|$, the mass enclosed by such sphere is calculated by:

$$M_{Jeans} = \frac{4\pi}{3}\left(\frac{2\pi}{|\vec{k_{Jeans}}|}\right)^3 nm_X = \frac{4\pi}{3}nm_X\left(\frac{\pi v_s^2}{G\rho}\right)^{\frac{3}{2}}, \tag{3.6}$$

where n is the number density of the boson being considered and m_X is its mass. The mass of the comoving sphere of radius equal to the Jeans wavelength $\lambda_{Jeans} = 1/k_{Jeans}$ is called Jeans mass. The dependence of energy density on the wave number k can be translated to the dependence of energy density on the Jeans mass:

- For $k > k_{Jeans}$, the mass M is smaller than Jeans mass M_{Jeans}. The means the energy density fluctuation oscillates sinusoidally.
- For $k < k_{Jeans}$, the mass M is larger than Jeans mass M_{Jeans}. The energy density fluctuations that could form clumps DM increase exponentially.

It is reasonable to assume that these dark matter compact objects are formed after the bosons become non-relativistic: $k_BT \ll m_X$. The equations of state are then:

$$\begin{aligned} \rho &= nm_X + \frac{3}{2}nk_BT, \\ p &= nk_BT, \end{aligned} \tag{3.7}$$

where the rest energy density nm_X is much bigger than the second term for non-relativistic dark matter. It is also reasonable to assume that the boson has decoupled from thermal equilibrium by the time of structure formation, which leads to the scaling of the number density $n \propto R^{-3} \propto T^{3/2}$. From this, the sound velocity can be calculated by:

$$v_s^2 = \frac{\delta p}{\delta \rho} = \frac{\frac{5}{2}k_BT^{3/2}}{\frac{3}{2}m_XT^{1/2}} = \frac{5k_BT}{3m_X}. \tag{3.8}$$

where we have neglected the second term on the right-hand side of ρ. Let the number density n take the value at the time the bosonx become non-relativistic n_i where

$m_i = k_B T_i$. n_i can be estimated by the black-body radiation number density [10]

$$n_i = \frac{30\zeta(3)}{\pi^3}\frac{a}{k_B}T_i^3 = 3.7\frac{a}{k_B}T_i^3, \tag{3.9}$$

where $\zeta(x)$ is the Riemann zeta function.

As the universe expands, the number density of the boson varies with temperature as $n \sim T^{3/2}$. In other words, we can write the number density anytime after the decoupling of the boson by:

$$n = n_i\left(\frac{T}{T_i}\right)^{\frac{3}{2}}. \tag{3.10}$$

From this, the Jeans mass can be estimated as:

$$M_{Jeans} = 4\left(\frac{\pi}{3}\right)^{\frac{5}{2}}\left(\frac{5k_B}{G}\right)^{\frac{3}{2}} T_i^{\frac{3}{4}} T^{\frac{3}{4}} n_i^{-\frac{1}{2}} m_X^{-2} \tag{3.11}$$

The corresponding Jeans wavelength gives us the order of magnitude of the radius of DM clumps of mass M_{Jeans}:

$$\begin{aligned}\lambda_{Jeans} &= \frac{2\pi}{k_{Jeans}} = 2\pi\left(\frac{4\pi G n m_X}{v_s^2}\right)^{-\frac{1}{2}} \\ &= 2\pi\left(\frac{5}{3}\frac{T}{T_i}\right)^{1/2}\left[4\pi G m_X n_i\left(\frac{T}{T_i}\right)^{3/2}\right]^{-1/2}.\end{aligned} \tag{3.12}$$

Both Jeans mass and Jeans wavelength depend on the temperature T, which decreases as the Universe expands. A rough estimate of the order of magnitude of the mass and the radius of such object can be made at the time where the energy density of the non-relativistic dark boson is equal to that of the radiation. Suppose that after the temperature drops below m_X, the model-dependent effective degrees of freedom of the model is g_{eff} (which is at least equal to that of the SM at $T = m_X$), the matter - radiation equilibrium temperature will then be calculated by:

$$\begin{aligned}\rho_M = \rho_R &\leftrightarrow n m_X = g_{eff} a T^4 \\ n_i\left(\frac{T}{T_i}\right)^{3/2} & kT_i = g_{eff} a T^4 \\ \rightarrow 3.7 a T_i^4\left(\frac{T}{T_i}\right)^{3/2} &= g_{eff} a T^4 \\ &\rightarrow T = T_i\left(\frac{3.7}{g_{eff}}\right)^{2/5}\end{aligned} \tag{3.13}$$

We call this temperature T_{MD}, the temperature at which energy density of the dark bosons is equal to that of radiation. The Jeans mass at this temperature can then be estimated as:

$$\begin{aligned} M_{Jeans} &= 4\left(\frac{\pi}{3}\right)^{\frac{5}{2}}\left(\frac{5k_B}{G}\right)^{\frac{3}{2}} T_i^{\frac{3}{4}} T^{\frac{3}{4}} n_i^{-\frac{1}{2}} m_X^{-2} \\ \Leftrightarrow M_{Jeans} &= 3.08 g_{eff}^{-\frac{3}{10}}\left(\frac{\pi}{3}\right)^{\frac{5}{2}}\left(\frac{5k_B}{G}\right)^{\frac{3}{2}}\left(\frac{a}{k_B}\right)^{-1/2} m_X^{-2}. \end{aligned} \tag{3.14}$$

What makes DACOs fundamentally different from the regular fermionic stars is the fact that DACOs do not have the Fermi pressure to support and balance the gravitational pressure. Therefore, to estimate the mass of DACOs, we have to follow the arguments of Yoshimura and Takasugi [20] on mass limits of Bose stars.

For a brief introduction to Yoshimura and Takasugi limit on Bose star, one can anticipate that the only force that balances the graviational pressure is the pressure created from the uncertainty of the confined bosons:

$$\Delta p \Delta x \geq h = 2\pi\hbar \leftrightarrow \Delta p \geq \frac{\pi}{R}, \tag{3.15}$$

where $\Delta x = 2R$ is the diameter of the star and $\hbar = c = 1$ were used as conventions. For a spherical Bose star of mass M, radius R, the balance between the gravitational pressure and the quantum uncertainty pressure requires that:

$$\frac{P}{R^1} \sim \frac{GM\rho}{R^2}, \tag{3.16}$$

which means that the mass of the Bose star depends on the relation between the pressure P and its density ρ.

In the non-relativistic limit, the pressure P is related to the momentum of each particle whose mass is m by:

$$P \sim \frac{p^2\rho}{m^2} \sim \frac{\rho}{m_X^2 R^2}, \tag{3.17}$$

where m_X is boson's mass. The mass of the Bose star in this case is:

$$M \sim \frac{m_{Pl}^2}{m_X^2 R}, \tag{3.18}$$

where m_{Pl} stands for the value of Planck's mass.

In the relativistic limit, the pressure is related to the momentum by $p = \rho/3$, and the mass of the Bose star will then be:

$$M \sim m_{Pl}^2 R. \tag{3.19}$$

From this, the turn-up at $m_X = R^{-1}$ where the maximum mass of the Bose star is:

$$M \sim \frac{m_{Pl}^2}{m}. \tag{3.20}$$

In the detailed calculation, the mass limit of the Bose star whose boson has mass m_X is given by:

$$M_{Y-T} = 0.57 \frac{m_{Pl}^2}{m_X}. \tag{3.21}$$

From this, we can calculate the ratio of the Jeans mass and the Yoshimura - Takasugi limit:

$$\frac{M_{Jeans}}{M_{Y-T}} = \frac{3.08 g_{eff}^{-\frac{3}{10}} \left(\frac{\pi}{3}\right)^{\frac{5}{2}} \left(\frac{5k}{G}\right)^{\frac{3}{2}} \left(\frac{a}{k}\right)^{-1/2} m_X^{-2}}{0.57 \frac{m_{Pl}^2}{m_X}} = g_{eff}^{-\frac{3}{10}} \left(\frac{10^{18}}{m_X \text{ TeV}}\right) \tag{3.22}$$

For a dark boson of mass in the order of 1 TeV, Jeans mass is about 17 to 18 orders bigger than the Yoshimura - Takasugi limit. However, before the Jeans mass is achieve, the DM sphere is not yet a clump and therefore, the Yoshimura - Takasughi limit is not yet applicable. This means that by the time the mass of the dark boson clump is large enough for energy density fluctuation to grow with time, its mass is already bigger than the maximum mass a boson clump can have. As a result, the dark boson clump will collapse to its core, increasing the central pressure to a much higher value. When all dark bosons collapse to the center of the clump, the pressure may be large enough to deconfine them into their constituents, which are fermions whose spin is 1/2. Once that process is completed, the dark compact object will be made of all dark fermions and will possess the same properties of a fermionic star. The outward Fermi pressure of the dark fermions will counter balance the inward gravitational pressure.

Let M_{crit} be the critical mass of a fermion star, which can be estimated by following approach of Oppenheimer - Volkoff [21], there are two scenarios that could happen. If the critical mass M_{crit} is smaller than Jeans mass M_{Jeans}, by the time a DM clump is created, it would collapse due to the fact that Jeans mass is much bigger than the Yoshimura - Takasugi limit. The DM clump will continue to collapse as the fermi press cannot keep up with the gravitational pressure. At the end of this process, we would end up with a black hole whose mass is at least equal to the Jeans mass. In the second scenario where Jeans mass is smaller than the critical mass, once the DM clump is created and its mass is between Jeans mass and critical mass, we would have a gravitationally stable DACO. If it happens that the DACO mass is bigger than the critical mass, the DACO would then collapse and become black hole.

Following the derivation of Oppenheimer-Volkoff [21] limit on neutron star, we can estimate the critical mass for DACOs over which it will collapse radially as follows: consider a degenerate gas of fermionic χ's particles at temperature $T \ll E_F/k$ enclosed in a sphere of radius R. In what followed, we used the analysis of [49]: let the Fermi energy of each particle be $E_F = m_\chi = k_F$, the number density of χ gas is then:

$$n_F = \frac{k_F^3}{6\pi^2} = \frac{N}{4\pi R^3/3} \rightarrow k_F = \left(\frac{9\pi}{2}\right)^{\frac{1}{3}} \frac{1}{R} N^{\frac{1}{3}}. \tag{3.23}$$

The gravitational energy per χ particle is:

$$E_G = -\frac{NGm_\chi^2}{R} \tag{3.24}$$

The condition for stability of the fermionic χ stars is now that the total energy each particle has is positive:

$$\begin{aligned}
&E_F + E_G < 0 \rightarrow -\frac{GNm_\chi^2}{R} + k_F = \left(\frac{9\pi}{2}\right)^{\frac{1}{3}} \frac{1}{R} N^{\frac{1}{3}} \\
&\rightarrow N > N_{crit} = \left(\frac{9\pi}{2}\right)^{\frac{1}{3}} \left(\frac{1}{Gm_\chi^2}\right)^{\frac{3}{2}}, \\
&\rightarrow M > M_{crit} = N_{crit} m_\chi = \left(\frac{9\pi}{2}\right)^{\frac{1}{3}} G^{-\frac{3}{2}} \frac{1}{m_\chi^2}, \\
&\rightarrow R > R_{crit} = \left(\frac{9\pi}{2}\right)^{\frac{1}{2}} N_{crit}^{\frac{1}{2}} \frac{1}{m_\chi}.
\end{aligned} \tag{3.25}$$

In Figure (3.3), the orange line shows the scale of the critical mass at different boson masses (which is equal to $4m_\chi$). The critical mass here is considered to be the upper limit for DACOs. For DACO of a mass that is higher than the critical value, the Fermi pressure is not enough to balance the gravitational pressure and that DACO will then collapse radially inward, which might possibly result in black hole. The range from the Jeans mass to the critical mass gives us the window of possible mass for the DACOs. These values are model independent and can be used as predictions to confirm any model which introduces strongly interacting bosons whose constituents are dark fermions.

Having constructed the fomulas for Jeans mass, Yoshimura - Takasugi limits and critical masses for DACO, we can now plug in some numeric values to see the typical values of the Jeans mass, Yoshimura - Takasugi limit and critical mass of DACO which is shown on Table 3.1, where g_{eff} was taken to be that of the SM. For a heavy boson of mass in the order of 1 TeV, the corresponding Jeans mass is about several Earth mass. This range makes it possible for us to use some current methods being used to look for exoplanets to search for DACOs.

m_X	1 TeV	10 TeV
$M_{Jeans}(M_E)$	6.25	6.25×10^{-2}
$M_{Y-T}(M_E)$	2.54×10^{-17}	2.54×10^{-18}
$M_{crit}(M_E)$	21.1	2.11×10^{-1}
$\lambda_{Jeans}(m)$	4.9×10^{-3}	4.9×10^{-5}
$R_{crit}(m)$	1.46×10^{-1}	1.46×10^{-3}

Table 3.1: Jeans mass, Yoshimura-Takasugi mass and critical mass of DACOs for different boson masses and g_{eff} is model-dependent and was taken to be that of the SM.

We can now see that as the critical mass is bigger than the Jeans mass, a DACO will be gravitationally stable if its mass is between Jeans mass and critical mass. However, if its mass is bigger than the critical mass, it would collapse to form a black hole as we have mentioned earlier. The mass of this type of black hole makes its lifetime longer than the age of the Universe (a black hole of mass 10^{11} kg would have its lifetime equal to the age of the Universe). This means both stable DACOs and DACO-originated black holes could exist together.

3.4 The Luminogenesis Model

Having discussed the conditions under which DACOs will be created and its possible mass range as a function of dark bosonic baryon mass, we can now represent a model whose dark bosonic baryon might possibly form DACOs: the Luminogenesis model. The Luminogenesis model [22] was written to accommodate the flowing scenario. It

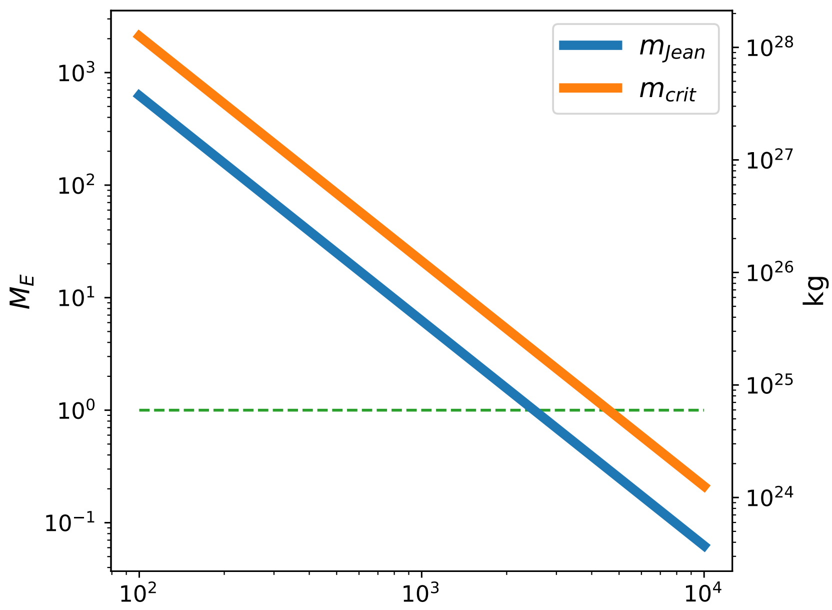

Figure 3.3: The DACO's mass is estimated to be in the region between the Jeans mass and the critical mass, where the critical mass is the Oppenheimer - Volkoff limit on the mass of a fermion star. The green dashed line indicates one Earth mass.

was assumed that there was an inflationary stage in the early universe. Furthermore, it was assumed that, at the end of inflation, the inflaton decayed primarily into dark matter and the energy density of the early universe was dominated by that of dark matter. A mechanism was proposed in which dark matter converted 15% of its energy density into luminous matter. In order to achieve this scenario, Refs. [22, 23] proposed that dark matter is endowed with a gauge group which is unified with the electroweak gauge group at some high energy scale Λ_{DUT} (DUT stands for Dark Unified Theory) into a larger gauge group $SU(6)$. The summary of the Luminogenesis model is given below:

- Above DUT scale Λ_{DUT}, the symmetry group is $SU(3)_C \times U(1)_Y \times SU(6)$. Here $SU(3)_C \times U(1)_Y$ denotes the usual SM QCD and weak hypercharge interactions which are "spectator" gauge group in the Luminogenesis model.

- At Λ_{DUT}, $SU(3)_C \times U(1)_Y \times SU(6) \to SU(3)_C \times U(1)_Y \times SU(4)_{DM} \times U(1)_{DM} \times SU(2)_W$.

- For $SU(3)_C \times U(1)_Y \times SU(6)$ to be anomaly-free, the model requires the presence of mirror fermions of opposite chiralities to those of the SM fermions. It turns out that these mirror fermions give rise to a model (EW ν_R model) with non-sterile electroweak-scale right-handed Majorana neutrinos, with the test of the seesaw mechanism being accessible at Large Hadron Collider [24]. The Luminogenesis model is a natural generalization of EW ν_R model.

- The $SU(6)$ representations which are relevant to the Luminogenesis model are listed in Table (3.2) [22]:

$SU(6)$	$SU(4)_{DM} \times SU(2)_L \times U(1)_{DM}$
6	$(\mathbf{1},\mathbf{2})_{\mathbf{2}} + (\mathbf{4},\mathbf{1})_{-\mathbf{1}}$
20	$(\mathbf{4},\mathbf{1})_{\mathbf{3}} + (\mathbf{4}^*,\mathbf{1})_{-\mathbf{3}} + (\mathbf{6},\mathbf{2})_{\mathbf{0}}$
35	$(\mathbf{1},\mathbf{1})_{\mathbf{0}} + (\mathbf{15},\mathbf{1})_{\mathbf{0}} + (\mathbf{1},\mathbf{3})_{\mathbf{0}} + (\mathbf{4},\mathbf{2})_{-\mathbf{3}} + (\mathbf{4}^*,\mathbf{2})_{\mathbf{3}}$

Table 3.2: Some $SU(6)$ representations where $(\mathbf{1},\mathbf{2})_{\mathbf{2}}$ represents luminous matter and $(\mathbf{4},\mathbf{1})_{\mathbf{3}} + (\mathbf{4}^*,\mathbf{1})_{-\mathbf{3}}$ represents dark matter.

Mirror quarks and leptons can be searched for at the LHC [11]. The electroweak-scale right-handed neutrinos, if exist, will be a direct test for seesaw mechanism. As emphasized in Ref. [53], the production of $\nu_R\nu_R$ at the LHC can result in many interesting signals such as like-sign dileptons. One of the most interesting processes of mirror quarks is their decay to SM quarks by radiating a SM-singlet Higgs scalar ($q_R^M \rightarrow q_L + \phi_S$) via the interaction of the form $g_{Sq}\bar{q}_L\phi_S q_R^M + h.c$, where q_L and q_R^M refer to the SM left-handed and mirror quark doublet, respectively. There is also a corresponding process for the lightest mirror lepton ($l_R^M \rightarrow l_L + \phi_S$) with $g_{Sl}\bar{l}_L\phi_S l_R^M + h.c.$

The inflaton ϕ_{inf} is represented by $(\mathbf{1},\mathbf{1})_{\mathbf{0}}$ of **35**, and since $\mathbf{20}\times\mathbf{20} = \mathbf{1_s} + \mathbf{35_a} + \mathbf{175_s} + \mathbf{189_a}$, the inflaton decays mainly to dark matter through the interaction $g_{20}\Psi_{20}^T\sigma_2\Psi_{20}\phi_{35}$ which contains the inflaton in $g_{20}\Psi_L^T\sigma_2\Psi_L^c\phi_{inf}$. The outcome of this process explains the predominance of dark matter over luminous matter. The dark matter created can then decay into luminous matter in a process called "luminogenesis". Some key points of process can be summarized as follows

- As noted in Ref. [22], for the $SU(4)_{DM}$ dark matter fermion χ, there is a small excess of n_χ over $n_{\bar{\chi}}$, which is known as the asymetric part: $\Delta n_\chi = n_\chi - n_{\bar{\chi}}$. The symmetric part of the number density are approximately equal to that of χ and $\bar{\chi}$: $n_{sym} \approx n_\chi \approx n_{\bar{\chi}}$, which means that $\Delta n_\chi \ll n_{sym}$. To explain the origin of this asymmetry in the DM number density, we assume that there is a global $U(1)_\chi$ for DM. The interaction carried by the gauge bosons for the coset group $SU(6)/SU(4) \times SU(2) \times U(1)_{DM}$ explicitly breaks the $U(1)_\chi$ symmetry, and their decay involving the interference between the tree-level and one-loop diagrams will ultimately produce a net DM asymmetry, assuming the presence of CP violation in the DM sector. (This process is similar to the one involving X and Y gauge bosons in $SU(5)$ Grand Unified Theory.)

- χ and $\bar{\chi}$ can annihilate to a SM fermion pair via γ_{DM}, the dark photon of $U(1)_{DM}$ with the effective Lagrangian given by $\frac{g^2}{M_{\gamma DM}}(\bar{\chi}\gamma_\mu\chi)(\bar{f}\gamma^\mu f)$. The luminous fermion pair will then annihilate to radiation.

- As χ and $\bar{\chi}$ annihilate, the symmetric number density n_{sym} will be affected while the asymmetric part Δn_χ will not. When the effective interaction goes out of equilibrium, the number density n_{sym} will be given by: $\frac{\alpha^2}{M^2_{\gamma DM}} n_{sym,D} \approx \frac{T_D^2}{m_{Pl}}$, where D stands for "decoupling" [22]. When χs become non-relativistic, i.e., for $T_0 \approx m_\chi$, since the asymmetric number density Δn_χ is small, the symmetric number density will approximately be $n_{sym,0} \approx n_{tot,0} \sim Cm_\chi^3$, where C is a constant. From this, $\frac{n_{sym,D}}{n_{sym,0}} = \frac{1}{C\alpha^2}\frac{M^2_{\gamma DM}T_D^2}{m_{Pl}m_\chi^3}$. For $m_\chi \sim 1$ TeV, $M_{\gamma DM} \sim \mathcal{O}(1\text{TeV})$, assume that $T_D = m\chi/10$, then $n_{sym,D} \approx 10^{-16} n_{sym,0}$. This means that at the decoupling time, most of the symmetric DM has annihilated to luminous fermion-antifermion pairs. Due to the Boltzmann suppression at $T_D \sim m_\chi/10$, $\rho_\chi/\rho_R < exp(-10) \approx 4.5 \times 10^{-5}$, which is well in the radiation epoch and before Big Bang Nuclesynthesis (BBN). Since the baryon-to-photon ratio should be 10^{-9}, where the main photon source comes from the radiation of fermion-antifermion pairs created from the annihilation of symmetric DM and where the main source of baryons is from the asymmetric part, it was estimated that $\Delta n_\chi \sim 10^{-9} n_{sym,0}$. Compare 10^{-16} to 10^{-9}, we can see that by number density of symmetric DM is much smaller compared to asymmetric DM well before BBN. Below T_D, any dark pions ($\bar{\chi}\chi$, dark "baryons" ($\chi\chi\chi\chi$) and dark "anti-baryons" ($\bar{\chi}\bar{\chi}\bar{\chi}\bar{\chi}$) formed after $SU(4)_{DM}$ confinement are converted via dark gamma γ_{DM} to radiation and can no longer be thermally produced. As a result, there will be no more anti-DM before BBN, unlike other models in literature.

- χ and $\bar{\chi}$ can also be converted to luminous matter via interactions with two scalar fields: $\Phi_{15}^{(L)}$ and $\Phi_{15}^{(R)}$, which is described by $\frac{g_6^2}{M_{15}^2}(\chi_L^T \sigma_2 l_L)(\chi_L^{c,T} \sigma_2 l_M^{M,c}) + h.c.$ This results in $\chi_L + \chi_R \rightarrow l_L + l_R^M$ and $\bar{\chi}_L + \bar{\chi_R} \rightarrow \bar{l}_L + \bar{l}_R^M$. In the early universe, mirror leptons l_M^R mainly decay to SM leptons.

- The annihilations of DM particles via γ_{DM} and via $\Phi_{15}^{(15)}$ and $\Phi_{\bar{15}}^{(R)}$ are independent of each other. After these interactions freeze out during matter dominated epoch, any DM left in the symmetric part annihilate to radiation while those in asymmetric part do not annihilate because there is no anti-DM in asymmetric part. This will give us the correct observations of 14% luminous matter and 86% of dark matter.

In the $SU(4)$ confinement, the bound state of 4 χ forms baryons called "CHIMP"s, which stands for "χ massive particle". A CHIMP, which is denoted by $X = (\chi\chi\chi\chi)$, is assumed to have spin 0. Similar to QCD where $SU(3)$ Nambu-Goldstone (NG) bosons appearing from the spontaneous breaking of chiral symmetry due to small masses of quarks, the dark pion ($\bar{\chi}\chi$ can acquire a small mass through a term $m_0\bar{\chi}\chi$ where m_0 is a Lagrangian mass term for χ. Following QCD, it should obey that $m_0 \ll \Lambda_4 \sim m_\chi$. It has been shown in Ref. [25] that the mass of CHIMP is constrained from 1 - 10 TeV and the mass of the dark pion $m_{\pi DM}$ was constrained from 1 - 10 MeV.

At this point, we can estimate DACOs mass for our Luminogenesis model. The required parameters are just the number of effective degrees of freedom, and the dark fermion mass, which was stated above. As the temperature drops below CHIMP mass, the relativistic particles in the model consist of all particle in SM, mirror counterparts of SM fermions, 4 Higgs singlets, 2 complex Higgs doublets, 1 complex Higgs triplet and 1 real Higgs triplet. The number of effective degrees of freedom is calculated as:

$$\begin{aligned} g_b &= 28(SM) + 4 + 2 \times 4 + 2 \times 3 + 3 = 49, \\ g_f &= 90 \times 2 = 180, \\ g_{eff} &= g_b + \frac{7}{8} g_f = 206.5. \end{aligned} \tag{3.26}$$

For this value of g_{eff}, the numerical values show that the possible mass range for DACOs of mass of 1 TeV is from 5 to 20 Earth mass, which makes it possible to look for these dark compact objects by the techniques used to search for exoplanets.

3.5 The energy dissipation mechanism for DACOS

In the previous sections, we have discussed the possible mass limits over which the energy density fluctuation will start to grow exponentially. For that condition to be achieved, the highly energetic DM particles must have a mechanism to lose energy and settle in the gravitational well. Without one, the CHIMP particles' gravitational attraction between each other will not be big enough to bring them together for the energy density fluctuation to grow.

It must be noted that the density profiles of luminous matter and dark matter in galaxies are fundamentally different. Due to the radiation of energy, the majority of luminus matter resides closer to the center of the hosting galaxy while dark matter has the tendency to extend throughout the extended halos due to its lack of cooling mechanism. It has been shown that such mechanism can be available for dark matter model that has two oppositely charged dark matter particles under an unbroken $U(1)_X$ symmetry. However, the model requires that one dark matter particle is at least 6 orders heavier than the other [44].

For the DACOs in the Luminogenesis model to lose their energy, we propose a cooling mechanism based on the "Bremsstrahlung" of dark pion π_{DM} $(\bar{\chi}\chi)$ illustrated in Figure (3.4). The interaction between the CHIMP and dark pion can be thought to take a similar interaction of the pion-nucleon vertex where the difference is that our CHIMPs have spin 0 instead of 1/2 for SM nucleons. The effective Lagrangian for the dark "baryon" - dark pion vertex is given by:

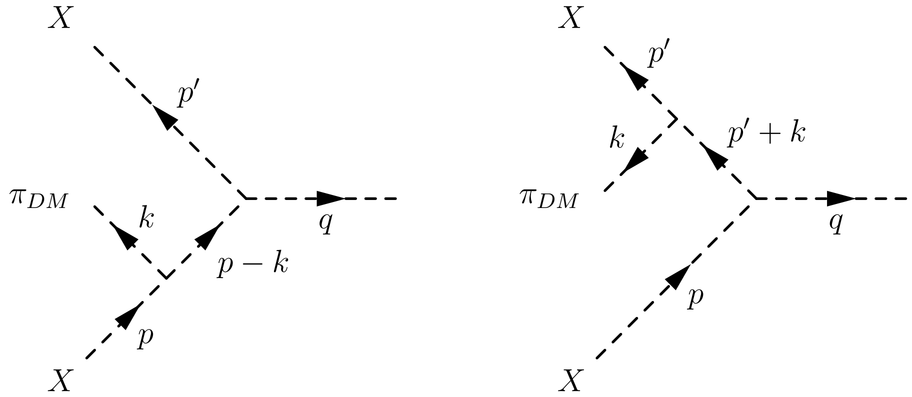

Figure 3.4: π_{DM} "Bremsstrahlung" of CHIMPs

$$L = g_X m_X XX\phi, \tag{3.27}$$

where X and ϕ denote CHIMPs and π_{DM}. Following the discussion given in [4], the scattering matrix for the process that includes π_{DM} "Bremsstrahlung" is given in term of scattering matrix without one is:

$$\begin{aligned} i\mathcal{M}(p,p') = -ig_X m_X \Bigg(& \mathcal{M}_0(p-k,p')\frac{1}{(p-l)^2 - m_X^2 + i\epsilon} \\ & + \mathcal{M}_0(p,p'+k)\frac{1}{(p'+k)^2 + m_X^2 + i\epsilon}\Bigg). \end{aligned} \tag{3.28}$$

It has been shown in [22] that $m_{\pi_{DM}}$ was constrained to be $\mathcal{O}(1)$ MeV. The detail calculation of the probability of such a dark pion "Bremsstrahlung" process to occur is in Appendix A. The probability of the π_{DM} "Bremsstrahlung" of CHIMPs are plotted on Fig. (3.5) at different velocity of non-relativistic CHIMPs and angle θ between p and p':

Due to the fact that DACOs in Luminogenesis model have a cooling mechanism, DACOs could be created during the history of the Universe. The next question one could ask is how could we find them. Due to the fact that DACO's mass is at the same scale of Earth mass, if one DACO travels across the Solar system or any star system, it could be captured by gravity and become a planet of that system that can change the original orbits of other planets in that system. This leads to some possible methods that could be used to detect DACOs, which will be discussed in the next section.

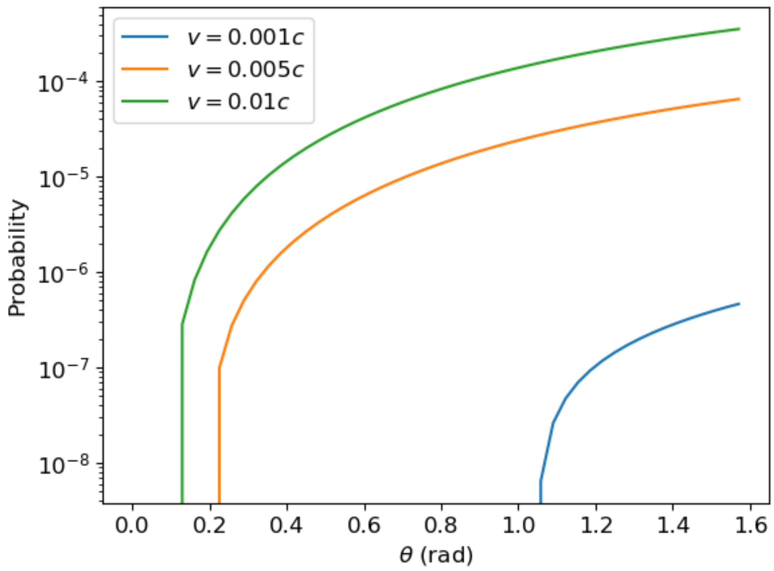

Figure 3.5: Probability of π_{DM} "Bremsstrahlung" of CHIMPs

3.6 Detection methods for DACOs

In previous section, we have estimated the possible mass range for DACOs, which can be from a few to tens of Earth mass. This mass range makes it possible that DACOs can be captured by a star to form a star - planet system whose signals are fundamentally different from those generated by luminous matter star-planet systems. Hence, the best ways to look for DACOs are methods that are being used to detect exoplanets in star - planet binary systems, which include: radial velocity, astrometry, imaging, transits, gravitational microlensing and timing methods. We briefly describe each method and whether or not it can be applied to look for DACOs:

- The radial velocity method [26] is based on the Doppler effect due to the motion of the star around the center of mass of the star-planet systems. This method cannot be used alone to measure the mass of the planet due to the inclination of the planet's plane of orbit with respect to the line-of-sign from the observer to the star.

- The astrometry method is based on the direct observations of stars in start-planet systems. The difference between this and the radial velocity method is that this astrometry method is used when the planets' plane of orbit is perpendicular to the line-of-sign and hence generates no Doppler effect. The signal for this method is the periodic motion of a star relative to stable background stars.

- The imaging method is a direct method, which differentiates the dim spectra generated from the planet from bright spectrum from stars. This method can be used to estimate the temperature but not the mass of the planet.

- The transit method [28] is used to detect the planet in the star-planet systems. In this method, one measures the variation of flux from the star. The decrease in flux can be seen when the start, the planet, and the observer align in that order. The amount of variation is proportional to the ratio of the area of the planet to that of the star.

- The gravitational microlensing method [27] is used to detect when a massive object close to us is passing through the line-of-sign from us to distant stars. The gravitational microlensing events of stars at the order of solar mass usually last a couple of days. If those stars are accompanied by planets, the effect of those planets may also create gravitational microlensing events, which last must shorter, in matter of hours.

- The timing method [28] is the method that are based on the variation of periodic signal from objects like pulsars, white dwarfs, etc., when these objects are accompanied by planets.

Out of these methods above, DACOs can be seen by using radial velocity, astrometry, gravitational microlensing, pulsar timing methods while being completely transparent if one uses imaging method or transit method. Therefore, an evidence for DACOs would be positive signals from any of the first 4 methods in conjunction with negative signals from the later two methods.

As we have mentioned in the previous chapter, the Luminogenesis model proposes a candidate for the DACO that possesses a cooling mechanism, which is crucial for dark matter to clump to form bigger structures such as planets, or galaxies. If the clump of dark matter is formed in the locations where a star is, it can be gravitationally captured by that star and will have impacts on the orbits of the other luminous planets that are orbing that star. By identifying the abnomality in the orbits of these planets, the mass and the distance of the dark objects can be identified or at least be constrained. An example for this is the proposal of the "planet X", and theoretically predicted object that orbit the Sun, which has the mass that is up to 10 times the Earth mass and is at the distance of about 700 AU [47]. Coincidently, our estimated mass for DACO in our model falls into the same range, which means it is not impossible that DACO is a candidate for "planet X".

Chapter 4

Heavy mirror mesons

4.1 Introduction

The validity of the SM has been solidified by the observations of particles at the Large Hadron Collider (LHC) that possesses the properties that resemble its prediction. However, the SM does not provide a clear understanding of many problems such as the existence of Dark Matter, the non-zero masses of neutrinos, the origin of the mass hierachy of fermions or the nature of the Cabibbo-Kobayashi-Maskawa (CKM) mixing matrix. To explain the fact that neutrinos are not massless, many models have been proposed. The first model generates tiny masses for neutrinos through Weinberg operator [30] of dimension 5 and is suppressed at scale M. This predicts the masses of neutrinos that are three to four orders smaller than the inferred values if M is at Planck's scale. The other direction is to extend the SM to include new particles. The first proposal is to extend the SM gauge symmetry to higher gauge symmetries, such as the left-right extension or $SO(10)$ Grand Unified Theory (GUT). The second way is to introduce more Higgs multiplets and select appropriate masses for these additional Higgs bosons and the corresponding Yukawa coulings. The third way is is to add three right-handed neutrinos and a second Higgs doublet to the SM that have a VEV at the KeV scale. The SM Higgs doublet in this model only couples to the charged SM fermions while the second Higgs doublet only couples to the neutrinos where the mass of these neutrinos depends on the Yukawa coulpings. The selection of Yukawa coupling that is at the same order of magnitude of electron Yukawa results in the correct level of neutrino mass. The fourth approach is what is called the "Electroweak fertile ν_R" model [22], which is an extension of SM with the addition of the mirror fermion sector. Specifically, the model introduces some additional fermion multiplets called mirror fermions which contain right-handed neutrinos whose Majorana masses are proportional to the EW scale, four additional Higgs doublets (2 Higgs doublets couple to the SM fermions and the other two couple to the mirror fermions), two triplets and four singlets. In this model, the right-handed neutrinos are doublets under the $SU(2)$ gauge symmetry and will have masses in the EW scale. The model explains the tininess of the neutrino mass via the seesaw mechanism and the neutrinos are of Majorana type. As the gauge symmetry of the group is actually that of the SM, all mirror fermions and the ν_R have masses in EW scale. This makes the model accessible experimentally and it can be confirmed by results from the Large Hadron Collider (LHC).

The EW-ν_R model has many interesting phenomenological implications related to the searches for mirror quarks and leptons at the LHC. It has been shown in Ref. [45] that the couplings of mirror fermions to SM fermions and the Higgs singlet are constrained to be of the order of $\mathcal{O}(10^{-4})$. The tininess of these Yukawa couplings indicates a possibility that the decays of mirror quarks and leptons to the SM quarks and leptons would only be observed at displaced vertices. In the discussion below, we will look at the possibilities that mirror mesons can be created from mirror quarks as well as their production mechanisms, their decays and their signatures.

4.2 The Model

In this section, we will briefly summarize the key features of the Electroweak Scale Right Handed neutrino model concentrating on the meaning and the use of the particle content in comparison to Left - Right model [31]. By making the energy scale of the seesaw mechanism down to the electroweak scale and making right-handed neutrino "non-sterile" or "fertile", we have the advantage of making the seesaw mechanism testable at colliders such as the LHC. As pointed out in Ref. [22], the requirement for this condition to be realized is the additions of the following: right-handed $SU(2)$ mirror quark and lepton doublets, left-handed mirror quark and lepton singlets, two Higgs triplets that include one real triplet and one complex triplet, two Higgs doublets and four Higgs singlets. The gauge group of the model is $SU(3)_C \times SU(2)_W \times U(1)_Y$, which is identical to that of the SM. By expanding the SM, we have increased the number of degrees of freedom. To illustrate the need and the physical meaning of that action, we will compare this model with the famous Left - Right Symmetry model whose gauge group is $SU(3)_C \times SU(2)_L \times SU(2)_R \times U(1)_{B-L}$. Below we summarize the EW ν_R model as proposed by P. Q. Hung:

1. **The gauge sector**

   The gauge sector of the EW ν_R model is that of the SM:

   $$SU(3)_C \times SU(2)_W \times U(1)_Y, \tag{4.1}$$

   while that of the Left - Right Symmetry model is:

   $$SU(3)_C \times SU(2)_L \times SU(2)_R \times U(1)_{B-L}. \tag{4.2}$$

   From this, it can be noted that the EW ν_R model is characterized by only one symmetry breaking scale $\Lambda_{EW} \sim 246$ GeV while the Left - Right Symmetry model has two symmetry breaking scales $\Lambda_L \sim \Lambda_{EW}$ and $\Lambda_R \gg \Lambda_L$, which is constrained to be larger than approximately 3 TeV.

2. **The Fermion sector**

   - For every left-handed SM doublet, there is a corresponding right handed mirror doublet:

     $$\text{SM}: \quad l_L = \begin{pmatrix} \nu_L \\ e_L \end{pmatrix}; \ \text{Mirror}: \quad l_R^M = \begin{pmatrix} \nu_R \\ e_R \end{pmatrix}. \tag{4.3}$$

     The right handed neutrino is "fertile" or "non-sterile" as it belongs to the right handed doublet. The mass of the right-handed neutrino will be discussed in the next section.

     $$\text{SM}: \quad q_L = \begin{pmatrix} u_L \\ d_L \end{pmatrix}; \ \text{Mirror}: \quad q_R^M = \begin{pmatrix} u_R \\ d_R \end{pmatrix} \tag{4.4}$$

   - For every right-handed SM singlet, there is a corresponding left-handed mirror singlet:

     $$\text{SM}: \quad u_R, d_R, e_R; \ \text{Mirror}: \quad u_L^M, d_L^M, e_L^M \tag{4.5}$$

- In comparison, the particle content of the Left - Right model is given by:

$$\begin{aligned} SU(2)_L: \quad l_L &= \begin{pmatrix} \nu_L \\ e_L \end{pmatrix} \\ SU(2)_R: \quad l_R &= \begin{pmatrix} \nu_R \\ e_R \end{pmatrix} \\ SU(2)_L: \quad q_L &= \begin{pmatrix} u_L \\ d_L \end{pmatrix} \\ SU(2)_R: \quad q_R &= \begin{pmatrix} u_R \\ d_R \end{pmatrix} \end{aligned} \tag{4.6}$$

3. **The Scalar Sector**

- The scalar sector in EW ν_R model:

  - Higgs doublets: There are 4 Higgs doublets: $\Phi_1^{SM}(Y/2 = -1/2)$, $\Phi_2^{SM}(Y/2 = +1/2)$, $\Phi_1^{M}(Y/2 = -1/2)$, $\Phi_2^{M}(Y/2 = +1/2)$ where the $Y/2 = \pm 1/2$ refers to the $U(1)_Y$ quantum numbers. The requirements for these Higgs doublets are given in [46]. Basically, for the Lagrangian of interest given by:

$$\mathcal{L} = \mathcal{L}_{Kin} + \mathcal{L}_{mass} + \mathcal{L}_{mixing}, \tag{4.7}$$

where

$$\begin{aligned} \mathcal{L}_{mass} =& g_u \bar{q}_L \Phi_1^{SM} u_R + g_d \bar{q}_L \Phi_2^{SM} d_R \\ &+ g_u^M \bar{q}_R^M \Phi_1^M u_L^M + g_d^M \bar{q}_R^M \Phi_2^M d_L^M + H.c \end{aligned}, \tag{4.8}$$

and

$$\mathcal{L}_{mixing} = g_{Sq} \bar{q}_L \phi_S q_R^M + g_{Su} \bar{u}_L^M \phi_S u_R + g_{Sd} \bar{d}_L^M \phi_S d_R + H.c. \tag{4.9}$$

$\mathcal{L}$ is invariant under the transformations of $U(1)_{SM} \times U(1)_{MF}$:

$$\begin{aligned} U(1)_{SM}: & q_L \to e^{-i\alpha_{SM}} q_L, \\ & (u_R, d_R) \to e^{i\alpha_{SM}} (u_R, d_R) \\ & \Phi_{1,2}^{SM} \to e^{-2i\alpha_{SM}} \Phi_{1,2}^{SM}. \end{aligned}$$

$$
\begin{aligned}
U(1)_{MF} : & q_R \to e^{i\alpha_{MF}} q_R, \\
& (u_L^M, d_L^M) \to e^{i\alpha_{MF}} (u_L^M, d_L^M) \\
& \Phi_{1,2}^{MF} \to e^{2i\alpha_{MF}} \Phi_{1,2}^{MF}.
\end{aligned}
$$

and

$$\phi_S \to e^{-i(\alpha_{SM}+\alpha_{MF})} \phi_S. \tag{4.10}$$

The reason for having these Higgs doublets is to have $\mathcal{L}$ invariant under $U(1)_{SM} \times U(1)_{MF}$ transformations.

– Higgs triplets include one complex triplet $(3, Y/2 = 1)$ and one real triplet with $\xi(3, Y/2 = 0)$ under $SU(2)_L \otimes SU(2)_R$. The two triplets, when combined, form a (3, 3) representation under the global $SU(2)_L \otimes SU(2)_R$ as:

$$\chi = \begin{pmatrix} \chi^0 & \xi^+ & \chi^{++} \\ \chi^- & \xi^0 & \chi^+ \\ \chi^{--} & \xi^- & \chi^{0*} \end{pmatrix}, \tag{4.11}$$

where the VEV of χ is given by:

$$\langle \chi \rangle = \begin{pmatrix} v_M & 0 & 0 \\ 0 & v_M & 0 \\ 0 & 0 & v_M \end{pmatrix}. \tag{4.12}$$

This VEV of χ breaks the symmetry $SU(2)_L \otimes SU(2)_R$ down to $SU(2)$ and guarantees the Custodial Symmetry of the model, which is to maintain the relationship $\rho = M_W^2/M_Z^2 cos^2\theta_W = 1$.

All the VEVs are related by:

$$\sum_{i=1,2} v_i^2 + v_i^{M,2} + 8v_M^2 = v^2 = (246 \text{ GeV})^2, \tag{4.13}$$

where $\langle \Phi_{1,2}^{SM} \rangle = v_{1,2}$ and $\langle \Phi_{1,2}^{MF} \rangle = v_{1,2}^M$ are the VEVs of the Higgs doublets that give masses to SM fermions and mirror fermions.

– 4 Higgs singlets are also needed to contruct neutrino mass matrices with the A_4 non-abelian discrete symmetry.

- Scalar sector in the Left - Right symmetry model includes:
  - Two complex Higgs triplets: $\Delta_R = (1,3)$ and $\Delta_L = (3,1)$ under $SU(2)_L \times SU(1)_R$ where $\langle\Delta_L\rangle = v_L \ll \Lambda_{EW}$ for ρ parameter to satisfy $\rho = 1$. It is also constrained that $\langle\Delta_R\rangle = v_R > 3$ TeV.
  - A bi-doublet $\phi_2 = (2,2)$ which is equal to two SM doublets.

4. **The role of the scalar sector**

To simplify the notation, ν_R^M will be writen as ν_R.

- Dirac and Majorana neutrino masses, charged fermion masses in the EW ν_R model:
  - The Majorana neutrino mass:

    As the right-handed neutrino is now part of right-handed lepton doublet, it is now non-sterile and can acquire a mass that is proportional to the electroweak scale by:

$$\begin{aligned} L_M &= g_M l_R^{M,T} \sigma_2 \tau_2 \tilde{\chi} l_R^M \\ &= g_M \nu_R^T \sigma_2 \nu_R \chi^0 - \frac{1}{\sqrt{2}} \nu_R^T \sigma_2 e_R^M \chi^+ \\ &- \frac{1}{\sqrt{2}} e_R^{M,T} \sigma_2 \nu_R \chi^+ + e_R^{M,T} \sigma_2 e_M^R \chi^{++}, \end{aligned} \tag{4.14}$$

    which gives us the neutrino's Majorana mass of $M_R = g_M v_M$. As the ν_R interacts with Z boson, it must follow that $M_R = g_M v_M > M_Z/2$, or $v_M > 46$ GeV. It has been shown in the originial paper that the real triplet $\xi(Y/2 = 0)$ is required to maintain the relationship $\rho = M_W^2/M_Z^2 cos^2\theta_W = 1$. This is a consequence of the custodial symmetry.
  - The Dirac neutrino mass: In EW ν_R model, the Dirac neutrino mass is obtained by the mixed coupling between SM and Mirror leptons with Higgs singlets. The singlet scalar field ϕ_S couples to fermion bilinears as:

$$\begin{aligned} L_S &= g_{Sl} \bar{l}_M \phi_S l_M^R + h.c \\ &= g_{Sl} (\bar{\nu}_L \nu_R + \bar{e}_L e_R) \phi_S + h.c, \end{aligned} \tag{4.15}$$

    which gives us the Dirac mass of neutrino as $m_D = g_{Sl} v_S$. The seesaw mechanism gives $m_\nu \sim (m_\nu^D)^2/M_R \sim \mathcal{O}(eV)$, or $g_{Sl} v_S < \mathcal{O}(100$ keV).

- Mass of charged leptons and quarks:

  As we have mentioned earlier, SM quarks and charged leptons acquire their masses by coupling to Φ_2 while mirror quarks and leptons acquire their masses by coupling to Φ_{2M}.

- **Dirac and Majorana neutrino masses, charged fermion masses in L-R models**

  - Majorana masses

    Right-handed neutrinos in $SU(2)_R$ and the SM right-handed charge lepton have their mass proportional to the VEV of Δ_R: $\langle \Delta_R \rangle = v_R > 3$ TeV, which means that the right-handed neutrinos in the Left- Right model must have masses in similar scale. In addition, ν_R in the Left - Right model can only be created from the exchange of W_R and Z_R, which are constrained to be above 3 TeV. As a result, the production cross section of the ν_R is much smaller compared to that of the EW-scale ν_R model.

  - Diract masses

    In the Left - Right symmetry model, Dirac neutrino masses are obtained by coupling to the Higgs bi-doublets, which means $m_D \sim \mathcal{O}(v_L \sim EW)$. Charged lepton and quark masses are obtained by coupling to the same Higgs bi-doublets we have mentioned earlier. In contrast, Dirac neutrino masses in EW-scale ν_R model come from couplings to the Higgs singlets while SM charged leptons and quarks and their mirror counterparts get their masses from coupling to Φ_2 and Φ_{2M}, respectively. The diffence in the couplings has been exploited to show the difference between the PMNS and CKM matrices in Ref. [33]

- **The scalar contribution to the electroweak radiative corrections**

  It has been noticed in Ref. [34] and Ref. [22] that triplet Higgs gives large negative contributions to the S-parameter and therefore, fine tuning is required to have a small contribution to the S-parameter coming from the Higgs triplet. In addition, the fine tuning disappears if the negative contribution from the Higgs triplet cancels the positive contribution from an extra fermion sector. This is satisfied by the fermion doublets in case of the EW-scale ν_R model.

4.3 Yukawa Interactions Between Mirror and SM Quarks

- **The interactions** As we have mentioned, the non-abelian discrete symmetry group A_4 was used to describe the Higgs singlet sector which is responsible for generating the Dirac masses of the neutrinos. The assigments of the SM fermions, mirror fermions and the scalars under A_4 are shown in Table (4.1). From this, the Yukawa interactions can be writen as:

$$\begin{aligned} L_S &= \bar{q}_L^d U_L^{d\dagger} M_\phi^d U_R^{d^M} q_R^{M,d} + h.c \\ &= \bar{q}_L^d \bar{M}_\phi^d q_R^{M,d} + h.c \end{aligned} \tag{4.16}$$

for down type quarks and:

$$\begin{aligned} L_S &= \bar{q}_L^u U_L^{u\dagger} M_\phi^u U_R^{u^M} q_R^{M,u} + h.c \\ &= \bar{q}_L^u \bar{M}_\phi^u q_R^{M,u} + h.c, \end{aligned} \tag{4.17}$$

where $q_L^d = (d_L, s_L, b_L)$, $q_L^u = (u_L, c_L, t_L)$, $q_R^{M,d} = (d_R^M, s_R^M, b_R^M)$, $q_R^{M,u} = (u_R^M, c_R^M, t_R^M)$ and where $M_\phi^{d,u}$ contains the couplings and mixing of mirror quarks and SM quarks:

$$M_\phi^{d,u} = \begin{pmatrix} g_{0S}^{d,u}\phi_{0S} & g_{1S}^{d,u}\phi_{3S} & g_{2S}^{d,u}\phi_{2S} \\ g_{2S}^{d,u}\phi_{3S} & g_{0S}^{d,u}\phi_{0S} & g_{1S}^{d,u}\phi_{1S} \\ g_{1S}^{d,u}\phi_{2S} & g_{2S}^{d,u}\phi_{1S} & g_{0S}^{d,u}\phi_{0S} \end{pmatrix} \tag{4.18}$$

Field	$(\nu, l)_L$	$(\nu, l^M)_R$	e_R	e_L^M	ϕ_{oS}	$\tilde{\phi}_S$	Φ_2
A_4	$\underline{3}$	$\underline{3}$	$\underline{3}$	$\underline{3}$	$\underline{1}$	$\underline{3}$	$\underline{1}$

Table 4.1: A_4 assignment for leptons and Higgs field

It must be noted that while the Yukawa couplings for lepton sector g_{Sl}, which is constrained by rare processes like $\mu \to e\gamma$, there are no constraints on the value of g_{Sq}. Therefore, if the combination of the coupling and the mixing are small enough, the decay length of the mirror quark to SM quark will sine displaced-vertex behaviours as we will show below.

- **The decay length** From the Yukawa coupling of the SM and mirror quarks to the scalar Higgs described above, the allowed decay mode of mirror quarks to the SM quarks is $q^M \to q\phi_S$ where the mass of the singlet scalars are supposed to be much smaller than that of the quarks and hence can be ignored in the calculation. Let g_{Sq} be the generic coupling of the mirror quark to SM quark that contains both the Yukawa coupling and the mixing angle, the decay width of this decay process is calculated as:

$$\Gamma(q^M \to q\phi) = \frac{g_{Sq}^2}{64\pi} m_{q^M} \left(1 - \frac{m_q^2}{m_{q^M}^2}\right)\left(1 + \frac{m_q}{m_{q^M}} - \frac{m_q^2}{2m_{q^M}^2}\right). \tag{4.19}$$

Since the decay length of this process is:

$$L = \frac{\gamma\beta\hbar c}{\Gamma(q^M \to q + \phi_S)}, \tag{4.20}$$

the decay length can be macroscopic if the generic coupling g_{Sq} is small enough. This behavior is displayed in Fig. (4.1), where the generic coupling is varied in $10^{-8} \sim 10^{-5}$. For the velocity of the mirror quark in the range of $\beta = 0.5$, the decay length can be from a few millimeters to a few centimeters.

It must be also noted that as the lowest decay time is of the order of 10^{-15} (s) for coupling g_{Sq} that is smaller than 10^{-5}, mirror quarks have enough time to hadronize. As a result, bound states of mirror quarks, which are mirror mesons and hybrid mesons, could be created.

4.4 Production and decays of mirror mesons

4.4.1 An overview of Quarkonia

As we have mentioned earlier, the heavy mirror meson is the bound state of an heavy mirror quark and a corresponding anti-mirror quark. In general, a bound state of an quark and an antiquark $\bar{Q}Q$ is called a quarkonium. Some examples of

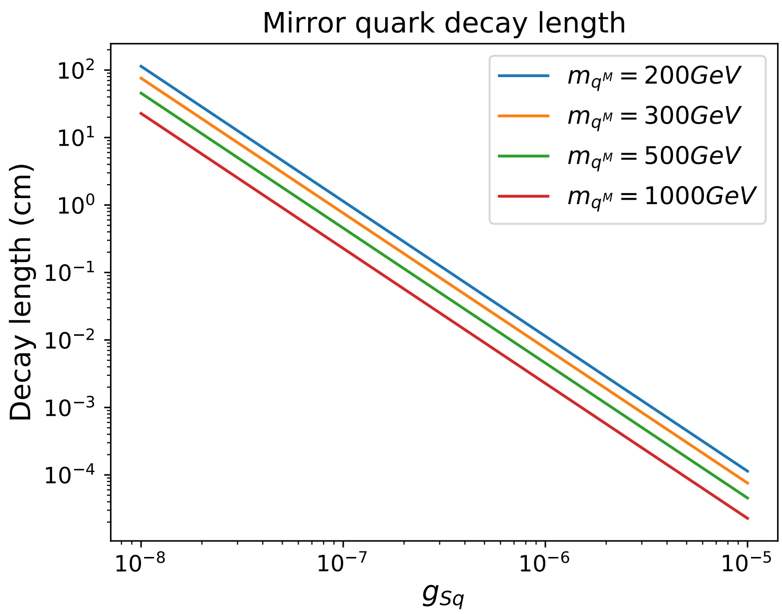

Figure 4.1: Decay length of mirror quarks to SM quarks

quarkonia are the charmonium resonances $\psi(\bar{c}c)$ and bottomonium resonances $\Upsilon(\bar{b}b)$ discovered in the e^+e^- collisions or in p-nucleus collisions.

In non-relativistic approximation, the total angular momentum of the quark - aniquark system is calculated by $\mathbf{J} = \mathbf{L} + \mathbf{S}$ where the spin states can be either $S = 0$ for antisymmetric cases or $S = 1$ for symmetric cases. The parity P and charge conjugation of quarkonium are defined as usual: $P = (-)^{L+1}$ and $C = (-)^{L+S}$. Table 4.2 lists some quantum numbers of quarkonium states. For quarkonium in our model, the mirror meson, we consider it to be at the lowest spin state which is $^1S_0$.

Angular momentum	J^{PC}		Spectroscopy notation
	$S = 0$	$S = 1$	
L= 0 (S)	$\eta(0^{-+})$	$\psi, \Upsilon, \theta(1^{--})$	$^1S_0$, $^3S1$
L = 1 (P)	$h(1^{+-})$	$\chi_{Jeans}(0^{++}, 1^{++}, 2^{++})$	$^1P_1$, ^3P_J
L = 2 (D)	2^{-+}	$1^{--}, 2^{--}, 3^{--}$	$^1D_2$, ^3D_J

Table 4.2: Quantum number of quarkonium states

A quarkonium $\bar{Q}Q$ whose mass is larger than the combination of two heavy mesons $\bar{Q}q$ and $\bar{q}Q$, it will decay strongly into the two heavy mesons. If we set the zero energy to be at $2m_Q$ where Q is the heavy quark, the threshold above which the quarkonium would decay to two heavy meson is: $E_T = 2m(\bar{Q}q) - 2m_Q$. This threshold is usually independent of m_Q for $m_Q \gg m_q$.

In the quarkonium bound states whose masses are much larger than the QCD scale, the dynamics of such bound states can be treated by using nonrelativistic quantum mechanics [38]. Specifically, the production and decay of heavy quarkonium bound states are calculated by using the Schrodinger equation where the interquark potential is parameterized by:

$$V(r) = -\frac{4\alpha_s(r)}{3r} + V_I(r) + ar, \tag{4.21}$$

where α_s is the strong coupling constant. The first term in the potential is from the Fourier transformation of the short-distance Coulomb-like one-gluon-exchange scattering amplitude. The third term that is linear in r is a confining potential with $a \simeq 0.2$ GeV^2. The second term in the potential is the parameterization of the region between the Coulomb-like and the linear terms, which are usually extracted from experimental data. The heavier the quarkonium is, the more important the Coulomb-like term is. In the following sections where our proposed mirror quarks are assumed to be heavy, we will only concentrate on this one-gluon-exchange potential.

For quarkonium mass that is large enough, it is reasonable to ignore the last two terms in the potential above. From this, the wave function for a quark at the origin can be approximated by:

$$|\psi_n(0)|^2 = \frac{1}{\pi}\left[\frac{2}{3n} m_Q \alpha_s(m_Q^2)\right]^3, \tag{4.22}$$

where n is the radial wave number. We will use this for our next calculation for production and decay of our mirror mesons.

4.4.2 Production

In the previous section, we have reviewed the Electroweak Scale right-handed Neutrino model whose particle content contains a mirror counterpart for every SM fermion. As a result, the bound state of a mirror quark and an antimirror quark can form to what we call "mirror meson". Similarly, the bound state of a mirror quark and a SM quark can form to what we call "hybrid mesons". Let us denote the mirror meson formed by the lightest mirror quark - antiquark pair η^M and the generic hybrid meson formed by the lightest mirror quarks and other much lighter SM antiquark pair η^H.

Because the gauge group of the EW-scale ν_R model is the same with that of SM, mirror quarks have the same strong interaction as that of the SM quarks. From this, mirror meson production will come from the gluon - gluon fusion process. The production cross section of that process can be inferred from the decay of a mirror meson η^M to a gluon pair in spin singlet state which is given by:

$$\Gamma(\eta^M \to gg) = \frac{8\alpha_S^2}{3}\frac{\pi|\psi(0)|^2}{m_{q^M}^2} = \frac{32\alpha_S^5}{27}m_{\eta^M}, \tag{4.23}$$

where the strong coupling constant must be evaluated at the m_{q^M} scale and where the wave function at the origin $\psi(0)$ is given by:

$$|\psi_n(0)|^2 = \frac{1}{\pi}\left[\frac{2}{3}n^{-1}m_{q^M}\alpha_S\right]^3 \tag{4.24}$$

By crossing, the spin and color average cross section of the gluon fusion to mirror meson $gg \to \eta_M$ is:

$$\sigma(gg \to \eta_M) = \frac{\pi^2}{64m_{q^M}^3}\Gamma(\eta^M \to gg) = \frac{\alpha_S^2\pi^3}{8m_{q^M}^5}|\psi(0)|^2 = \frac{\alpha_S^5\pi^2}{27m_{q^M}^2}. \tag{4.25}$$

4.4.3 Decays of mirror meson and hybrid meson

The mirror mesons can decay via two different mechanisms that show different signatures in the collider as is shown in Figs. (4.2) and (4.4) or they can be propagators of the gluon annihilation to two mirror mesons. In the first decay mechanism showed in Fig. (4.2), there is a scalar Higgs ϕ_S exchanged between the mirror quark and antiquarks and the final states are the SM quark and antiquark pair. In the second decay mechanism showed in Fig. (4.4), there is a SM quark exchange between two mirror quarks and the final products are two undetectable scalar Higgs ϕ_S. As we will show in the following calculation, the decays of this type are associated with the annihilation of two mirror quarks with exchange of ϕ_S to SM quarks. As the mass of the ϕ_S is considered to be very small, the second decay is negligible compared to the first one. In addition, the fact that there is no detectable signal for the second decay makes it less significant compared to the first one. One example of the decay of this type would be the case where the SM quark in the process is b quark. If that is the case, the signal of the process will be b quark jets.

In the process shown in Fig. (4.3), the mirror meson η^M is a propagator for the process $gg \to \eta^H \eta^H$. The mirror quark in the hybrid meson will eventually decay to an SM quark and the scalar Higgs ϕ_S, the final state of this decay is a pair of SM mesons and missing energy that is carried out by the scalar Higgs which is not part of the first mechanism. One example we could have for this process is the case where the mirror quarks decay to SM b quark. The mesons in the production would depend on the type of inner line SM quark. If the inner line SM quark was u quark, we would have $B^{+,-}$ mesons in the output. If the inner line SM quark was d quark, we would have $B^0, \bar{B}^0$ mesons in the final state.

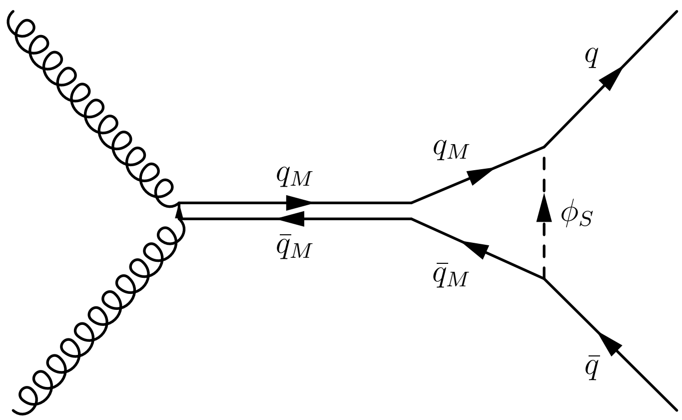

Figure 4.2: $g + g \to \eta^M \to q\bar{q}$ without missing energy.

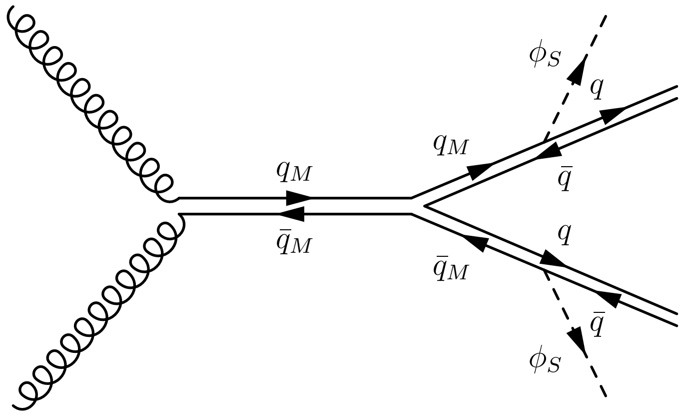

Figure 4.3: $g + g \to \eta^M \to$ 2SM mesons $+ 2\phi_S$ with missing energy.

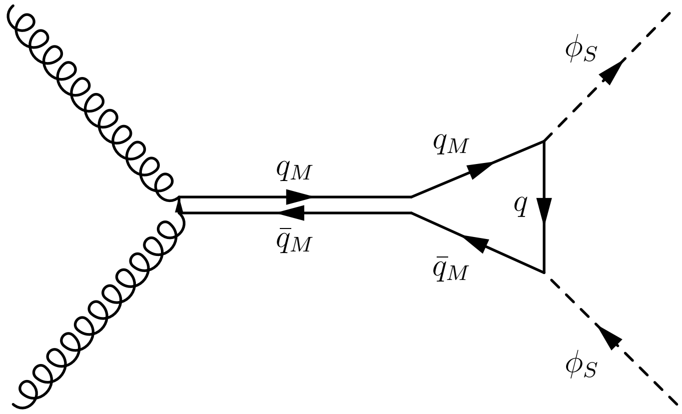

Figure 4.4: $g + g \to \eta^M \to 2\phi_S$ with complete missing energy

Decay without missing energy

The decay of a mirror meson η^M to the SM quark - antiquark pair is can be calculated with help from the process of free mirror quark annihilation via ϕ_S exchange: $q_M\bar{q}_M \to q\bar{q}$.

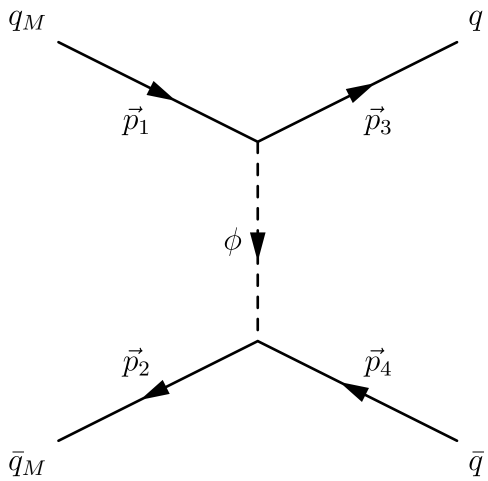

Figure 4.5: Free mirror quarks annihilation via Φ_S exchange

Following the method described in Ref. [35] and use the center of mass frame such that $p_1 - p_2 = (0, 2\vec{p})$ and $p_1 + p_2 = (2m_{q^M}, 0)$, the free-quark scattering matrix is given by:

$$\mathcal{A} = \frac{g_{Sq}^2}{t}(\bar{u}_{3L}u_{1R})(\bar{v}_{2R}v_{4L}). \tag{4.26}$$

Using a Feirz Transformation, we can rewrite the product above as:

$$\begin{aligned}\mathcal{A} = \frac{1}{4}\frac{g_{Sq}^2}{t}\Big[&(\bar{u}_{3L}v_{4L})(\bar{v}_{2R}u_{1R}) + (\bar{u}_{3L}\gamma^{\mu}v_{4L})(\bar{v}_{2R}\gamma_{\mu}u_{1R}) \\ &+ \frac{1}{2}(\bar{u}_{3L}\sigma^{\mu\nu}v_{4L})(\bar{v}_{2R}\sigma_{\mu\nu}u_{1R}) - (\bar{u}_{3L}\gamma^{\mu}\gamma_5 v_{4L})(\bar{v}_{2R}\gamma_{\mu}\gamma_5 u_{1R}) \\ &+ (\bar{u}_{3L}\gamma_5 v_{4L})(\bar{v}_{2R}\gamma_5 u_{1R})\Big] \end{aligned} \tag{4.27}$$

By using chiral properties, we can eliminate all terms except for the first and the last ones in the expression above, which simplifies to:

$$\begin{aligned}\mathcal{A} &= \frac{1}{4}\frac{g_{Sq}^2}{t}\left[(\bar{u}_{3L}v_{4L})(\bar{v}_{2R}u_{1R}) + (\bar{u}_{3L}\gamma_5\frac{1+\gamma_5}{2}v_{4L})(\bar{v}_{2R}\gamma_5\frac{1+\gamma_5}{2}u_{1R})\right] \\ &= \frac{1}{2}\frac{g_{Sq}^2}{t}(\bar{u}_{3L}v_{4L})(\bar{v}_{2R}u_{1R}) \\ &= \frac{1}{2}\frac{g_{Sq}^2}{t}(\bar{u}_3\frac{1+\gamma_5}{2}v_4)(\bar{v}_2\frac{1+\gamma_5}{2}u_1)\end{aligned} \tag{4.28}$$

The mirror meson decay amplitude is then calculated by:

$$\mathcal{M}(^1S_0) = \frac{\sqrt{3}\Psi(0)}{\sqrt{2m_{q^M}}}\frac{1}{2}\frac{g_{Sq}^2}{t}(\bar{u}_3\frac{1+\gamma_5}{2}v_4)Tr\left[\frac{1+\gamma_5}{2}(\not{p}_1 - m_{q^M})\right], \tag{4.29}$$

where $\Psi(0)$ is the coordinate-space wave function at the origin. We only consider here the spin 0 state of the mirror meson, since the fusion of the two gluons can only give a scalar mirror meson:

$$\mathcal{M}(^1S_0) = \frac{\sqrt{3m_{q^M}}\Psi_S(0)}{\sqrt{2}}\frac{g_{Sq}^2}{t}(\bar{u}_3\frac{1+\gamma_5}{2}v_4) \Rightarrow \left|\mathcal{M}(^1S_0)\right|^2 = \frac{6g_{Sq}^4\Psi_S^2(0)}{m_{q^M}} \tag{4.30}$$

The decay width of mirror meson is then:

$$\begin{aligned}\Gamma(\eta^M \to q\bar{q}) &= \frac{p}{8\pi(2m_{q^M})^2}\left|\mathcal{M}(^1S_0)\right|^2 \\ &= \frac{m_{q^M}}{32\pi m_{q^M}^2}\frac{6g_{Sq}^4\Psi_S^2(0)}{m_{q^M}} = \frac{3g_{Sq}^4\Psi_S^2(0)}{16\pi m_{q^M}^2} \\ &= \frac{g_{Sq}^4\alpha_S^3}{18\pi^2}m_{q^M}.\end{aligned} \tag{4.31}$$

The decay length $\gamma\beta\hbar c/\Gamma$ of the mirror meson into SM quarks are illustrated on Fig. (4.6) for $\beta = v/c = 10^{-3}$ and $\beta = 10^{-1}$ at different mirror quark masses. It can be seen that for the coupling g_{Sq} smaller than $\mathcal{O}(10^{-3})$, the decay length can reach to the macroscopic sizes (1 mm). The Fig. (4.6) also plots the radius of the CMS's Silicon Strip Tracker. The macroscopic size of this radius allows these detectors to observe the displaced-vertex events of mirror mesons and hyrid mesons.

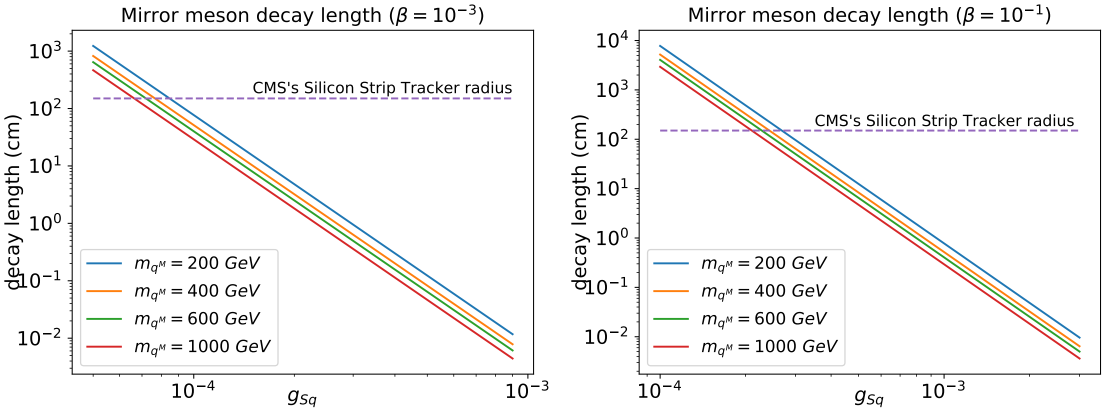

Figure 4.6: Macroscopic mirror meson decay lengths at small couplings g_{Sq}.

To simplify the process of gluon fusion to a mirror meson followed by the mirror meson decaying to SM quarks, we can use an effective Lagrangian that describes the gluon-mirror meson vertex and mirror meson-SM quark vertex as follows:

$$\mathcal{L} = \frac{1}{4}\frac{g_1}{m_{\eta^M}} F_{\mu\nu}F^{\mu\nu}\eta^M + g_2\bar{q}^M q^M \eta^M, \tag{4.32}$$

where g_1 is the effective coupling constant for gluon - mirror meson vertex and g_2 is mirror meson - SM quark vertex. From this, the decay width of a mirror meson to gluon pair and to quark pairs are:

$$\Gamma(\eta^M \to gg) = \frac{g_1^2}{128\pi} m_{\eta^M}, \tag{4.33}$$

$$\Gamma(\eta^M \to q\bar{q}) = \frac{g_2^2 m_{\eta^M}}{16\pi}\left(1 - \frac{2m_q^2}{m_{\eta^M}^2}\right)\left(1 - \frac{4m_q^2}{m_{\eta^M}^2}\right)^{1/2} \tag{4.34}$$

By comparing equations (4.23) and (4.31) with equations (4.33) and (4.34) respectively, we get:

$$\begin{aligned} g_1 &\approx 22\alpha_S^{5/2} \approx 10^{-2} - 10^{-1} \\ g_2 &\approx 1.1 g_{Sq}^2 \alpha_S^{3/2} \approx 10^{-9} - 10^{-8}. \end{aligned} \tag{4.35}$$

where g_{Sq} has been chosen to be $\mathcal{O}(10^{-3})$ for the reason mentioned above.

These effective couplings are the parameters being used to simulate the process of $gg \to \eta^M \to \bar{q}q$. For demonstration purposes, the b quark was chosen to be the resulted SM quark of the process. Various mirror meson η^M masses have been used for the simulation and the transverse momentum distributions are plotted in Fig. (4.7) where energy of the proton beam was set at 13 TeV.

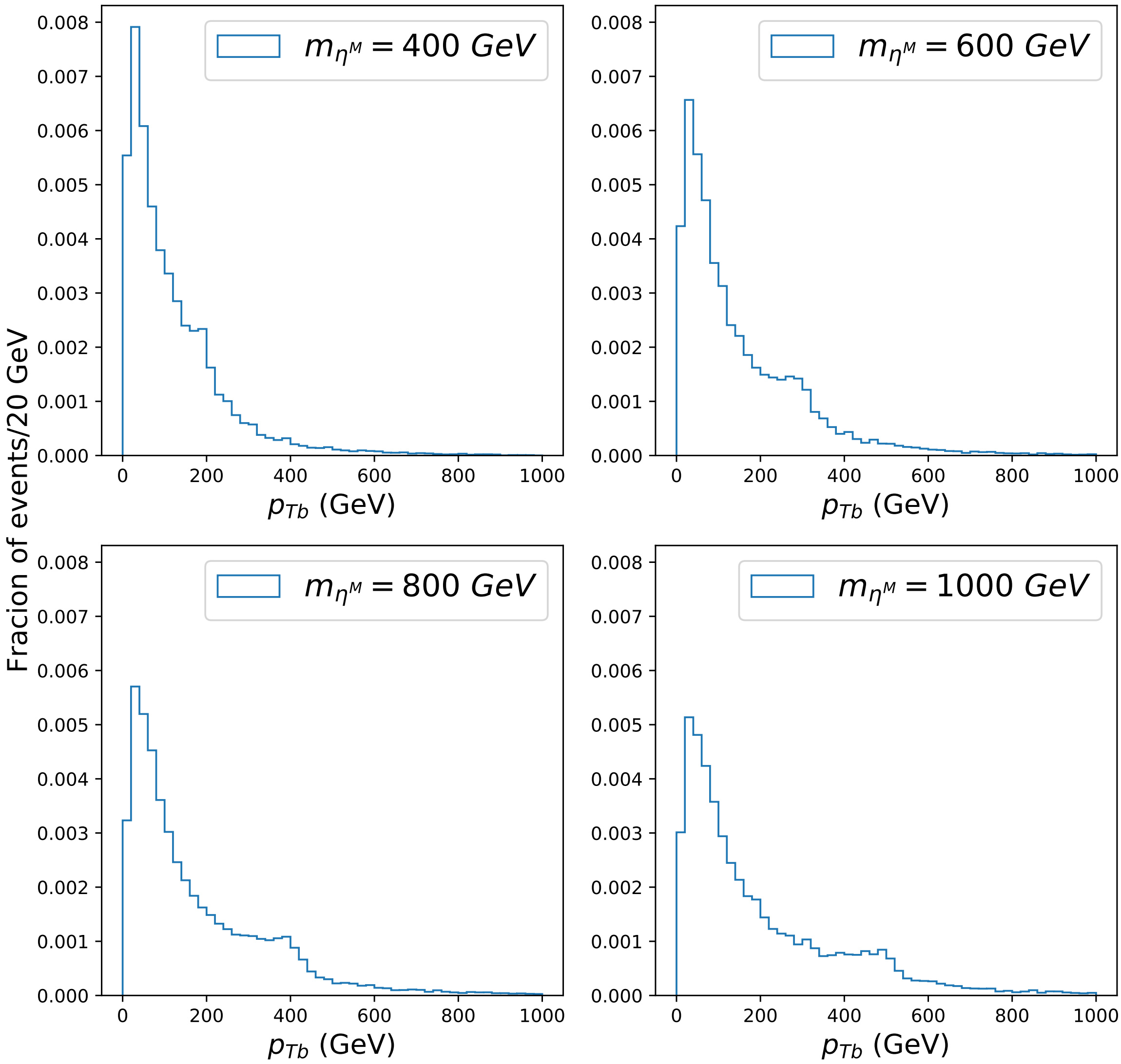

Figure 4.7: p_T distribution of b quark after decaying from mirror mesons as predicted by Madgraph.

Process with missing energy

The second process involves the hybrid mesons η^H, which is created from gluon annihilation to a mirror meson in the s-channel, decaying to SM mesons as jets and a pair of scalar Higgs ϕ_S. As the scalar Higgs singlet carries part of the energy and momentum of the gluons, the signature of this process will be the missing energy and momentum of the fused gluons. The effective Lagrangian of the η^M - η^H and η^H - ϕ_S vertices can be written as:

$$\mathcal{L} = \frac{1}{4}\frac{g_1}{m_{\eta^M}} F_{\mu\nu}F^{\mu\nu}\eta^M + g_3 m_{\eta^M}\eta^H\eta^H\eta^M + g_4\frac{m_{\eta^H}}{2}\eta^H J_{SM}\Phi_S \tag{4.36}$$

where J_{SM} is any SM meson and will be observed as jets.

The coupling contant g_4 can be taken to be the same with g_{Sq} as the underlying process of the decay $\eta^H \to J_{SM} + \phi_S$ is the decay of mirror quark $q^M \to q_{SM} + \phi_S$. The decay width of hybrid meson can be calculated by:

$$\Gamma(\eta^H \to J_{SM} + \Phi_S) = \frac{g_4^2}{16\pi} m_{\eta^H}\left(1 - \frac{m_{J_{SM}}^2}{m_{\eta^H}^2}\right) = \frac{g_{Sq}^2}{16\pi} m_{\eta^H}\left(1 - \frac{m_{J_{SM}}^2}{m_{\eta^H}^2}\right). \tag{4.37}$$

The decay length of the hybrid meson at various mirror quark mass and coupling constant g_{Sq} are shown in Fig. (4.8). From this, if the combination of the coupling constant and the mixing angle is smaller than $10^{-8} \sim 10^{-7}$, the decay length of the hybrid meson to will achieve macroscopic levels and hence will show displaced vertex behaviors.

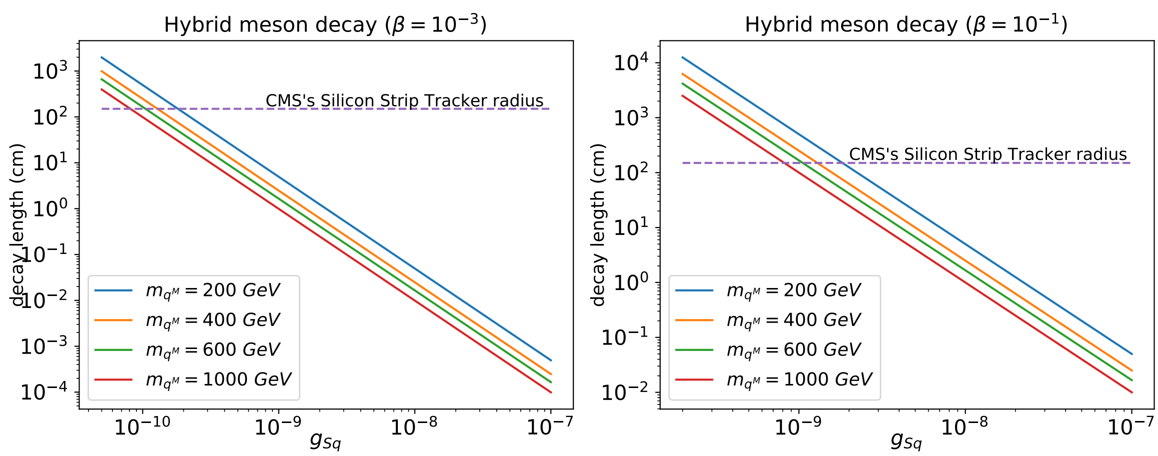

Figure 4.8: Macroscopic hybrid meson decay lengths at small couplings g_{Sq}.

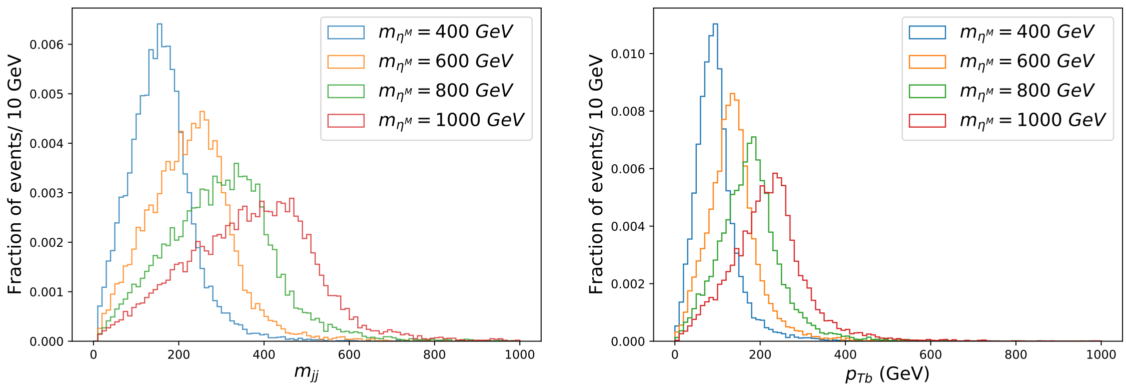

Figure 4.9: Invariant mass and transverse momentum distributions of the SM meson pair from hybrid meson decay as predicted by Madgraph.

To estimate the coupling g_3 of the η^H - η^M vertex, we can look at a similar decay of f_0 meson of mass $400 \sim 700$ MeV into two pion π^0:

$$\Gamma(f_0 \to \pi\pi) = \frac{g^2}{16\pi} m_{f_0} \left(1 - \frac{4m_\pi^2}{m_{f_0}^2}\right)^{1/2} , \tag{4.38}$$

from which, we could estimate $g \approx \mathcal{O}(1)$ and assume that the coupling g_3 should also be at the same magnitude. By using these chosen parameters, the distribution of the invariant mass and the transverse momentum can be acquired from Pythia simulation at different mirror meson masses. The SM meson was selected to be the neutral pion for the simulations. The fact that the scalar Higgs singlet carries part of the energy from the incoming gluons can be seen on the SM meson pair invariant mass distribution, which shows that the distribution is shifted to the left.

Chapter 5

Conclusions

The Standard Model is a great tool for studying elementary particle Physics. Despite being the most successful theory, it has many proceblems that make it not a perfect theory. Some of those include the explantion for the gravitational interaction, the explanation for dark matter and dark energy, the non-zero mass of neutrinos, the matter-antimatter asymmetry, etc.

In this thesis, we have addressed two of these problems. we have reviewed the Luminogenesis model [22], whose dark matter is proposed to be belonging to the gauge group $SU(4)_{DM}$. The baryonic bound state of $SU(4)_{DM}$ fermions was assumed to be dark matter in the universe. By looking at the stability conditions for this dark astronomical compact objects, we have predicted the possible mass range for DACOs and proposed some experimental techniques for deteccting such objects. The fact that the DACOs' mass is about a few times of that the Earth has enabled us to use the same tichniques being used to look for exoplanets to look for DACOs. We also proposed a cooling mechanism for DACOs, which is crucial for highly energetic particles in the universe to form a graviational potential well to attract other particles to form bigger structures.

The problem of non-zero mass of the neutrinos was addressed by reviewing the Electroweak-scale Right-handed neutrinos model [17]. By introducing the additional scalar singlets and triplets, one can generate small mass of the neutrino by seesaw mechanism in electroweak scale. As the the right-handed neutrinos are now non-sterile and having the mass in the electroweak scale, they are accessible at the high energy colliders such as the LHC. The model introduced mirror mesons to satisfy the anomaly cancellation requirements. We have looked at the possibility of long-live mesons that are bound states of mirror quark - anti mirror quark and of mirror quark - SM antiquark. The fact that the coupling of these mirror quarks to the SM quarks is not constrained and can be very small has been used to reason the possibility of existence of mirror mesons and hybrid mesons and as well as proposing the possible displaced vertex behavior of these mesons. By using simulation tools such as Madgraph and Pythia, we are able to simulate the signatures of these events at higher energy colliders.

At the scope of this thesis, there are some interesting problems that we were not able to discuss. For example, the distribution of DACOs in the Universe, the mixing of mirror quarks and SM quarks, etc. We hope that these and other aspects of these problem would be addressed in later research.

Appendices

Appendix A

Rate of Dark Pion "Bremsstrahlung"

The interaction between the CHIMP and dark pion can be thought as similar to the interaction between pion-nucleon vertex where the difference is that our CHIMPs have spin 0 instead of 1/2 for SM nucleons. The effective Lagrangian for the dark 'baryon" - dark pion vertex is given by:

$$L = g_X m_X X X \phi, \tag{A.1}$$

where X and ϕ denote CHIMPs and π_{DM}. Following the discussion given in [4], the scattering matrix for the process that includes π_{DM} "Bremsstrahlung" is given in term of scattering matrix without one is:

$$\begin{aligned} i\mathcal{M}(p,p') = -ig_X m_X \Bigg(& \mathcal{M}_0(p-k,p')\frac{1}{(p-l)^2 - m_X^2 + i\epsilon} \\ & + \mathcal{M}_0(p,p'+k)\frac{1}{(p'+k)^2 + m_X^2 + i\epsilon}\Bigg). \end{aligned} \tag{A.2}$$

For $k \ll |p-p'|$, we can replace $\mathcal{M}_0(p-k,p')$ and $\mathcal{M}_0(p,p'+k)$ with $\mathcal{M}_0(p,p')$:

$$i\mathcal{M}(p,p') = -ig_X m_X \mathcal{M}_0(p,p')\left(\frac{1}{-2pk} + \frac{1}{2p'k}\right) \tag{A.3}$$

$$\Leftrightarrow d\sigma(p \to p'+k) = d\sigma(p \to p')\int \frac{d^3k}{(2\pi)^3}\frac{1}{2E_k}\frac{g_X^2 m_X^2}{4}\left(\frac{1}{p'k} - \frac{1}{pk}\right)^2. \tag{A.4}$$

Choose a frame in which $p = E(1,\mathbf{v})$, $p' = E(1,\mathbf{v}')$, $k = E_k(1,\hat{k}) = \sqrt{\mathbf{k}^2 + m_{\pi_{DM}}}(1,\hat{k})$ where the π_{DM} is considered to be relativistic as its mass is about 3 orders smaller than that of CHIMPs. The probability for a "Bremsstrahlung" to happen is the ratio of the cross section of the process with dark pion "Bremstrahhlung" to the process without it:

$$\begin{aligned} d(Prob) &= \int \frac{d^3k}{(2\pi)^3} \frac{1}{8E_k} \frac{g_x^2 m_X^2}{\mathbf{k}^2 + m_{\pi_{DM}^2}} \left(\frac{1}{p'k} - \frac{1}{pk}\right)^2 \\ &= \int \frac{\mathbf{k}^2 d\mathbf{k} d\Omega_{\mathbf{k}}}{(2\pi)^3 8E_k} \frac{g_X^2 m_X^2}{\mathbf{k}^2 + m_{\pi_{DM}^2}} \left(\frac{-2}{(p'\hat{k})(p\hat{k})} + \frac{1}{(p'k)^2} + \frac{1}{(pk)^2}\right) \\ &= \frac{g_X^2 m_X^2}{16\pi^2} \int \frac{\mathbf{k}^2 d\mathbf{k}}{(\mathbf{k}^2 + m_{\pi_{DM}}^2)^{3/2}} \int \frac{d\Omega_{\mathbf{k}}}{4\pi} \left(\frac{-2}{(p'\hat{k})(p\hat{k})} + \frac{1}{(p'\hat{k})^2} + \frac{1}{(p\hat{k})^2}\right). \end{aligned} \tag{A.5}$$

The non-zero mass of dark pion makes the first integral convergent as opposed the situation of gamma Bremsstrahlung in QED. For second integral, the last two terms can be simplified to:

$$\begin{aligned} \int \frac{d\Omega_{\mathbf{k}}}{4\pi} \frac{1}{(p'\hat{k})^2} &= \frac{1}{2} \int_{-1}^{1} d(\cos\theta) \frac{1}{(p_0' - p'\cos\theta)^2} = \frac{1}{2} \frac{1}{p'} \left(\frac{1}{p_0' - p'} - \frac{1}{p_0' + p'}\right) \\ &= \frac{1}{E^2 (1 - (v')^2)} \approx \frac{1}{m_B^2}. \\ \int \frac{d\Omega_{\mathbf{k}}}{4\pi} \frac{1}{(p\hat{k})^2} &= \frac{1}{E^2 (1 - (v)^2)} \approx \frac{1}{m_B^2}. \end{aligned} \tag{A.6}$$

The first term in the second integral in Eq. (A.5) requires using Feynmann parameters:

$$\begin{aligned} \int \frac{d\Omega_{\mathbf{k}}}{4\pi} \frac{-2}{(p'\hat{k})(p\hat{k})} &= \int_0^1 dx \int \frac{d\Omega_{\mathbf{k}}}{4\pi} \frac{-2}{[xp'\hat{k} + (1-x)p\hat{k}]^2} \\ &= \int_0^1 dx \int_0^{\pi} \frac{-\sin\theta d\theta}{[x(p_0' - p'(\cos\alpha\cos\theta - \sin\alpha\sin\theta)) + (1-x)(p_0 - pcos\theta]^2}, \end{aligned} \tag{A.7}$$

where θ is the angle between p and p'. For small momentum transfer, we can approximate $sin(\alpha) \approx 0$.

$$\begin{aligned} \int \frac{d\Omega_{\mathbf{k}}}{4\pi} \frac{-2}{(p'\hat{k})(p\hat{k})} &= -\int_0^1 dx \int_{-1}^{1} d(\cos\theta) \frac{1}{[x(p_0' - p'\cos\theta) + (1-x)(p_0 - p\cos\theta)]^2} \\ &= \int_0^1 dx \frac{-2}{-[(xp' + (1-x)p]^2 + [xp_0' + (1-x)p_0]^2} \\ &= \int_0^1 dx \frac{-2}{[xp' + (1-x)p]^2} = \int_0^1 dx \frac{-2}{m_B^2 - x(1-x)q^2}. \end{aligned} \tag{A.8}$$

Put these to Eq. A.5, we have:

$$\begin{aligned} d(Prob) &= \frac{g_X^2 m_X^2}{16\pi^2} \int_0^{|\mathbf{q}|} \frac{\mathbf{k}^2 d\mathbf{k}}{(\mathbf{k}^2 + m_{\pi_{DM}}^2)^{3/2}} \left(\frac{2}{m_X^2} - \int_0^1 dx \frac{2}{m_X^2 - x(1-x)q^2}\right) \\ &= \frac{\alpha_{DM}^2}{\pi} \ln\left(\frac{-q^2}{m_{\pi_{DM}^2}}\right) \left(1 - \int_0^1 \frac{1}{1 - x(1-x)\frac{q^2}{m_X^2}}\right). \end{aligned} \tag{A.9}$$

Bibliography

[1] Griffiths, David (1987). Introduction to Elementary Particles. John Wiley & Sons. ISBN 0-471-60386-4.

[2] M.Gell-Mann, Phys.Rev.92(1953)833.

[3] C. Patrignani et al. (Particle Data Group), Chinese Physics C, 40, 100001 (2016)

[4] An Introduction to quantum field theory - Peskin, Michael E. et al.

[5] C. N. Yang and R. Mills, Phys. Rev. 96 191 (1954).

[6] Quarks And Leptons: An Introductory Course In Modern Particle Physics - Halzen, F. et al. New York, Usa: Wiley (1984)

[7] S. J. Warren, P. C. Hewett, P. S. Osmer & M. J. Irwin. Nature 330, 453 (1987).

[8] Planck Collaboration (2015). "Planck 2015 results. XIII. Cosmological parameters". Astronomy & Astrophysics. 594: A13. arXiv:1502.01589.

[9] V.C. Rubin, W.K. Ford, N. Thonnard, Astrophys. J.238, 471 (1980).

[10] E.W. Kolb, M.S Turner. The Early Universe (1989).

[11] S. Weinber. Gravitation and Cosmology: Principles and Application of the General Relativity (1972).

[12] J. J. Condon and A. M. Matthews 2018 PASP 130 073001.

[13] J.S. Bullock. arXiv:1009.4505 [astro-ph.CO]

[14] P.H. Frampton and P.Q. Hung. Phys. Lett. B675, 411 (2009). arXiv:0903.0358[hep-ph].

[15] P.H. Frampton and P.Q. Hung, arXiv:1309.1723[hep-ph].

[16] P.Q. Hung and Kevin J. Ludwick, JCAP 09, 031 (2015). arXiv:1411.1731[hep-ph].

[17] P.Q Hung, Phys. Lett. B 649 (2007) 275. arXiv:hep-ph/0612004.

[18] P.Q. Hung and Kevin J. Ludwick, JCAP 09, 031 (2015). arXiv:1411.1731[hep-ph]

[19] P.Q. Hung and S. Nussinov

[20] E. Takasugi, M. Yoshimura,Zeitschrift für Physik C Particles and Fields, 1984, Volume 26, Number 2.

[21] Oppenheimer, J. R., Volkoff G. M., Phys. Rev. 55, 374 (1939).

[22] P.H. Frampton and P.Q. Hung, arXiv:1309.1723[hep-ph].

[23] P.H. Frampton and P.Q. Hung, Phys. Lett. B675, 411 (2009). arXiv:0903.0358[hep-ph].

[24] P. Q. Hung, Phys. Lett. B 649, 275 (2007) [hep-ph/0612004].

[25] P. Q. Hung, K. J. Ludwick, arXiv:1411.1731 [hep-ph].

[26] M. Mayor, D. Queloz, Nature volume 378, 355.

[27] Sjur Refsdal, H. Bondi; The Gravitational Lens Effect, Monthly Notices of the Royal Astronomical Society, Volume 128, Issue 4, 1 September 1964, Pages 295–306

[28] Miralda-Escude, The Astrophysical Journal. 564 (2): 1019–1023. arXiv:astro-ph/0104034.

[29] J. J. Hermes. arXiv:1708.00896

[30] S. Weinberg, Phys. Rev. Lett. 43, 1566 (1979).

[31] J. C. Pati and A. Salam, Phys. Rev. D 10, 275 (1974) [Phys. Rev. D 11, 703 (1975)];R. N. Mohapatra and J. C. Pati, Phys. Rev. D 11, 2558 (1975); G. Senjanovic and R. N. Mohapatra, Phys. Rev. D 12, 1502 (1975);

[32] S. Chakdar, K. Ghosh, V. Hoang, P. Q. Hung, S. Nandi, arXiv:1508.07318 [hep-ph]

[33] P. Q. Hung, Trinh Le, arXiv:1501.02538 [hep-ph].

[34] F.Borzumati and Y. Nomura, Phys. Rev. D64, 053005 (2001) doi:10.1103/PhysRevD.64.053005 [hep-ph/0007018].

[35] Vernon D. Barger, Roger J.N. Phillips, *Collider Physics*.

[36] T.Song, H. Berrehrah, Phys. Rev. C 94, 034901, arXiv:1601.04449 [nucl-th]

[37] J.Kristian, A. Sandage and J. Westphal, Ap. J. 221, 383 (1978)

[38] T. Kawanai, S. Sasaki, arXiv:1311.1253v1 [hep-lat]

[39] G. Jungman, M. Kamionkowski, K. Griest, arXiv:hep-ph/9506380

[40] Julio F. Navarro, Carlos S. Frenk, Simon D.M. White, arXiv:astro-ph/9508025

[41] T. Fukushige, J. Makino, arXiv:astro-ph/9610005

[42] S.H.Oh, C. Brook, F. Governato, E. Brinks, L Mayer, A. Brooks, F. Walter, arXiv:1011.2777 [astro-ph.CO]

[43] A. A. Klypin, A. V. Kravtsov, O. Valenzuela, F. Prada, arXiv:astro-ph/9901240

[44] Matthew R. Buckley and Anthony DiFranzo, arXiv:1707.03829v2 [hep-ph]

[45] S. Chakdar, K. Ghosh, V. Hoang, P. Q. Hung and S. Nandi, Phys. Rev. D 93, no. 3, 035007 (2016); S. Chakdar, K. Ghosh, V. Hoang, P. Q. Hung and S. Nandi, ibid. 95, no. 1, 015014 (2017).

[46] P. Q. Hung, arXiv:1712.09701 [hep-ph]

[47] Batygin, Konstantin, E. Brown, Michael. The Astronomical Journal. 151.22.10.3847/0004-6256/151/2/22.

[48] Anatoly A. Klypin, Andrey V. Kravtsov, and Octavio Valenzuela, arXiv:astro-ph/9901240[astro-ph].

[49] Original draft by P. Q. Hung and S. Nussinov.

[50] Adam G. Riess, Stefano Casertano, Wenlong Yuan, Lucas M. Macri, Dan Scolnic. arXiv:1903.07603v2 [astro-ph.CO]

[51] Ryan J. Cooke, Max Pettini, Kenneth M. Nollett, Regina Jorgenson. arXiv:1607.03900v1 [astro-ph.CO]

[52] Cyril Pitrou, Alain Coc, Jean-Philippe Uzan, Elisabeth Vangioni. arXiv:1801.08023 [astro-ph.CO]

[53] Shreyashi Chakdar, K. Ghosh, V. Hoang, P. Q. Hung, S. Nandi. Phys. Rev. D 95, 015014 (2017)